



**HAL**  
open science

# Assistive control of motion in sensorimotor impairments based on functional electrical stimulation

Benoît Sijobert

► **To cite this version:**

Benoît Sijobert. Assistive control of motion in sensorimotor impairments based on functional electrical stimulation. Other. Université Montpellier, 2018. English. NNT : 2018MONTTS079 . tel-02139184

**HAL Id: tel-02139184**

**<https://theses.hal.science/tel-02139184>**

Submitted on 24 May 2019

**HAL** is a multi-disciplinary open access archive for the deposit and dissemination of scientific research documents, whether they are published or not. The documents may come from teaching and research institutions in France or abroad, or from public or private research centers.

L'archive ouverte pluridisciplinaire **HAL**, est destinée au dépôt et à la diffusion de documents scientifiques de niveau recherche, publiés ou non, émanant des établissements d'enseignement et de recherche français ou étrangers, des laboratoires publics ou privés.

# THÈSE POUR OBTENIR LE GRADE DE DOCTEUR DE L'UNIVERSITÉ DE MONTPELLIER

En Systèmes Automatiques et Microélectroniques

École doctorale I2S

Unité de recherche CAMIN

Assistive control of motion in sensorimotor impairments  
based on functional electrical stimulation

Présentée par Benoît SIJOBERT

Le 28 septembre 2018

Sous la direction de Christine AZEVEDO  
et David ANDREU

Devant le jury composé de

Brian ANDREWS	Professeur	Université d'Oxford	Rapporteur
Philippe SOUERES	Directeur de Recherche	CNRS - LAAS Toulouse	Rapporteur
Christian GENY	Praticien Hospitalier	CHU Montpellier	Examineur
Philippe FRAISSE	Professeur	Université de Montpellier	Examineur, Président du Jury
Christine AZEVEDO	Directrice de Recherche	INRIA	Directrice de Thèse
David ANDREU	Maître de Conférence, HDR	Université de Montpellier	Co-directeur de Thèse
Charles FATTAL	Praticien Hospitalier, HDR	CRRF La Châtaigneraie	Invité



UNIVERSITÉ  
DE MONTPELLIER



*A ma famille.*



# Acknowledgements

A Christine, pour ces années à apprendre à tes côtés, merci... de m'avoir transmis ta passion, ta vision de la recherche, tes valeurs professionnelles et personnelles, de m'avoir apporté ton soutien et ton énergie sans faille, de m'avoir fait confiance dans ce travail, et bien sûr pour tous ces moments épiques passés en manip', aux quatre coins du globe ou du côté de Montbazin !

A David.A, merci, pour tes précieux conseils, ta disponibilité, ton investissement, ton énergie communicative et ton soutien à toute épreuve tout au long de cette thèse!

A l'équipe DEMAR, CAMIN, David, Paweł, Mélissa, Mourad, Annie, Jennifer, Thomas, Xin Yue, Alejandro, François, Marion, Anthony, Olivier, Ronan, Guillaume, Mitsuhiro...tous ceux qui ont marqué l'équipe en partageant l'esprit « DEMAR », ces moments forts au sein d'une équipe de recherche exceptionnelle et soudée, rythmée avec humanité, humilité, passion de la recherche (mais rigueur tout de même !).

A l'équipe FREEWHEELS, Jérôme, pour ton engagement hors norme, ta philosophie et ton optimisme contagieux, Charles, pour ton abondante humanité, pour ta passion du patient, ta disponibilité à la partager, et pour ton humour « fatal » à l'égal de ton humilité, Anne, pour ton travail engagé, ton implication assidue dans cette belle aventure, et pour m'avoir permis d'approfondir l'usage du vélo électrique dans les côtes Dijonnaises.

A Roger, pour ta rigueur, ton savoir et tes nombreuses astuces ingénieuses ô combien utiles, qui auront été d'une grande aide au long de cette thèse.

A Christian et Jérôme, pour m'avoir soutenu, fait confiance et m'avoir permis de découvrir le milieu tellement passionnant de la recherche clinique.

A François, pour ces longues heures de manip' qui n'auraient jamais été les mêmes sans tes croissants matinaux, ta bonne humeur et ton implication constante.

To Jessica and James, thank you for these wonderful moments spent in Stanford, for your visit in Menucourt, for sharing your enthusiastic vision of the clinical research with me and for your collaboration.

Aux TS1, parce que les TP de Physique de Mr Bonneau et les cours d'anglais de Mme Rius y sont certainement pour quelque chose,

Aux Shakes et aux Shuffle Canari, pour avoir rythmé de douces mélodies ces années musicales Montpelliéraines.

*« On réussit lorsqu'on prend pour point de départ le respect de la personne humaine ».*  
Abbé Glasberg, Fondateur du COS Divio Dijon

# Table of Contents

<b>Acknowledgements</b> .....	<b>5</b>
<b>Résumé</b> .....	<b>9</b>
<b>Nomenclature</b> .....	<b>15</b>
<b>1 Introduction</b> .....	<b>16</b>
<b>1.1 FES: an assistive solution in lower limbs sensorimotor deficiencies</b> .....	<b>18</b>
1.1.1 FES principle.....	18
1.1.2 FES: general usage and constraints in lower limb rehabilitation ...	21
1.1.3 FES : instrumentation and control .....	26
a. In theory .....	26
b. In practice .....	28
<b>1.2 Prerequisite: motion estimation in a clinical and ambulatory context</b>	<b>31</b>
<b>2 Observing and analyzing lower limb motions</b> .....	<b>34</b>
<b>2.1 Wearable sensors: inertial measurement unit based motion analysis</b>	<b>35</b>
2.1.1 Inertial sensors: basic principles.....	35
a. Prerequisites.....	35
b. Sensors .....	37
c. Known issues.....	39
d. Calibration .....	41
e. Basic filtering .....	43
2.1.2 Attitude and Heading Reference System (AHRS) sensor fusion techniques.....	45
a. State-of-the-art and explanations: in theory .....	45
b. Implementation and validation: in practice .....	49
2.1.3 From IMU generic principles to lower limbs motion analysis .....	50

<b>2.2</b>	<b>Healthy and Parkinsonian gait: a 2D approach.....</b>	<b>52</b>
2.2.1	2D stride length estimation.....	52
a.	Gait segmentation and ZVU introduction .....	53
b.	Calibration and Filtering .....	58
c.	2D stride length: algorithm .....	59
d.	2D stride length: experimental validation.....	60
e.	2D stride length: experimental results .....	62
2.2.2	Application : FOGC criterion computation for FOG detection in Parkinson's Disease deficiency .....	67
<b>2.3</b>	<b>Pathological gait: a 3D approach .....</b>	<b>71</b>
2.3.1	Attitude based 3D Trajectory.....	75
2.3.2	3D Goniometer .....	78
2.3.3	Application: stroke and cerebral palsy .....	78
<b>3</b>	<b>Controlling and acting on the motion.....</b>	<b>85</b>
3.1	Open-loop control in Parkinson's Disease: triggering sensitive electrical stimulation at heel off.....	86
3.1.1	Electrical Stimulation .....	88
3.1.2	IMU based triggering .....	90
3.1.3	Experimental protocol .....	92
3.1.4	Functional results and discussion.....	95
<b>3.2</b>	<b>Open-loop control in SCI subjects: FES cycling.....</b>	<b>103</b>
3.2.1	Participation to the Cybathlon: a longitudinal study .....	104
a.	Inclusion and exclusion criteria.....	105
b.	Pilot profile .....	105
c.	Tricycle description.....	106
d.	Electrical stimulation information .....	108
e.	Longitudinal study .....	110
f.	Performances and results .....	111
3.2.2	Towards IMU based closed-loop control.....	113
a.	Quantifying the FES system output .....	114
b.	Future closed-loop control solutions .....	119

<b>3.3</b>	<b>Closing the loop: online FES knee control in central neurological pathologies for stance phase improvement .....</b>	<b>122</b>
3.3.1	Experimental Protocol .....	125
a.	Evaluation criteria .....	126
b.	Balance training .....	128
c.	FES assisted gait protocol.....	128
3.3.2	Control modality .....	129
a.	Pre-stance event.....	129
b.	Knee control.....	133
3.3.3	Preliminary results and discussion.....	135
<b>4</b>	<b>Discussions – Conclusions .....</b>	<b>141</b>
<b>4.1</b>	<b>Clinical Protocol: design, follow-up and data processing... </b>	<b>142</b>
<b>4.2</b>	<b>An hardware and software architecture challenge .....</b>	<b>145</b>
4.2.1	Problematic .....	145
4.2.2	Iterations: toward a decentralized solution .....	145
4.2.3	A scalable solution.....	149
4.2.4	Software implementation .....	153
<b>4.3</b>	<b>Patient-centered solutions for an ambulatory use in a clinical context: a constrained challenge .....</b>	<b>156</b>
<b>4.4</b>	<b>Conclusion – Perspectives .....</b>	<b>158</b>
<b>5</b>	<b>References.....</b>	<b>160</b>

# Résumé

Suite à une lésion (ex: blessure médullaire, accident vasculaire cérébral) ou une maladie neurodégénérative (ex: maladie de Parkinson), le système nerveux central humain peut être sujet à de multiples déficiences sensori-motrices menant à des handicaps plus ou moins lourds au cours du temps.

Différentes technologies d'assistance et de suppléance peuvent être envisagées pour améliorer la condition des personnes atteintes de telles déficiences, en facilitant leur vie quotidienne et leur réadaptation.

Les progrès considérables dans le domaine des neurosciences et de l'ingénierie biomédicale ont donné lieu à de nombreuses avancées au cours des trente dernières années, aboutissant notamment à différentes solutions capables de restaurer ou d'améliorer les fonctions sensori-motrices basées sur la rééducation neurologique.

La rééducation neurologique a pour objectif d'utiliser les structures neuromusculaires préservées d'un individu avec une atteinte du système nerveux central afin de promouvoir la récupération de ses capacités physiques. Dans la majorité des cas de déficiences sensori-motrices d'origine neurologique, les sujets atteints présentent des difficultés à contrôler leur membres inférieurs, rendant alors difficile, par exemple, la réalisation d'une marche normale. Dans ce cas de figure, la rééducation neurologique de la marche pourrait être envisagée grâce à l'utilisation d'une stimulation électrique des muscles paralysés de la jambe, finement paramétrée pour délivrer au moment adéquat une série d'impulsions activant la contraction des muscles visés.

Cependant, en dépit d'importantes avancées technologiques, la rééducation neurologique appliquée au contrôle moteur (ex : préhension, déambulation,

verticalisation...) reste confinée à un usage sporadique comparée à d'autres domaines d'application de la stimulation tels que les implants cochléaires et les pacemakers, bénéficiant aujourd'hui d'une notoriété et d'un usage largement répandu. Malgré la présence d'une technologie performante et d'un savoir faire suffisant, comment expliquer le faible nombre de personnes atteintes de déficiences sensori-motrices bénéficiant aujourd'hui d'une telle assistance fonctionnelle ?

Une déficience sensori-motrice entraîne généralement un cycle de déconditionnement au cours duquel les variables psychologiques et physiques du sujet se dégradent. La plupart des technologies de rééducation neurologiques actuelles appliquées au contrôle moteur demandent un contrôle fin et une synchronisation précise pour être efficaces. Cependant elles se révèlent pour la plupart relativement complexes d'utilisation, demandant d'être opérées par un utilisateur averti et menant généralement à une surcharge technologique supplémentaire pour la personne déficiente. Ce constat met en exergue une probable explication au faible succès de l'utilisation de la stimulation électrique appliquée à la restauration d'une fonction motrice (alias la stimulation électrique fonctionnelle, SEF). Il paraît donc essentiel d'étudier de nouvelles solutions innovantes afin de promouvoir l'utilisabilité et l'accessibilité de cette technologie et permettre à un maximum de personnes atteintes de déficiences sensori-motrices d'améliorer leur qualité de vie quotidienne, tout en assurant un contrôle fin et adéquat de l'assistance apportée.

Motivé par ce paradoxe, ce travail de thèse repose sur l'ambition de proposer de nouvelles voies réalistes de solutions d'assistance basées sur la stimulation électrique fonctionnelle et l'utilisation de réseaux de capteurs embarqués face à plusieurs problématiques cliniques et technologiques visant à la rééducation neurologique des membres inférieurs.

Complexifiées par de multiples contraintes intrinsèques à l'étude de solutions orientées-patients (utilisabilité, fonctionnalité, accessibilité) dans un contexte ambulatoire et clinique, de nouvelles stratégies de commande et d'analyse du mouvement ont été étudiées et validées dans le cadre de différentes pathologies affectant le mouvement des membres inférieurs : l'accident vasculaire cérébral, la maladie de Parkinson et la paraplégie.

Reposant sur un réseau de capteurs génériques à bas coût embarqués sur la personne, la commande de la stimulation électrique fonctionnelle a demandé un travail initial important afin d'être capable d'observer et d'analyser le mouvement pathologique à assister en temps réel. La connaissance du mouvement en conditions ambulatoires est nécessaire pour développer un contrôle efficace et fin de la stimulation et du mouvement généré. Peu de technologies sont capables d'offrir une précision suffisante quant à l'évaluation du mouvement en ambulatoire, les habituels tapis de marche instrumentés et systèmes de capture de mouvement optiques étant inappropriés à ce cas d'usage. Pour ce faire, une technologie initialement utilisée dans l'aéronautique a été dérivée et embarquée sur le sujet porteur d'un handicap : les centrales inertielles. Basés sur cette technologie, plusieurs algorithmes ont été étudiés et mis au point pour l'observation et l'analyse du mouvement sain et pathologique et validés au cours de différents protocoles cliniques expérimentaux.

Fort de cette connaissance, différentes stratégies de commande en boucle ouverte ou fermée ont été développées et expérimentées comme solutions d'assistance chez des personnes atteintes d'une déficience sensori-motrice, en combinant l'analyse du mouvement à la stimulation électrique fonctionnelle (SEF) des membres inférieurs.

Mais qu'est-ce que la SEF ? La SEF est une technique de rééducation neurologique qui consiste à suppléer artificiellement la commande motrice lésée, normalement vectrice d'une contraction musculaire volontaire, par l'envoi d'impulsions électriques à proximité du nerf ou directement sur la plaque motrice du muscle visé. Pouvant être utilisée comme une alternative aux orthèses mécaniques classiques, la SEF peut donner lieu à différentes utilisations appliquées à la restauration du mouvement des membres inférieurs. Initialement développée pour corriger le syndrome du pied tombant (absence de dorsiflexion pendant la phase de balancement) chez le sujet hémiplegique, elle est aussi ponctuellement utilisée dans la restauration de la marche chez des blessés médullaires (stimulation multicanal) ou encore au travers d'activités de loisirs telle que l'aviron ou le cyclisme assistés par stimulation électrique des muscles sous-lésionnels (ex : quadriceps et ischio-jambiers pour la propulsion d'un vélo à trois roues).

Dans la quasi-totalité des stimulateurs commerciaux, le pilotage de la stimulation électrique est effectué en boucle ouverte ; un contacteur placé dans le talon de la chaussure ou un capteur sur le pédalier du vélo fournit l'information nécessaire au déclenchement et à l'arrêt de la stimulation. Si cette approche offre une certaine utilisabilité au quotidien, elle n'est pas adaptée à un contrôle individualisé et efficace de la stimulation et limite considérablement son champ d'application en ne considérant pas, en outre, une contrainte majeure liée à la SEF : la fatigue musculaire précoce induite. Les propriétés musculosquelettiques et leur responsivité à la stimulation ne peuvent être parfaitement modélisées au point de négliger la prise en compte réelle du mouvement généré. Dans ce contexte, une connaissance précise du mouvement (ex : longueur et hauteur de foulée, angle de dorsiflexion, angle du genou, pourcentage du cycle de marche...) peut servir plusieurs buts :

- la définition d'un événement précis de stimulation, fonction du mouvement volontaire,
- une rétro-action pour le contrôle en boucle fermée,
- un outil objectif d'évaluation pour le clinicien.

Mais comment calculer ce mouvement à partir de capteurs embarqués ? Une centrale inertielle est généralement composée de trois capteurs (accéléromètre, gyromètre, magnétomètre) mesurant des grandeurs physiques. Le traitement et l'intégration des valeurs brutes mesurées au cours du temps permet de reconstruire une position, une trajectoire ou une orientation, et ce nécessairement en trois dimensions pour certaines pathologies. En combinant deux capteurs il est possible de calculer alors un angle articulaire entre deux segments. Ces principes de base sont cependant limités par l'apparition d'erreurs intrinsèques à l'intégration numérique, à la conception et l'environnement du capteur, à la calibration, à la fréquence d'échantillonnage ou à l'algorithme utilisé. Des algorithmes de fusion de capteurs permettent une plus grande robustesse de la mesure au cours du temps mais nécessitent pour la plupart une puissance de calcul importante.

A travers cette thèse, le travail en amont réalisé à partir de centrales inertielles génériques a permis de valider leur capacité à évaluer : une marche saine et pathologique (sujets Parkinsoniens, sujets hémiplegiques), un angle de dorsiflexion (sujets hémiplegiques), un angle de genou (sujets hémiplegiques et paraplégique) ou encore à détecter l'apparition de troubles locomoteurs, tels que le « freezing of gait » chez le sujet Parkinsonien (tremblements entraînant un blocage de la marche menant parfois à la chute), tout en garantissant une utilisabilité optimale : minimum de paramétrage et de capteurs, calibration facilitée, robustesse et tolérance d'utilisation, etc...

Basées sur ce travail, plusieurs stratégies de stimulation en boucle ouverte et fermée des membres inférieurs ont été développées et expérimentées en collaboration avec des équipes médicales :

- déclenchement d'un indiçage somatosensoriel utilisant une centrale inertielle localisée sur le pied de sujets atteints de la maladie de Parkinson pour délivrer une stimulation électrique sensitive de la voûte plantaire au

décollage du talon (diminution de l'occurrence du freezing et amélioration de la vitesse de marche).

- développement et étude d'une solution de pédalage assisté par stimulation électrique fonctionnelle chez un blessé médullaire (participation au Cybathlon, Zurich).
- contrôle embarqué en boucle fermée du genou de sujets atteints d'hémiplégie pour l'amélioration du report d'appui.

Une solution embarquée générique, évolutive et adaptable à différentes applications basées sur la SEF et le contrôle moteur a été réalisée via le développement d'une architecture matérielle et logicielle orientée-patient.

Indépendamment de résultats cliniques encourageants, la réussite scientifique et technique des stratégies d'assistance des membres inférieurs étudiées au cours de ce travail de thèse atteste de la faisabilité et de l'importance de développer des solutions innovantes orientées-patients. La mise au point de solutions de rééducation neurologique performantes et accessibles reste cependant particulièrement difficile dans le contexte actuel, malgré un réel besoin exprimé à la fois par la personne en situation de déficience et les équipes médicales. Les progrès et avancées technologiques liées à l'ingénierie des neuroprothèses implantées laisse présager une future démocratisation de la rééducation neurologique par des dispositifs implantés. L'usage de la SEF externe comme une étape intermédiaire vers un dispositif de neurostimulation implantable pourrait s'avérer alors particulièrement utile à la compréhension préalable du contrôle moteur et de son intégration technologique. La combinaison d'actionneurs mécaniques (ex : exosquelettes) et de capteurs embarqués (ex : centrales inertielles, électromyographe,...) à de la stimulation électrique fonctionnelle pourraient également ouvrir de nouvelles perspectives d'utilisation vers des neuroprothèses hybrides.

# Nomenclature

AHRS: Attitude and Heading Reference System  
ASIA: American Spinal Injury Association  
BAN: Body Area Network  
BMI: Body Mass Index  
BMD: Bone Mineral Density  
CNS: Central Nervous Disorder  
DXA: Dual energy X-ray Absorptiometry  
E-FAP: Emory Functional Ambulation Profile  
EKF: Extended Kalman Filter  
EMG: Electromyography  
FES: Functional Electrical Stimulation  
FOG: Freezing Of Gait  
FNS: Functional Neuromuscular Stimulation  
FTP: File Transfer Protocol  
IMU: Inertial Measurement Unit  
I2C: Inter-Integrated Circuit  
MEMS: Micro Electro Mechanical Systems  
NMES: Neuromuscular Electrical Stimulation  
OMCS: Optical Motion Capture System  
PCI: Physiological Cost Index  
PD: Parkinson's Disease  
SCI: Spinal Cord Injuries / Injured  
SSH: Secure Shell  
UAV: Unmanned Aerial Vehicles  
WBAN: Wireless Body Area Network  
ZVU: Zero Velocity Update

# 1 Introduction

The human central nervous system (CNS) can be subject to multiple dysfunctions. Potentially due to physical lesions (e.g.: spinal cord injuries, hemorrhagic or ischemic stroke) or to neurodegenerative disorders (e.g.: Parkinson's disease), these deficiencies often result in major functional impairments throughout the years, that make even the simplest tasks impossible to complete.

Various technological assistances could be provided to people suffering from these kinds of sensorimotor deficiencies, in order to improve their daily life condition, or to help enhancing rehabilitation process.

Rehabilitation engineering and neuroscience-based research have jointly received much attention over the last forty years. A lot has been done to improve health and to restore functions by studying pioneering approaches based on neurorehabilitation. Originally developed for stroke subjects, neurorehabilitation aims at using preserved neuro-muscular structures in an individual with motor disabilities, to promote recovery of functions following the lesion or disease. For instance, neurologically impaired subjects have often difficulties to perform lower limb movements, thereby hardly eliciting natural walking. In this case, neurorehabilitation of walking could be achieved by integrating electrical stimulation of the leg muscles, finely timed to drive the appropriate muscular group.

In contrast, despite a dramatic technological development, the field of motor control and neurorehabilitation technology for humans with sensorimotor disabilities has been subject to a very slow acceptance and remains within a sporadic use compared to other medical devices successes also based on electrical stimulation, such as cochlear implants or heart pacemakers. Why is this field of application developing slowly in the presence of both technology and know-how?

---

A sensorimotor disability often triggers a cycle of de-conditioning in which psychological and physical functioning deteriorate. Most of the existing motor neurorehabilitation technologies may turn out to be relatively complex for the users, requiring skilled experts and a technological overload for the subject. This likely answer highlights the importance of developing user-friendly and accessible neurorehabilitation tools, not only restricted to a clinical use, to promote their usability and allow humans with disabilities to enjoy their life again.

Challenged by this paradox, the ambition of this thesis has been motivated by investigating assistance modalities, keeping in mind the intrinsic constraints associated to a patient-centered approach: to promote functionality, ease of use, genericity and affordability. Using functional electrical stimulation (FES) as a neurorehabilitation of lower limb movements, several approaches and algorithms were studied through this work and experimentally validated in various clinical and pathological contexts, fitting the constant and recurring constraints of a patient-centered solution while providing an accurate control of motion.

To meet this requirement, the choice was made to use wearable sensors in order to assess pathological motions and be able to design a specific command.

While the first part of this document introduces the general context, the second chapter presents all the different aspects and investigated algorithms needed to provide a robust and accurate lower limb pathological motion assessment based on wearable sensors. Using this information, the third chapter addresses multiple neurorehabilitation approaches based on wearable sensors to control motor functions in a clinical and ambulatory context. The final chapter highlights the different difficulties encountered to go from theory to clinical protocols, concludes and opens the way to a broad prospective of the field for future research.

## 1.1 FES: an assistive solution in lower limbs sensorimotor deficiencies

After central nervous injuries, functional electrical stimulation (FES) of paralyzed muscles enables to assist individuals in executing functional movement. Also called neuromuscular electrical stimulation (NMES) or functional neuromuscular stimulation (FNS) in literature, the concept aims to either activate moto neurons to elicit a motor response or to activate reflex pathways by stimulating sensory nerve fibers.

### 1.1.1 FES principle

The ultimate goal of using FES on a paralyzed, yet preserved, muscle is to be able to supplement the deficient CNS command by imitating as close as possible the “natural” activation occurring in the absence of lesion or disorder.

The CNS command is coded and transmitted as a series of electrical pulses called action potentials, which represent a brief change in cell electric potential. The more action potentials occur in a unit of time, the higher the intensity of the transmitted signal.

In FES systems, the action potentials are artificially elicited by generating sufficient electrical charges in the vicinity of the nerve. This localized depolarization of the nerve cells result in the start of action potentials toward both ends of the axon. Action potentials that propagate towards the muscle (orthodromic propagation) until reaching the neuromuscular junction cause muscle fibers to contract and generate muscle force.

The electrical charges can be delivered through the skin via surface electrodes (external stimulation) or under the skin directly at the muscle or nerve level (implanted stimulation) via intramuscular, cuff or intrafascicular neural electrodes. Throughout this thesis, only external stimulation is addressed and referred to as FES.

---

The trains of electrical pulses delivered via the electrodes are usually characterized by multiple parameters expressed as (Figure 1): the frequency  $f$  (Hz), the amplitude  $I$  (generally in mA or in V), and the width of the pulse  $PW$  (standing for pulse width, generally expressed in  $\mu s$ ). Modulating either the amplitude or the pulse width enables to control the number of recruited motor units and thus the force generated.

By modulating the stimulation frequency, a summation mechanism over time also affects the force output. A sufficient stimulation firing rate causes a sustained contraction, also called tetanic contraction, from which the muscular mechanical response becomes smooth and homogeneous. Needed to avoid muscle tremors, this tetanic contraction however limits the functionality of the movement and partly contributes to a major limitation of FES: muscular fatigue.

Artificially induced contraction early fatigues skeletal muscles compared to volitional contraction. Rapid fatigue during FES results from a recruitment order which, contrary to volitional contraction, firstly activates the most fatigable muscular fibers (type II, rapid fibers), always in the same order in regards to electrode positioning. The fatigability can be limited by, for instance, choosing the lowest but minimum stimulation needed to obtain a sustained contraction: between 18 and 25 Hz for the lower limbs [1]. Meanwhile, rapid fatigue can be worsened by physiological changes intrinsic to a CNS lesion. For instance, in spinal cord injured (SCI) individuals, muscular atrophy tends to naturally convert type I fibers (slow fibers) into type II fibers [1].

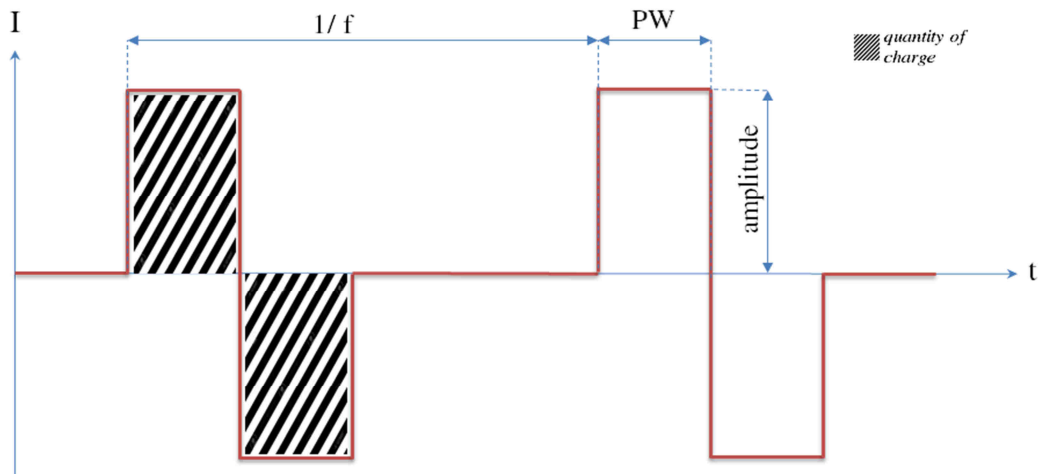


Figure 1. Illustration of a charge-balanced biphasic pulse. FES delivers trains of electrical pulses to mimic the natural flow of excitation generated by the CNS when non-impaired. Pulses are defined by their frequency ( $f$ ), their amplitude ( $I$ ) and their width ( $PW$ ).

Two different configurations can be used to deliver FES in multi-channel stimulation: the monopolar or bipolar configuration. In the first case, active electrodes are positioned close to the muscles to be stimulated while a single common electrode is positioned somewhere along the neural pathway to the CNS, at a certain distance of the active electrodes. In the second case, the bipolar configuration consists in using two electrodes to close the electrical circuit nearby the nerve. The monopolar configuration requires a lowered number of electrodes and can be useful in case of a high number of muscles needs to be stimulated, while the bipolar configuration enables a better stimulation accuracy but requires more electrodes. Most of the current commercially available stimulators use a bipolar configuration.

The pulse waveform is generally rectangular or if not, nonrectangular but with a rise time sufficiently fast to open the nerve membrane channels.

Most of the FES stimulators modulate the number of recruited fibers by regulating the quantity of charge delivered, which equals to the integral of amplitude by the pulse width (Figure 1). The waveform can be monophasic or biphasic (such as illustrated in Figure 1). Most of the stimulators use biphasic

---

pulses. Among many advantages, the stimulation is more comfortable and the potential risk to damage the tissues is lessened by balancing the electrical charges going through the skin (Figure 1).

### 1.1.2 FES: general usage and constraints in lower limb rehabilitation

FES can be used in individuals with stable neurologic lesions and where the recovery process reached a plateau. It is considered as an effective therapeutic tool to develop or reactivate injured voluntary functions [2] associated to paralyzed yet innervated muscles of the corresponding intact Alpha motoneurons.

Neuromuscular stimulation can be used as an alternative to orthoses for restoring gait. By activating paralyzed muscles, FES is able to supplement the lost motor command and favor motor learning, thereby limiting neuro-orthopedic consequences associated to the lesion while enhancing rehabilitation process. Multiple stimulation strategies have been investigated over the past years to assist or restore gait. Liberson et al. [3] were the first to introduce the stimulation of the peroneal nerve in 1961 (original patent) to correct the foot drop syndrome (absence of voluntary foot dorsiflexion during swing phase) in post stroke individuals. The first demonstrated application took place 8 years later with an experimental study performed by Gracanic et al. [4]. However, due to weak paretic limbs, only stimulating the peroneal nerve in acute strokes and SC injuries turned out to be not efficient enough to enable gait [5]. The stimulation of a muscular group targeting a specific joint leads to an isolated action, such as knee flexion or extension. Using this property, some devices have been investigated to restore gait in short distances (limited by the quadriceps fatigue) using multiple stimulation channels [5]. The use of a multi-channel stimulator for helping during stance and swing phase was firstly investigated in 1978 by Stanic et al [6]. Postans et al. [7] presented a study using two stimulation channels to stimulate the quadriceps in stance phase and the peroneal nerve in swing phase in SCI individuals. Stimulation duration was preset according to the duration of swing and stance phases measured before with an instrumented mat. Yan et al. [8] used

a multi-channel stimulation delivered on the paretic limb and were able to stimulate via two stimulators both the quadriceps, hamstrings, tibialis anterior and medial gastrocnemius (Figure 2) in bedridden post stroke individuals. The activation sequence was close to the timing of a healthy walk pattern. Results showed an increase in torque produced by the ankle and a decrease in muscle spasticity (i.e. unusual stiffness of muscles). Popovic et al. [9] proposed a similar multichannel stimulation protocol for increasing walking range in post stroke subjects. Three stimulation channels were used to stimulate quadriceps, gastrocnemius and tibialis anterior in order to improve stance phase, to obtain a better push at the end of the stance phase, a better stability at initial contact and a higher foot clearance during swing phase.

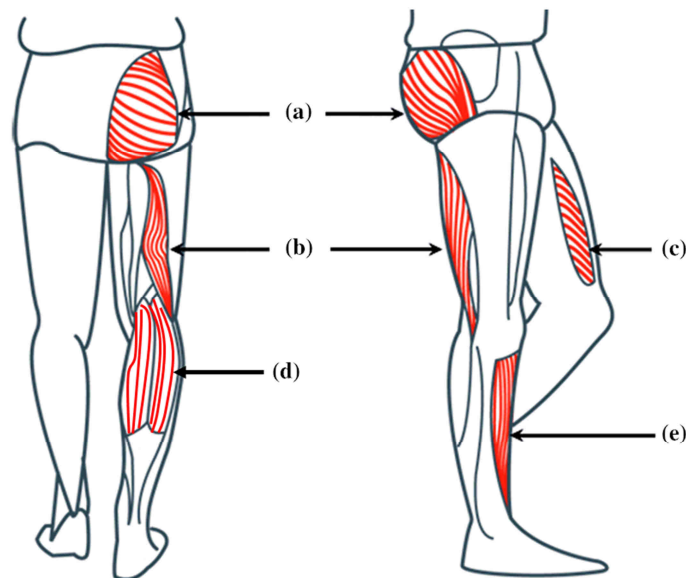


Figure 2. Illustration of muscles able to be stimulated in FES-based lower limb rehabilitation. (a) gluteal muscle, (b) hamstrings (biceps femoris), (c) quadriceps (vastus lateralis), (d) gastrocnemius, and (e) tibialis anterior. (source: interstices.info)

Most of the few FES systems commercially available for lower limb rehabilitation have been designed for restoring walking by only stimulating dorsiflexors. They are mainly used in clinical rehabilitation protocols in post-stroke individuals.

One of the simplest stimulator still in use today is the Odstock Foot-drop Stimulator (ODFS, the Department of Medical Physics and Biomedical Engineering, Salisbury District Hospital, Salisbury, Wiltshire, UK). It is a single channel foot-drop stimulator providing electrical stimulation to the tibialis anterior muscle or to the common peroneal nerve (Figure 3a). The stimulation is triggered on the affected side using a switch located inside the shoe. The pulses are sent after the heel rises from the ground until heel strike. The switch can also be placed under the toes of the contralateral limb if heel contact is inconsistent. The rise and fall of the stimulation pattern can be adjusted to obtain a smooth contraction and prevent a premature ending of dorsiflexion.

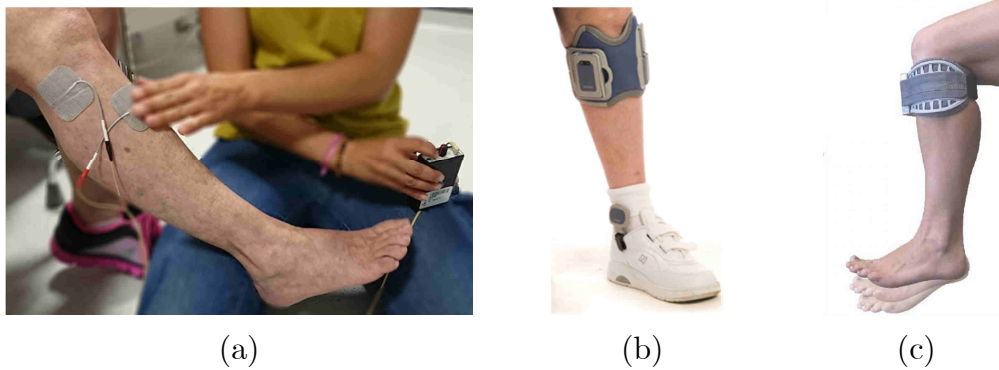


Figure 3. Stimulation of the tibialis anterior muscle or of the common peroneal nerve to correct the foot-drop syndrome using (a) an Odstock stimulator or (b) a NESS L300 (source: [www.bioness.com](http://www.bioness.com)) or (c) a WalkAid (source [www.walkaide.com](http://www.walkaide.com))

The NESS L300<sup>©</sup> (Bioness, Santa Clarita, USA) relies on the same triggering modality, except that the heel switch is wireless (Figure 3b). To enhance a user-friendly approach, the stimulator and the electrodes are self-contained inside a brace which is placed around the knee, for enabling the user to easily localize the stimulation sites. The dorsiflexors stimulation can be combined with hamstrings or quadriceps stimulation by adding a second brace around the thigh (NESS L300 Plus<sup>©</sup>).

Another self-contained FES system (Walk-Aid<sup>©</sup>, Innovative Neurotronic, USA, Figure 3c) was adapted from Dai et al. study [10] using a magneto resistive

---

tilt sensor to determine gait phases. The stimulus is turned on when the tilt signal rises above a threshold corresponding to a forward leg position. It is then turned off if the tilt falls below a second level or if the total stimulus duration exceeds a preset maximum period. Despite offering several important advantages over traditional stimulators controlled by foot switches, the stimulator has been commercialized but the distribution failed to make it a market success [2]. Based on a broadly similar approach, a new device (NESS L300 GO<sup>©</sup>) has been recently launched on the market. The stimulation can be adjusted between a preset percentage of the gait cycle time (e.g. stimulation turned on at  $t=30\%$  of the mean duration of the last strides) estimated using a 3-axis gyroscope and accelerometer embedded in the stimulator.

Lower limb stimulation can also elicit motor responses by stimulating sensory nerve fibers. Multiple studies and technological developments investigated the use of a different stimulation paradigm, the withdrawal reflex, to induce knee and hip flexion in SCI and post-stroke gait [11], [12]. Based on a nociceptive stimulus (i.e. slightly evoking pain), the method consists in stimulating the arch of the foot thereby eliciting a spinal reflex of the autonomic nervous system to this perceived threat. Combined with a quadriceps stimulation in stance phase, this specific stimulation pattern (four trains of five electrical pulses, described in [13]) enables to facilitate the initiation and to improve knee and hip flexion during swing phase. It is commonly triggered using a foot switch similar to the other FES drop foot systems. However, the effectiveness of the stimulation highly depends on the stimulation site. Some subjects reported too much discomfort and pain. Nociceptive stimulation also sometimes results in activation of the intrinsic foot muscles, thereby causing an unwanted flexion of the toes [14].

In addition to restore gait, FES stimulation of lower limb in subjects with CNS disorders has also been investigated through different studies and commercialized devices as a recreational and sport activity, included in multiple rehabilitation programs.

In SCI subjects, a clinical use of FES to stimulate lower limb muscles has proven to decrease cardiovascular and other risks related to a prolonged sitting posture (e.g. the occurrence of pressure sores, atrophy...) by maintaining a muscular activity [15], [16]. FES assisted cycling and rowing have demonstrated to be particularly efficient to prevent psychological and physical functions deterioration by stimulating thigh and glutei muscles to propel a bike or a rowing machine [17]. While increasing self-esteem and wellness, FES-induced cycling and rowing positively affect the cardiopulmonary system [18], [19], bone mineral density [20] and muscle strength [21], [22]. In order to activate the largest possible muscle mass, the combination of FES-assisted lower-extremity exercise with upper-extremity exercise enhances training effects and cardiovascular fitness, such as FES rowing or FES cycling combined with hand propelling [23].

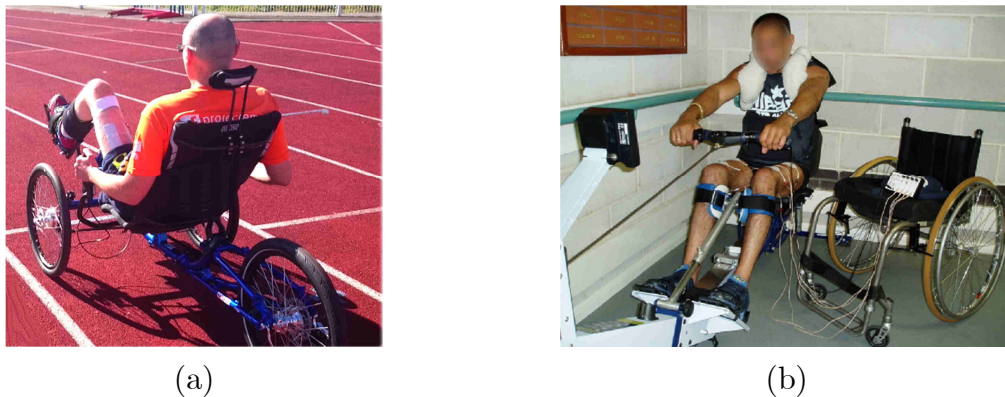


Figure 4. FES assisted cycling and rowing have demonstrated to be particularly efficient to prevent psychological and physical functions deterioration by stimulating thigh and glutei muscles to propel a bike (a) or a rowing machine (b). (source: freewheels.inria.fr & fesrowing.com)

Literature on FES cycling is particularly abundant and reflects a growing interest over the past thirty years [24]. In most of these studies, FES-cycling is achieved by means of a fixed ergocycle (e.g. RT300, Restorative Therapies, Baltimore, USA). However, multiple studies demonstrated that adding a recreational dimension to the exercise could improve the attractiveness of FES-assisted exercises and increase the psychological wellness of the user. This could be achieved using instrumented mobile tricycles. Few affordable systems are commercially available and specifically designed for this use. One of the most

widespread device is the BerkelBike<sup>©</sup> trike (Sint-Michielsgestel, Netherlands). Designed for an outdoor use, the stimulation is alternatively sent to quadriceps, hamstrings and glutei depending on the crank angle. The user can also propel the bike with the hands to decrease the effort on the lower limbs.

This state-of-the-art highlights the wide heterogeneity of the different FES systems able to assist or enhance daily life in people with CNS disorders by stimulating their lower limbs. The various applications and associated results also identify the complexity and inherent constraints of such FES solutions and the need to provide a specific instrumentation and individualized control.

The following sections give a particular focus on how to artificially control motion via FES systems and introduce the multiple constraints to face when put into practice.

### 1.1.3 FES : instrumentation and control

#### a. In theory

To restore and control motor functions following a CNS injury or disorder, FES systems are generally made up of multiple associated components needed for the stimulator to be able to: receive adequate command signals, generate the pulses and deliver them to the stimulation target via the electrodes [2] (Figure 5).

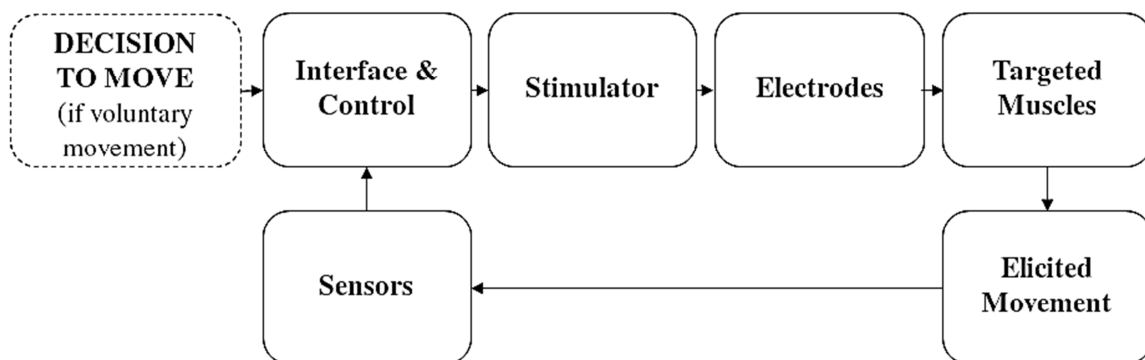


Figure 5. Diagram showing the global instrumentation of a FES system used to restore motor functions.

Generally speaking, the control of the musculoskeletal system can be directly compared to a control applied in automation, thereby describing the system with state variables and cost functions from control engineering: joint angles, angular velocities, acceleration, power produced, torque and forces...

The control of one to multiple states can be achieved via actuators (i.e. the muscles) by applying an appropriate stimulation generated according to the controller's command depending on a setpoint (trajectory, joint angle, muscular force...). Several control strategies requiring different complexity levels can be considered depending on the assistive aid to provide.

An open-loop stimulation consists in applying pre-computed stimulation patterns without taking into account potential errors between the desired setpoint and the actual setpoint obtained by stimulating the muscles. An open-loop controller only delivers command signals to trigger the stimulation sequences.

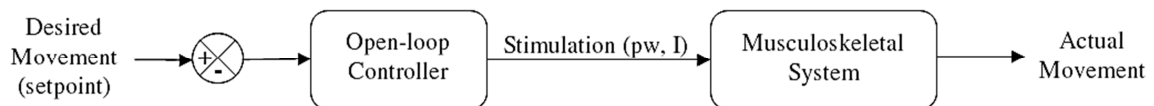


Figure 6. Illustration of an open-loop stimulation control strategy.

The use of an open-loop strategy to control lower limb movements may seem inadequate, as even in the absence of disturbances, musculoskeletal properties and their responsivity to stimulation cannot be perfectly modeled and pre-computed. This control strategy is however used to trigger the stimulation in almost all commercial FES applications introduced in the following sections.

To adapt the stimulation taking into account possible disturbances and errors due to musculoskeletal properties, it is necessary to use the actual output of the system (i.e. actual motion) as a feedback, closing the loop by feeding an error-driven FES controller:

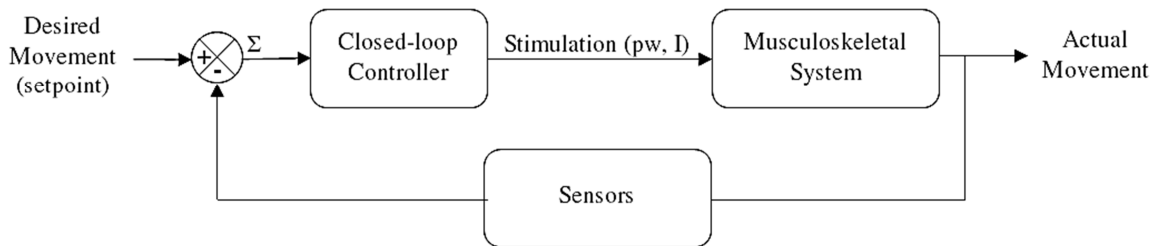


Figure 7. Illustration of a closed-loop stimulation control strategy.

In practice, numerous additional parameters and constraints (e.g. muscular fatigue, falls risks, technological and physical latencies...) have to be taken into account and make particularly complex the control of the lower limbs based on an FES system.

### b. In practice

The different applications introduced in section 1.1.2 reflect the variety of sensors and control strategies used for restoring lower limb motion. Meanwhile, if the control and instrumentation of FES systems seems in theory relatively simple, in practice the design of a FES solution has to face numerous constraints to maximize efficiency and usability of the proposed approaches while ensuring safety.

Section 1.1.2 introduced different FES systems to restore gait in SCI and post-stroke individuals. In the multichannel system designed by Popovic et al. [9], the stimulation timing was copied from muscle activation phases recorded from able bodied individuals walking at a low pace. Two major issues arose from this study:

- the activation pattern translated from healthy subjects did not match to the voluntary muscular activation of post stroke subjects.
- the post stroke participants adapted their muscular activation pattern if the stimulation was not triggered in phase with the voluntary motion.

In Kojovic et al. study [25], authors compared the recovery caused by functional electrical therapy based on predefined timing of stimulation used in Popovic et al. [9] with a sensor-driven therapy in post-stroke gait rehabilitation. They used machine learning from EMG, accelerometric and force sensing resistor

---

data recorded on the non-paretic leg to define IF-THEN rules to trigger the stimulation on the paretic side. The results suggested greater benefits from the new stimulation paradigm compared to predefined timing of stimulation. Their automatic control provided timing of muscle activation synchronized with required voluntary movements, while the predefined stimulation timings in Popovic et al. [9] were not synchronized with voluntary efforts.

In the context of the foot-drop syndrome, the Walk-Aid system or the L300 GO aimed at increasing the usability and reliability of the foot-drop stimulator by adding a magnetoresistive tilt sensor or an inertial sensor for computing gait phases and triggering the stimulation at an appropriate timing. It has the advantages of eliminating the footswitch, not fully reliable because of false triggering and malfunctioning [2] and the external wiring from the sensor to the stimulator. However the control modality requires to accurately preset several thresholds and could present errors in detecting step intention in subjects with limited swinging movements [10].

The section 1.1.2 also introduced the use of lower limb FES systems for cycling and rowing. These modalities also lead to numerous studies investigating control strategies. In Wheeler et al. FES rowing study [26], the stimulation of the quadriceps was manually synchronized with voluntary rowing movements of the upper limbs via a button pressed by the user when the maximum knee flexion was reached. FES rowing studies investigated the ability to automatically control the electrical stimulation of the paralyzed leg muscles using finite state machine controllers to improve FES efficiency and usability of the device [27], [28].

Regarding FES cycling, the BerkelBike trike was designed to be used by an inexperienced user. The stimulation is sent to the different muscles depending on the crank angle and a preset stimulation pattern. However, manually designing the stimulation pattern and setting the stimulation parameters for each muscular group require the assistance of a skilled user. Multiple studies investigated the possibility to use different sensors inputs (EMG [29], inertial sensors [30], oxygen measurement [31], pedal forces [32]...) to automatically design cycling stimulation

---

patterns and enhance usability. The BerkelBike device also makes possible to use the hands to help the legs to propel the bike in case of fatigue. However the level of stimulation intensity can only be manually adjusted by the bike driver. Numerous control strategies (neural network [33], fuzzy logic [34]) have been investigated to improve the maximum covered distance or force in FES cycling and complex FES controllers were studied but did not give the best functional results compared to simple ones [35]. Other works tried to improve the control strategy by changing the stimulation frequency [36], the recruited muscles [37], the cadence or the mechanical design [38], [39].

All of these illustrations reflect the global complexity and accuracy of control needed to be able to obtain the best efficiency of a neuromuscular electrical stimulation system in lower limb motion rehabilitation. On the contrary, it is essential to keep in mind that most of these applications are intended for a clinical or personal use. The potential users are either the medical practitioners or the patients themselves. If the practitioner can be trained, a patient with sensorimotor disorders may already be subject to a psychological distress and physical constraints that cannot be compatible with numerous complex solutions from literature. How to improve control strategies and stimulation efficiency while ensuring a maximum ease of use, adaptability and tailored solutions for the user?

## 1.2 Prerequisite: motion estimation in a clinical and ambulatory context

The previous sections identify the need to instrument FES systems with sensors, in order to determine the actual state of the system and adapt the stimulation. An accurate knowledge of the elicited motion is essential and can serve multiple purposes:

- an event to trigger the stimulation (e.g. depending on the voluntary motion)
- a feedback for closed-loop control of lower limb movements
- an objective assessment tool for the practitioner to follow the effects of the neurorehabilitation program (e.g. monitoring stride length, gait speed, max. joint angles...)

But how to obtain the needed knowledge of the actual movement with the minimum number of embedded sensors and in the particular ambulatory context of lower limb rehabilitation?

Being able to observe and assess a pathological motion is a recurrent need for practitioners. After a stroke, individuals are often hampered by walking difficulties [40]. Step-by-step kinematic and spatio-temporal parameters have been shown to be clinically relevant markers of impaired walking performances in individuals with CNS disorders [41]. If the motion's knowledge is essential, not every available system are able to provide the same accuracy, ease of use and affordability. Moreover, mobility of the system plays a key role in the ability to assess the motion in ecological conditions (i.e. outside-of-the-lab motion analysis).

The use of tape measures and manual goniometers can provide information in a 2D plane and static conditions. In the context of gait analysis, the use of instrumented mats such as the GAITRite<sup>®</sup> (spatial accuracy  $\pm 0.0127$  m, CIR Systems, Inc., Havertown, PA, USA) is considered as a reference system and has been widely used and validated in literature [42], [43] to provide 2D spatio-temporal information. Such instrumented mats can also be combined with force

---

platforms (e.g. AMTI Accugait<sup>©</sup>, Watertown USA or Zebris FDM<sup>©</sup>, Isny Germany) or force insoles to additionally give pressure distribution measurements. Few systems enable the clinician to gain information about dynamic three-dimensional movements. For this purpose, most of the motion analysis laboratories are equipped with optical motion capture systems. These video-based optoelectronic systems use retro-reflective markers visualized by multiple video cameras and are considered as the gold standard for 3D motion analysis (e.g. the Vicon<sup>©</sup> system, Oxford UK, with a global accuracy of 0.15mm [44]).

Meanwhile, none of these mentioned systems are able to meet the needs of an affordable, mobile, accurate and ambulatory device to be used in a FES system. This brings out a common need of accurately quantifying kinematics in CNS disorders, whether for assessing gait performance or for artificially controlling motion. Using low-cost wearable technologies may be considered as a potential alternative.

Initially designed for aircraft navigation, wearable sensors have been increasingly explored over the past few years as a mobile gait and motion analysis solution [45]. Numerous authors have suggested methods involving Inertial Measurement Units (IMU) sensors in order to estimate gait temporal or spatio-temporal parameters [46] as well as to compute joint angles during walking [47]. Literature has also reflected the growing interest in using such sensors in FES systems. Used in upper limbs for quantifying tremors in Parkinson's Disease and calibrating Deep Brain Stimulation (DBS) systems [48], this technology has been also investigated to coordinate upper and lower body during FES-assisted transfers in SCI individuals [49]. In Wiesener et al. [30], IMUs were used to detect flexion and extension of the legs to control the stimulation in FES cycling. Combined with FES, IMUs have been the most widely used for restoring gait in post-stroke individuals. In Azevedo et al. [50], an IMU was placed on the unaffected shank and was used to estimate a gait cycle index in order to later trigger the stimulation of the common peroneal nerve at a specific timing. In

---

Maleseciv et al. [51], a foot mounted IMU was used to determine the optimal stimulation site depending on the foot motion via a multipad electrode in drop-foot syndrome rehabilitation. In Williamson et al. works [52], [53], IMUs were investigated to detect gait events and monitor joint angles to be later used to real time control a lower limb FES system.

Few studies investigated the use of IMUs to feed an FES controller or to assess motion in a clinical context taking into account all the specific constraints of a patient-centered solution:

- maximum functionality and minimum technological overload: lowest number of sensors, ease of use, minimum of tuning, simple calibration...
- affordability and genericity: low-cost sensors, algorithms adapted to any kind of IMUs and to a wide range of pathologies.

This thesis aims to propose new FES rehabilitation approaches with the objective of elaborating patient-centered solutions using wearable sensors. The following chapter presents several preliminary investigated methods in order to assess motion using IMUs, while respecting these initial constraints and aims.

---

## 2 Observing and analyzing lower limb motions

The following sections introduce various prerequisites and notions in order to understand the different algorithms and approaches related to inertial sensors manipulation. How to correctly represent 3D orientations in the context of human motion analysis? What is concretely an inertial sensor? What are the different associated issues and how to correct them?

*The results presented in this chapter have been published in the following papers: [54]–[62]*

## 2.1 Wearable sensors: inertial measurement unit based motion analysis

### 2.1.1 Inertial sensors: basic principles

#### a. Prerequisites

Assessing human motion is commonly done using techniques of rigid body dynamics. A "rigid body" is usually defined as a body with volume and mass which has the specificity of having a solid and inelastic shape that cannot be changed. Using this notion for human motion analysis implies the important assumption that body segments can be modeled as rigid bodies.

To represent rigid body orientations, it is necessary to conventionally define a coordinate system attached to an inertial frame and express the rotations relative to these coordinates. A commonly used frame is the so-called 'Earth' frame, or "North-East-Down" (NED) frame, where the origin is located on the Earth surface,  $x$  pointing to the local north,  $y$  to the east and  $z$  downwards. The "Earth" frame constituting a "global" frame, it is also necessary for each rigid body to define a "local" frame, also called "body fixed" frame, related to the coordinate system attached to the rigid body. The description of the orientation of a rigid body expresses the link between these two coordinates systems, the "global" and the "local" frames.

Three methods are generally used to represent rigid body rotations with respect to a coordinate system: rotation matrices, Euler angles and quaternions.

Euler angles refer to a sequence of rotations around the axes of a coordinate system following a predefined order (e.g. z-y-x. x-y-z) The axes may be orthogonally body-fixed, earth-fixed or gimbal axes.

Commonly used in aircraft navigation, the rotations are named under the following convention: a rotation around the "north" axis is called "roll" or "bank" angle, around "east" axis, "pitch" or "attitude" angle and a rotation around "down" axis is denoted "yaw" or "heading" angle.

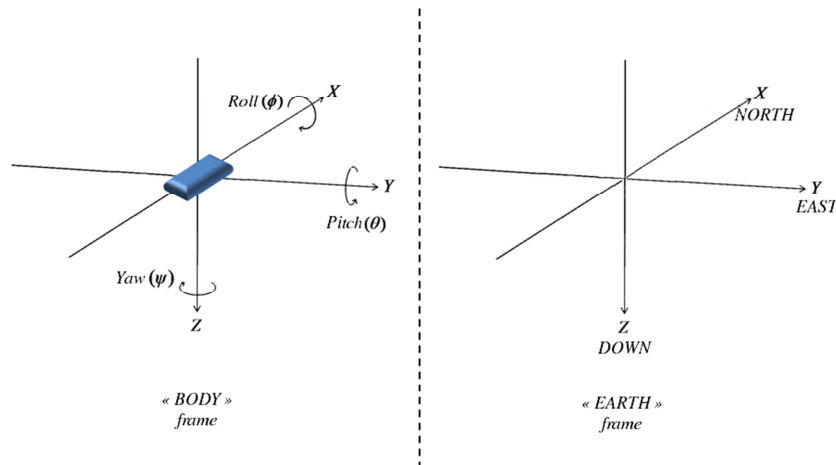


Figure 8. Euler angles and axes expressing “body” and “Earth” frames used to represent rigid body orientations.

The use of Euler angles to internally represent orientation makes however possible the occurrence of singularities in some orientations. Indeed, when a rigid body points straight up or down (e.g. pitch angle =  $\pm 90^\circ$ ), roll and yaw gimbal axes become collinear. Therefore, in this case neither roll or yaw angles are uniquely defined. This well-known singularity is called “gimbal lock”, corresponding to the loss of one degree of freedom. Although it may not be an issue when dealing with 3D rotations, in the different approaches presented in this thesis, it could have been a serious limitation when tracking lower limb movements [63], [64].

The use of rotation matrices results in a high computational cost and leads to an heavy memory usage [65].

Consequently, in order to be able to track any orientation without singularities and to shorten calculation time compared to the use of rotation matrices, the choice has been made to mainly deal with quaternion representations.

Throughout this document, the quaternion notation  $q$  is used as defined in [66] as four scalar numbers, one real dimension  $w$  and an imaginary (or also called vector) part  $(x_i, y_j, z_k)$ :

$$q = (w, x_i, y_j, z_k) \quad (1)$$

Quaternion representation is particularly efficient in the context of rigid body dynamics as it allows the use of numerous inherent properties.

For instance, let us defined the norm  $N$  of a quaternion:

$$N(q) = \sqrt{w^2 + x^2 + y^2 + z^2} \quad (2)$$

A quaternion with a unity norm is called unit quaternion. In the different algorithms presented through this work, quaternions were systematically normalized as:  $q_{\text{unit}} = \frac{q}{\text{Norm}(q)}$  to be able to use the so-called “unit quaternion properties”. For example, if we note  ${}^F_B q$  the quaternion describing orientations of B (e.g. the sensor) relative to F (e.g. the Earth frame), for a united quaternion,  ${}^F_B q$  equals  ${}^B_F \bar{q}$ , with  $\bar{q}$  defined as the quaternion conjugate and computed as:

$$\bar{q} = (w, -x_i, -y_j, -z_k) \quad (3)$$

Using this property, if we defined a unit quaternion  ${}^F_B q_{\text{orig}}$  corresponding to the initial orientation of the sensor in the global frame and  ${}^F_B q_{\text{rot}}$  the new orientation of the sensor after a certain rotation in the same global frame. It is possible to directly compute the quaternion expressing the rotation of the sensor relative to the starting orientation, as:

$$q_{\text{rot}}^{F_{\text{orig}}} = {}^F_B \bar{q}_{\text{orig}} ** {}^F_B q_{\text{rot}} \quad (4)$$

with  $**$  the specific quaternion multiplication, known as Hamilton product [66].

## b. Sensors

In order to understand the multiple issues and choices made in this thesis to estimate human motion from inertial sensors, it is also necessary to identify what such a sensor is composed of.

Inertial Measurement Units (IMU), sometimes referred to as MARG (Magnetic, Angular Rate, and Gravity) units, are usually made up of three types of sensors (an accelerometer, a magnetometer and a gyrometer), measuring three physical values: acceleration, magnetic field and angular rate.

Earth generates a force on massive bodies around it, commonly called “gravity”  $g$  and oriented toward its center. This force can also be seen as an

acceleration, with the relation  $F = m \cdot a$  (Force, mass, acceleration) from the second Newton law. What measures an accelerometer can be compared to what the inner ear senses: a combination of the gravitational field and the acceleration due to the movement. An ideal accelerometer sensor should thus record a magnitude  $N$  of  $1g$  ( $9.81m \cdot s^{-2}$ ) when lying in static conditions:

$$N(\text{acc})_{\text{static}} = \sqrt{a_x^2 + a_y^2 + a_z^2} = 9.81m \cdot s^{-2} \quad (5)$$

Earth also generates a geomagnetic field due to the motion of convection currents of molten iron in the Earth's outer core. This magnetic field can be locally represented as a constant three dimensional vector. This vector has a magnitude expressed in Tesla (T) and is related to a declination angle (the angle between the geographic North and the horizontal component) and an inclination angle (the angle between the horizontal plane and the magnetic field vector). The value measured by a magnetometer sensor fluctuates depending on the location and orientation. In France the geomagnetic field is about 47000 nT and is oriented towards the ground with an angle of about 60 degrees with the horizontal. It is essential here to keep in mind that magnetic measurements are therefore sensitive to magnetic field disturbances.

The third and last sensor to be introduced is the gyrometer. In opposite to the accelerometers and magnetometers which measure quantities which are not directly related to the motion, gyrometers measure movement quantity. It is interesting here to understand how this kind of sensor works, as it will be related to different issues addressed later in this document.

If the IMUs have become increasingly used in a high variety of devices (submarines, ships, aircrafts, smartphones, watches, game controllers...) it is important to highlight the important price, quality and technological ranges between the widespread low-cost sensors and the ones based on costly technologies (e.g. laser, fiber-optic, fluid-suspended...).

In most of low-cost IMUs, gyrometers are micromechanical systems (MEMS) built with a micro-machined mass which is connected to an outer housing by a set of springs. Any rotation of the system will induce Coriolis acceleration in the

mass. The Coriolis force is detected by capacitive sense fingers along the mass housing and the rigid structure. Thus the sensor can detect both the magnitude and direction of the angular velocities of the system. Depending on the chosen springs, capacitive fingers and amplifier characteristics, the sensor offers different levels of sensitivity.

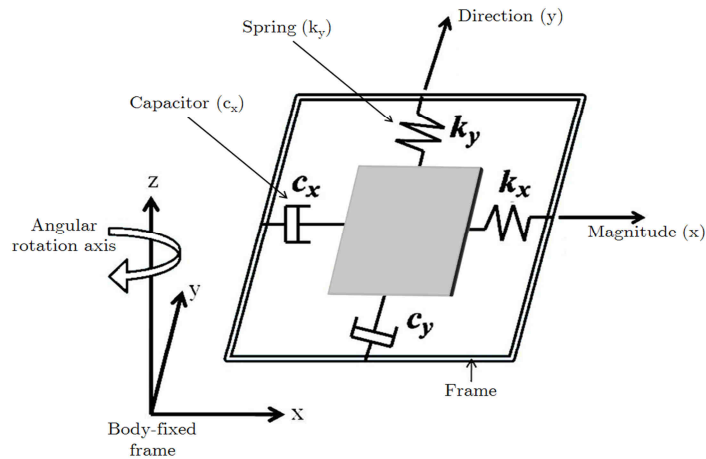


Figure 9. Schematic illustration of a MEMS vibratory gyrometer measuring angular rotation around its Z axis. The capacity  $C_x$  changes relatively to the magnitude ( $x$ ) of the rotation. The capacity  $C_y$  changes regarding the direction of motion.

### c. Known issues

Ideally, a gyrometer as mentioned above would therefore be enough to compute an orientation by itself. Integrating the angular rates (rad/s) along time would give the rotation angles (rad) from the initial orientation.

Similarly, by integrating acceleration ( $m.s^{-2}$ ) measurement from an initial position would give velocity ( $m.s^{-1}$ ) and velocity integration would give the position (m).

Nevertheless, these basic principles cannot be straight forwardly applied due to different well known issues.

The first and main issue is related to data integration and error accumulation.

Error can be due to different causes. To convert analog data from an electromechanical system to physical numerical values, a digital analog conversion results in a discretization and a time sampling. Therefore, regarding the

integration method used and the sampling rate, an error will keep increasing and will cause what is commonly called an “integration drift”.

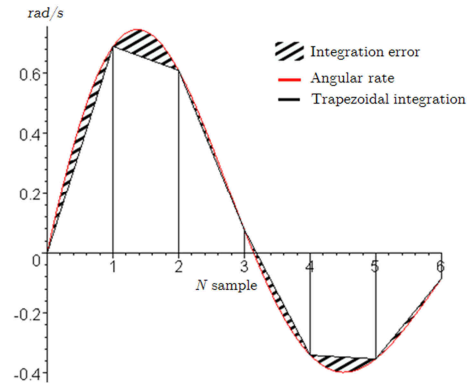


Figure 10. Illustration of integration error using trapezoid rule integration on an angular rate signal drawing.

A higher sampling rate and an adequate integration method can minimize integration error but will not prevent its increase over time. Trapezoidal integration is the most widespread method used to integrate inertial data, although some studies demonstrated slightly better results using Simpson or Romberg integration rules [67].

A second important source of integration error is the commonly called “bias error”. Defined as - any nonzero sensor output when the input is zero - and partly due to the electromechanical characteristics of these sensors (e.g. sensitivity to temperature changes), bias prediction and removal have led to numerous inherent studies [68] and technological improvements over the past few years.

This sensor feature is a critical aspect of inertial based motion analysis. If not removed from the measurement, a constant bias in acceleration becomes a linear error in velocity and a quadratic error in position. Similarly, a constant bias in angular rate coming from the gyrometer becomes a linear angular error.

The use of magnetometer measurement could provide a reliable and accurate compass to compute IMU global orientation related to the geomagnetic field and was shown to be a potential solution to remove bias error [69]. Meanwhile, this sensor also suffers from measurement error as various studies showed the

---

magnetometer could not provide accurate values when located closer than 20 cm from a metal alloy [70].

Last but not least, integration being performed from an initial position, an error can also be introduced if the sensor has moved regarding its initial mounting location, e.g. in case of the sensor is not firmly attached on the limbs, which is usually the case in gait analysis.

#### **d. Calibration**

Different solutions have been investigated through this thesis to be able to deal with most of the previously explained issues. The first primary and critical task to achieve efficient algorithms turned out to be the optimization of sensors calibration.

As previously explained, IMU are partly composed of mass-spring systems. As a mechanical to numerical conversion, values are subject to distortions, vibrations, temperature changes... Multiple existing calibration algorithms have been developed in the past few years with different levels of complexity, depending also on the available equipment. Some of them are based on highly accurate external devices, such as optical motion capture systems [71], [72] while other rely on various physical properties. Accelerometers can for instance be calibrated using the ‘drop method’. This method is based on the fact that when a sensor is dropped from a predetermined height, the only acceleration the object records is supposed to be the acceleration due to gravity. Measuring acceleration from different predetermined heights enable to calibrate the sensor to fit  $9.81 \text{ m/s}^2$  for any drop height. A second calibration method for accelerometers relies on a fundamental approach to compute an object’s acceleration which is the pendulum motion. Used in Choi et al. work [73], it relies on the property that a pendulum motion implies a gravity force always in the same direction (down) and always of the same magnitude. With a limited use, this method requires an accurate measurement system to monitor pendulum motion and be able to consider acceleration seen by the sensor as a sinusoid. Usually, the sensors are mounted on an electrodynamic shaker driven by a sinusoidal vibration. The

results are measured at different frequencies, checking linearity of the response for various acceleration ranges [74].

With the constant objective of designing a clinical oriented solution in the previously described contexts, none of the previous calibration solutions were selected. They were judged inadequate to a user-friendly and low-cost approach.

Based on the most widely used method, called multi-position calibration [75], a specific calibration process was rather investigated.

This calibration process is based on the previously introduced physical property that the norm of the acceleration, in static conditions, is equal to gravity acceleration  $g$ :

IMU sensor was placed in different random orientations. For each orientation, the sensor output was recorded while maintaining it in a strictly static state. The aim was to fit the gravity measurement in all orientations. Different optimization methods were tried and the one offering the best performances was the approach described in Frosio et al [76]. It has the advantages of incorporating not only the bias and scale factor for each axis but also the cross-axis symmetrical actors computed through Gauss-Newton nonlinear optimization. Thus, calibrated acceleration values  $A_c$  were systematically expressed as raw acceleration value  $A_r$ , minus offset  $O$  multiplied by the scale factors:

$$A_c = S (A_r - O) \quad (6)$$

with:

$$S = \begin{bmatrix} S_{xx} & S_{xy} & S_{xz} \\ S_{yx} & S_{yy} & S_{yz} \\ S_{zx} & S_{zy} & S_{zz} \end{bmatrix} \quad O = \begin{bmatrix} O_x \\ O_y \\ O_z \end{bmatrix} \quad (7)$$

Numerous methods have been also investigated in literature regarding magnetometer sensor calibration. Similarly to accelerometer calibration solutions, most of them require expensive devices, such as the used of Helmholtz coils [77] and do not seem to fall in line with a user-friendly approach. The compass swinging procedure [78] could be used instead. It consists in rotating the magnetometer in a series of known headings and measuring the sensor output. However, this procedure requires the use of external devices to accurately measure heading.

Instead, simpler approaches are possible by only using information related to Earth magnetic field magnitude (also called scalar checking) or inclination angle. Proposed in [79], [80], the method is based on field magnitude measurement and a sphere fitting approach. By minimizing algebraic distances between the Earth magnetic field and calibration data acquired by rotating the sensor in every orientations, offset and scale factors similar to accelerometer ones are computed.

As previously introduced, a large range of gyrometer sensors are available for purchase, with a cost highly related to their design quality, accuracy and sensitivity to dynamical and thermal changes. Multiple methods have been investigated for reducing offset and drift related to sensor miscalibration [81]. The usual method consists in using optical trackers and making rotate the gyrometer at different predefined angular speeds [82]. The outputs are then compared between the reference system and the gyrometer's data to compute a scale factor. However, this method requires a mechanical platform combined with accurate optical sensors that exceed the cost of the sensor by itself and was thus unsuitable to the desired approach described in this thesis.

For each study presented in the following sections, the only calibration performed on the gyrometer data was an offset removal. The method consisted in recording during at least 10 s the gyrometer values in static conditions (ideally equal to 0 rad/s) and removing the estimated bias to the dynamic measurements. In clinical conditions (e.g. gait assessment with PD and hemiparetic subjects), each recording session started by a motionless period where the subject was asked to stay still. An offset vector was approximated as the mean value of the gyrometer output during this static recording.

#### **e. Basic filtering**

In addition to calibration issues and similarly to many analog sensors, IMUs recordings are also subject to noise.

As previously introduced, in static condition the sensor 2D orientation could be ideally computed using only accelerometer magnitude and trigonometry. The

gravity  $g$  pointing downwards, in a 2D representation the tilting angle  $\theta$  between the sensor and the horizontal could easily be expressed as:  $\sin\theta = \frac{a_x}{g}$ .

This last statement is true if the accelerometer is not subject to motion. It is for instance the usual way a smartphone is able to detect its orientation relative to horizon and flips its screen relative to its tilting angle. However, a simple frequency domain analysis shows as soon as the accelerometer sensor is subject to motion, that high frequency noises disturb the accelerometer accuracy [83], in addition to acceleration disturbances related to motion. A common practice to reduce the noise consists in filtering accelerometer data with a standard first order low pass filter [84].

Thus, while these last statements are valid in static conditions, in dynamic conditions the use of gyrometer data is a crucial factor to compute orientation combined with information obtained from accelerometer. However, gyrometer values are also subject to noise.

Previously mentioned, the “bias error” is a constant bias that leads to a linear angular error once the angular speed integrated. A simple test consists in letting a gyrometer lying down on a table and integrating it over time. Although the gyrometer does not move, a significant drift is estimated.

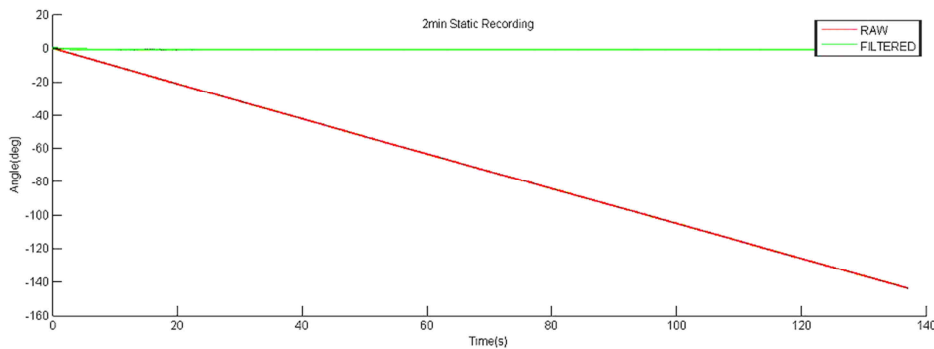


Figure 11. Static recording of Z-axis gyrometer from HikoB<sup>©</sup> FOX sampled at 200Hz and integrated using trapezoid rule. Raw data integration leads to a drift error of more than 120° in orientation after two minutes, while high pass filter based recording stays nearly constant.

This constant bias can be considered as a very low frequency component [85]. Thus, a usual method consists in high pass filtering gyrometer values. However,

---

the problem with this approach is that motions under relatively constant angular speeds are likely to be filtered out.

In addition, the use of standard frequency filters (e.g. Butterworth) is not a fully satisfactory solution as it introduces a well-known shift in time, usually called phase delay. As inertial data based algorithms usually combine data from multiple sensors and filtered in different ways, a phase distortion between the sensors data will decrease algorithm performances and accuracy. A possible solution to overcome this issue is to use linear phase filters or zero phase filters. The first one implies that all frequency components of the input signal are shifted in time by the same factor. The second one processes the input data, in both the forward and reverse directions (also called forward backward filters). Meanwhile, it introduces a processing delay which may prevent to use this kind of frequency filter for fast real-time processing. Therefore, more complex methods have been investigated to provide a robust and accurate processing of inertial data and are addressed in the following section.

### **2.1.2 Attitude and Heading Reference System (AHRS) sensor fusion techniques**

#### **a. State-of-the-art and explanations: in theory**

Combining information from multiple complementary data (e.g. filtered accelerometer and gyrometer values) refers to a sensor fusion technique widely used in inertial sensing based attitude computation and called a “complementary filter”.

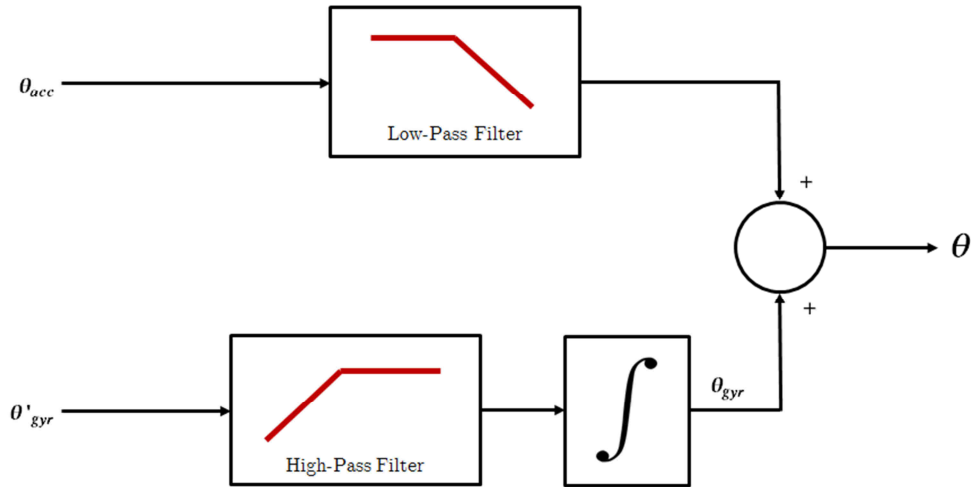


Figure 12. Example of a basic complementary filter as described in Colton et al. [84] for 2D balance (tilting) angle estimation. Tilting angle estimated from accelerometer passes through a low-pass filter, the angular rate from gyrometer passes through a high pass filter and is integrated to obtain rotational angle. Outputs are then fused (added) to estimate angle from complementary data.

Literature on this topic is abundant. The most significant contribution is the works of Mahony et al. [86], [87] in 2005. This work was followed by Colton et al. in 2007 [84], Premerlani et al. [88] and Starlino et al. [89] in 2009, Madgwick et al. [90] in 2010 and more recently Valenti et al. [91] in 2015, with different updates and improvement attempts.

A particular focus was given to Mahony and Madgwick complementary filters, as they have become standards and are now widely used by the community, especially with low-cost MEMS IMU.

Mahony's original idea was to correct the input  $\omega$ , the angular rate vector coming from gyroscope, by a correction vector  $e$  provided via a P (Proportional) controller. Part of a global transfer function expressing estimated orientation, the error vector is expressed as a mean difference between previous estimated orientation and the one measured from accelerometer vector [86]. In a later work, the author facilitated gyrometer drift estimation by using a PI (Proportional Integral) controller [92]. Inspired by Mahony's work, in Madgwick et al. [93] the

---

authors also proposed a gyroscope drift compensation based on a PI controller. The major differences lie in the use of a quaternion representation of orientation, the use of a gradient descent method to improve algorithm performance and a magnetic distortion compensation algorithm. Indeed, in addition to previously introduced advantages of using quaternions (no singularity, a fastest computation time, etc...), their mathematical properties allowed the authors to use data in an analytically derived and optimised gradient steepest descent algorithm, in order to compute the direction of the error as a quaternion derivative. According to the authors, this last method shows advantages, such as being less sensitive to low sample rate, but the use of a gradient technique is prone to lead to multiple solutions depending on the noise generated by the sensors. Thus, another fusion sensor approach has been widely used over the past few years and is able to take into account noises from sensors and more parameters: Kalman filters [94].

Indeed, in opposition to the previously stated deterministic algorithms, the use of Kalman filters as a stochastic method to fuse sensors data, enables to create an estimator via mathematical models of the sensors to estimate the state of the system, depending on previous measurements and inner parameters. Orientation filters based on a Kalman approach have become increasingly studied in literature [95]–[98] and represent the scientific basis upon most of the most accurate commercialized devices such as XSens<sup>©</sup> [99], Bosch<sup>©</sup>, VectorNav [100], InterSense [101], PNI [102] or Yost [103] rely on. Meanwhile, the numerous works available in literature reflect the complexity and the multiple possibilities related to an estimator based sensor fusion approach [97], [98], [104]–[106]. The use of a Kalman process implies linear regression iterations and demands high sampling rates, way higher than human motion bandwidth. Where arm motion leads to frequencies from 100 Hz up to 200 Hz, gait around 25 Hz [107], Kalman based algorithms need sampling frequencies between 10 KHz [108] to 30 KHz [109]. Moreover, for describing tridimensionnal rotational states, the use of large state vectors and Extended Kalman Filters (EKF) are therefore required [98], [104], [110]. This stochastic estimation technique no longer requires proving its accuracy

---

and performance when properly tuned. It represents by far the most widely used approach, essentially inside aerospace engineering community [111]. However, as said earlier, the numerous parameters to choose make it particularly complex to use. Most of all, the high computational load inherent to EKF requires powerful processors, which cannot be an issue when dealing with inertial systems in submarines, ships, aircraft or unmanned aerial vehicles (UAV), but which is a major obstacle in low-cost embedded devices, characterised by low-resolution signals subject to high noise levels and limited processing power.

For many of ambulatory low-cost applications, the algorithms need to run on embedded processors with a substantially less processing power than those available in most of the commercialized inertial navigation systems. Different studies have tried to deal with an efficient alternative to extended stochastic linear estimation techniques able to take into account both acceleration and magnetic disturbances and gyrometer biases [112]–[114]. The main principle is based on combining deterministic complementary filters, such as the one previously described from Mahony et al. [86], with non-linear observers. One of the most advanced work on this design technique is Martin et al. [115] study. The global principle is to build a state observer (i.e. a mathematical structure for estimating the inertial system output) relying on the fact that the state of our system (i.e. the inertial sensor) is supposed to be invariant by a rotation in the body-fixed frame and a translation on the gyrometer bias. The aim is to converge towards the lowest error between the observer estimated output and the output from the complementary filter. Martin et al. algorithm design guarantees that the error converges to zero, at least locally and the behaviour in the face of acceleration disturbances should stay consistent. The second advantage is that the magnetic measurement is used to estimate only the yaw angle, so that a magnetic disturbance does not affect the estimated pitch angle. The method is also able to indirectly deal with noise through the tuning of the observer gains. Last but not least, in order to demonstrate the computational simplicity of their work, Martin et al. implemented and tested it on a low-power 8-bit

---

microcontroller unable to run an EKF implementation. The aim was to check if they could obtain a correct estimation at a 50Hz update rate. They compared their results to a commercial device running an EKF and a complex observer running offline on Matlab-Simulink. Both estimations were very similar and satisfactory.

### **b. Implementation and validation: in practice**

From the three main attitude and heading estimation approaches previously presented (Complementary filters, EKF and Martin’s observer), a logical and easy solution could have been to directly buy a commercialized device equipped with on-board processors and EKF algorithms, such as the previously stated systems (e.g. XSens<sup>©</sup> MTi 100) to assess human motion and feed an FES controller. Most of recent works use these type of “plug and play” devices for motion analysis [116], where quaternions are directly given by the sensors through a “black box” unknown to the operator. However, a different choice was initially made, taking into account the initial constraints introduced in this thesis.

One of the different challenges related to this work was to investigate solutions able to be the most generic, scalable and affordable in order to be later implemented inside assistive devices for rehabilitation. Moreover, most of the commercial devices available were not “opened” to programming and already dedicated to one specific task, which made difficult the study of new algorithms and innovative assistive solutions.

Therefore, a decision was made to use generic low-cost inertial sensors. Based on the state of the art, Martin et al. algorithm seemed to be the best compromise for implementation on low-power devices for fusing data. However, to ensure the most adequate method was chosen among the different AHRS methods previously presented, three approaches were initially programmed and experimentally validated in clinical environments [56]: Mahony et al. [86], Madgwick et al. [117] and Martin et al. [118].

A generic and low-cost inertial sensor (Fox HikoB<sup>©</sup> Villeurbanne) featuring a 3-axis accelerometer, a 3-axis magnetometer (ST<sup>©</sup> LSM303DLHC), a 3-axis

gyrometer (ST<sup>©</sup> L3G4200DH) and a 32-bit micro-controller was bought and used to record raw data on post-stroke individuals. Mounted on the feet, the IMU was strapped on a rigid support together with 4 reflective markers tracked by an optical motion capture system (OMCS, Vicon<sup>©</sup> Bonita MX). Foot angle relative to the floor was monitored on a 5-meter path. Inertial data were recorded offline and post-processed for fusing. Vicon markers and the IMU were affixed onto a rigid mount which had the advantage of ensuring both systems measured the exact same motion, in order to get rid of a possible bias due to sensor displacement regarding the initial location. Mean drift was measured at  $t=20s$  and on 30 repetitions. In addition to best fitting with the reference signal dynamic, Martin et al. was indeed the method with the lowest drift ( $<6^\circ$ ) compared to Mahony ( $<20^\circ$ ) and Madgwick ( $<25^\circ$ ). The results validated the state of the art.

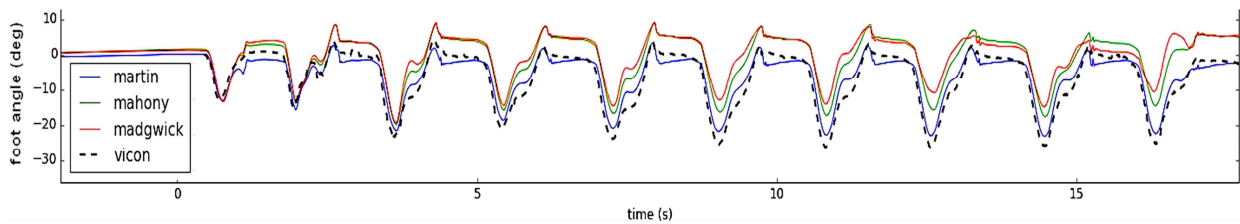


Figure 13. Foot angle relative to the floor (i.e. tilt angle) while walking on a 5-meter path, computed through three sensor fusion algorithms (Mahony et al. [86], Madgwick et al. [117] and Martin et al. [118]) from literature and compared to a motion capture system (Vicon).

### 2.1.3 From IMU generic principles to lower limbs motion analysis

The previous paragraphs exposed all the basic and generic principles related to the use of inertial sensors in a general context, how to deal with rotations, how to improve accuracy of the sensor or how to fuse raw data to compute the orientation of a sensor in a global frame. But how to use them in the context of assessing human motion? How to transpose theory initially designed for aerospace engineering to record pathological motion? How to convert a sensor orientation to estimate a joint angle or to compute a paretic foot trajectory? Through the next sections, different approaches investigated in this thesis are presented and

---

highlight the additional constraints and solutions to face when dealing with lower limbs motion assessment in different sensorimotor deficiencies. While some specificities related to these use cases will prove to be useful (e.g. “zero velocity update” combined with gait segmentation to limit drift error) the following paragraphs will also highlight the difficulty to design algorithms robust enough to be later considered as an input for an assistive control of motion based on FES, while keeping in mind to investigate a convenient and evolutionary patient centered approach.

The first and main problematic addressed in this work is gait rehabilitation.

## 2.2 Healthy and Parkinsonian gait: a 2D approach

Among multiple gait parameters, stride length is frequently observed for rehabilitation and diagnostic purposes. Applied to neurological diseases, it represents an extremely helpful marker for practitioners to analyze pathological effects on gait and therapy efficiency.

Numerous works showed the complexity and the diversity of accurately analyzing gait parameters in clinical applications, using wearable and non-wearable systems [119]. Most of the existing works on IMU-based stride length estimation only provide an average stride length (ex: RehaWatch© device). Usually based on the estimation of the distance covered in a fixed time interval, the stride is computed from the whole recording trial [120]. Other works performed stride length calculation with at least two IMUs [121], [122], or using motion pattern identification [123], thereby requiring either a technological overload or a prior knowledge of the subject's biomechanical model. While increasing installation time and complexity to properly tune the system, these solutions were not considered here because not adapted to a closed-loop control approach addressed in following sections. An averaged stride length is not satisfactory as an input to control an FES device, this kind of approach requiring an instantaneous knowledge of the monitored variable for an immediate feedback.

### 2.2.1 2D stride length estimation

A first algorithm was then investigated, set with the strongest constraints and the worst hypothesis but applied on subjects with either a normal walk or with a slightly altered gait pattern (people with Parkinson's disease). Keeping in mind the initial challenge of conceiving a light and noninvasive patient-centered solution, quickly implementable and easy to put ON and OFF, the objective was to demonstrate the feasibility of computing each individual stride length from a maximum of one IMU per leg, located either on the shank or on the foot. In

addition, the algorithm had to be developed if possible without using the magnetometer data, in order to prevent the estimation to be disturbed in presence of ferromagnetic materials. Finally, a minimum of prior knowledge had to be requested to ease the installation.

Only two accurate enough (error  $<10\%$ ) solutions based on one IMU without using magnetometer values were available in the literature to our knowledge at the time. The study of Köse et al. [124] is able to provide the instantaneous stride length calculated from an inertial sensor located on the pelvis of able-bodied subjects. Meanwhile, due to an algorithm based on acceleration patterns identification and pelvis displacement estimation, the authors exposed some limitations regarding pathological gait that could have been problematic if used in hemiparetic gait for instance. The second one is the solution proposed by Mariani et al. [125], which presents a 3D gait assessment method validated on both young and elderly valid subjects. Using a foot-worn inertial sensor, it uses a complex de-drifting method based on sigmoid-like curve subtraction modeled from a p-chip interpolation function [126].

In the following paragraphs, a first simple clinical use designed solution is presented and compared to the state of the art. Results have been validated using a reference system: a GAITRite<sup>©</sup> instrumented mat.

### a. Gait segmentation and ZVU introduction

In order to understand the following algorithms, the first main notions to be introduced are the gait cycle and its specific resulting properties when addressed with IMUs.

Human gait is divided into gait phases. The locomotion is basically divided into two main components: the stance and the swing phases. Each phase can be associated to one limb and divided into different sub-phases or gait events. The stance phase can be described by five sub-phases:

- the Initial Contact (IC), or also called Heel Strike (HS) or Heel On (HO): the first contact to the ground (usually the heel in case of a healthy walk).

- the Loading Response (LR): following IC, when the weight shift occurs due to the lift of contralateral limb.
- the Mid-Stance (MS): when both the heel and forefoot start to touch the ground.
- the Terminal Stance (TS): when the heel starts taking off and only the forefoot touches the ground.
- the Pre-Swing (PS): just prior to the lift from the ground and toe-off (TO).

The swing phase is divided into three sub-phases:

- the Initial Swing (IS) or Foot Off (FO): begins at toe off and continues until maximum knee flexion occurs.
- the Mid-Swing (MS): from maximum knee flexion until the tibia is vertical to the ground.
- the Terminal Swing (TS): where the tibia is vertical, ends at initial contact.

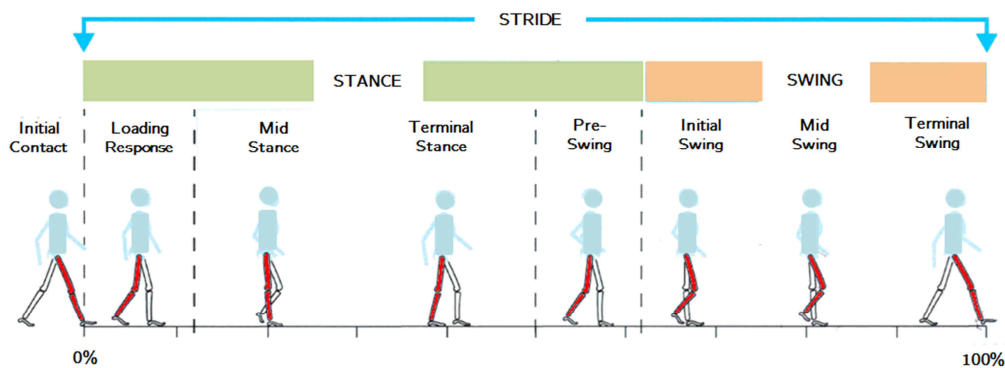


Figure 14. Gait cycle, from 0% to 100%, divided into two main parts: the stance and the swing phases. One stride corresponds to a complete gait cycle.

A stride corresponds to a full gait cycle. It can also be defined as two consecutive initial contacts (IC) of the same foot. One stride is equivalent to two steps, defined as two consecutive IC by different feet.

A high number of studies proposed different approaches to segment gait using wearable and non-wearable sensors [127]. Among wearable sensors, footswitches

---

and foot pressure insoles are usually considered as the gold standard. However, they suffer of multiple inherent limitations. The footswitch is generally located inside the shoe, right under the heel and relies on a technology based on force sensing resistors (FSR). It has two major disadvantages when used to segment pathological gait: weak ICs and toe-walks are not correctly detected and segmented and directly depend on the footswitch location inside the shoe. The FSR technology also suffers from multiple inner issues leading to inaccurate measurements (hysteresis, temperature sensitivity...)[128]. Based on a similar technology and thereby suffering from the same disadvantages than the footswitches, the foot pressure insoles do not either constitute an adequate solution for gait cycle segmentation. Despite their ease-of-use, the existing devices (e.g. Tekscan<sup>©</sup>, Pedar<sup>©</sup>...) are relatively costly and often require possessing every appropriate shoe size. They could be also unsuitable with a certain type of shoes. This partly explains the growing interest in the use of IMUs for gait segmentation.

Many different approaches have been investigated over the past few years to partition gait from IMUs data, able to provide different levels of spatio-temporal granularity. To evaluate gait recovery status in patients after rehabilitation [129], to classify daily life activities [130] or to distinguish between normal and pathological gaits [131], the state-of-the-art of the different gait partitioning algorithms is as various as the numerous possible applications.

The use of accelerometers tends to be the most widespread solution to segment gait phases, with different combinations and placements. Selles et al. [132] proposed an automated accelerometry-based system for estimating initial contact (IC) and terminal contact (TC) from accelerometers located on the shank of fifteen healthy adult subjects and ten unilateral transtibial adult amputees. The first local minimum in the longitudinal low-pass filtered acceleration represented the start of the stance, and the second one was the end of the stance phase. Williamson et al. used Rough Sets (RS) and Adaptive Logic Networks (ALN) induction algorithms applied on data coming from an accelerometer attached to

the shank of able bodied subjects [52] and were able to detect five gait subphases to an overall accuracy of 82-89% and 86-91%, respectively. Using footswitch signals as reference, Rueterbories et al. [133] designed an algorithm able to detect curve features of the vectorial sum of radial and tangential accelerations from an accelerometer attached to the foot and to map those to discrete gait states. They obtained an accuracy of about 95% on healthy and hemiplegic subjects. Most of the previously presented methods' accuracy is however directly related to the sensitive axis chosen to monitor acceleration and implies a precise sensor localization. While complex machine-learning algorithms have been used to detect gait phases, literature also shows that both longitudinal and antero-posterior linear acceleration specific peaks at the start and end of the stance phase could finally be sufficient to easily detect gait phases, by means of a threshold algorithm in able bodied subjects [134]. Despite some studies investigated gait partitioning from IMU located on the trunk, regardless the methodology used the sagittal acceleration of the foot was found to be the best choice to obtain optimal results [134]. Meanwhile, the use of accelerometers implies critical issues already addressed in part 2.1.1.c that partly explain an equally high number of gait partitioning methods based on gyrometers.

Indeed, to use angular velocity coming from gyrometers presents three major advantages compared to accelerometers: the measurement is neither impacted by the gravity nor by the vibrations occurring at heel strike (HS)[135] and the sensor does not require to be accurately placed [136]. The angular velocity recorded in the sagittal plane presents multiple features that make relatively easy to partition healthy gaits directly from the waveform profile. Most of the existing algorithms rely on the detection of four main events that can be robustly identified with simple peak detection algorithms or thresholds: the swing phase peak, the IC and FO events and the “zero velocity” event. One of the easiest features to detect is the maximum peak in angular velocity. It corresponds to the middle of the swing phase. Around this swing phase peak, two negative minimum in the shank or foot angular velocity signal can be robustly identified. The negative minimum

---

preceding the swing phase peak equates to the FO event. The negative minimum following the swing phase peak corresponds to the IC event [137]. Between IC and FO, the angular velocity reaches a plateau around zero, which is equivalent to the middle of the stance phase.

This last event is particularly interesting when dealing with IMU and gait assessment and is commonly called the “zero velocity” event. This feature represents the moment when the foot is supposed to lie flat on the floor and the shank to be vertical, parallel to the direction of gravity [138]. Addressed in different ways through this thesis, the fact of using this typical event to reset accumulated error over time is commonly called in literature ZUPT or ZVU, standing for: Zero Velocity Update [139]. By simply zeroing the velocity during each detected stance phase enables to limit drift error integration accumulation described in 2.1.1.c when the user is walking. This typical event also provides useful information to update actual sensor state (e.g. parallel to the gravity, with no velocity, lying flat on the floor,..).

Thus, partitioning gait phases using accelerometers or gyrometers enables to use gait events for 1) bounding gait cycle and integration of motion and for 2) updating the estimated sensor state depending on its actual physical state, in order to reduce error accumulation.

Meanwhile, despite being essential to most of IMU based lower limb motion assessment algorithms, in some cases partitioning gait cycle is not as straightforward as previously explained, especially when dealing with pathological gait patterns. While some studies merged IMU and footswitches or foot pressure insoles to overcome limitations of each technology and design robust gait partitioning algorithms [140], different approaches will be addressed through this thesis using only IMUs, to minimize the number of sensors thereby providing a simple and practical patient centered solution.

In the study presented in this section, gait cycle was segmented using angular velocity recorded in the sagittal plane. A simple automatized detection was performed as shown in Figure 15:

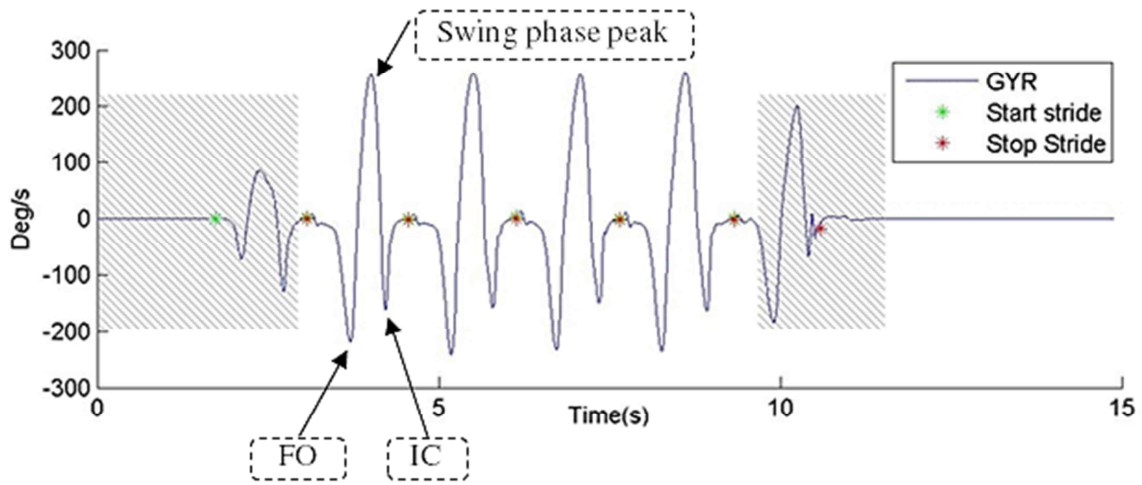


Figure 15. Illustration of the angular velocity based gait partitioning method on four strides (the first and last strides are not considered) applied on gyrometer data from an able bodied subject.

### b. Calibration and Filtering

The algorithm presented in this section used data from one 3D gyrometer and one 3D accelerometer embedded in a previously introduced Fox HikoB<sup>®</sup> IMU strapped to the leg (Figure 16). The acquisition frequencies were 200Hz for both sensors, data were post-processed offline.

As introduced in section 2.1.1.d, calibration and filtering of raw inertial data are prerequisites to any IMU based algorithms in order to ensure the best computation accuracy. Accelerometer data were filtered with a forward-backward lowpass Butterworth filter (order 1,  $F_{\text{cutoff}} = 5$  Hz). Gyrometer data were filtered via a forward-backward highpass Butterworth filter (order 1,  $F_{\text{cutoff}} = 0.001$  Hz) for reducing integration drift. As already described in the same section, accelerometer data were calibrated using Frosio et al. [76] model and each recording session started by a five-second motionless period to compensate an eventual existing gyrometer offset. No AHRS algorithms were initially used, in order to first try to design the simplest method to implement.

### c. 2D stride length: algorithm

The principle of stride length estimation is to calculate the horizontal movement of the inertial sensor during one stride cycle in the sagittal plane. Inspired by the algorithm originally proposed by Li et al. [141] and improved later by Laudanski et al. [138] which computes the walking speed from a shank-mounted IMU, we adapted it for calculating the stride length, by correcting and integrating the linear velocity along the stride duration, thereby obtaining the length of each stride. A simplification of the original algorithm was performed, as only the horizontal velocity was needed. As an effort to provide an easy-to-implement solution, the hypothesis that the sensor is initially set in the sagittal plane and does not move during the experiment was made, thereby working in a 2D frame.

To begin, the sensor orientation  $\theta(t)$  has to be computed by integrating the measured angular velocity  $\omega(t)$  on a stride cycle (from  $t = 0$  to  $t = t_{\text{end}}$ , the initial tilt at the beginning of the cycle  $\theta(0) = 0$ , assuming the sensor is aligned to the limb):

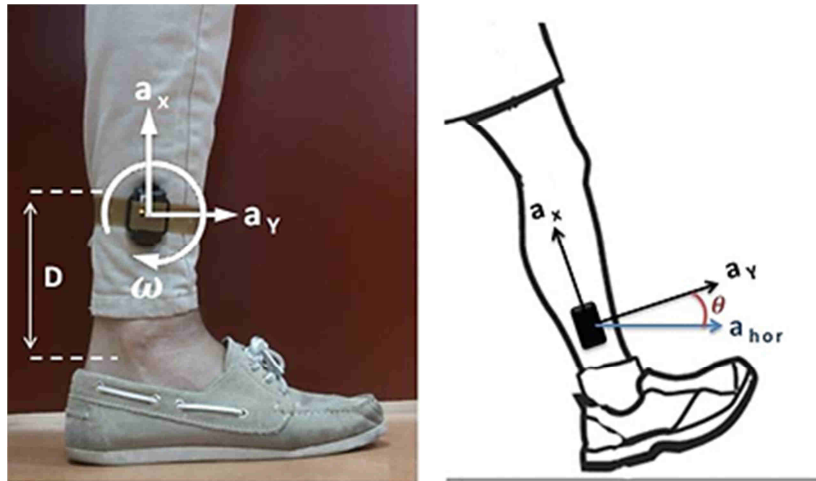


Figure 16. Frame schema: the IMU is located on the shank side, in sagittal plane. The angular velocity  $\omega$  is clockwise positive.  $D$  is the distance between the sensor and the ankle joint (malleolus) and  $\theta$  is the sensor orientation.

$$\theta(t) = \int_0^{t_{end}} \omega(t) dt \quad (8)$$

The horizontal component acceleration  $\mathbf{a}_{hor}(\mathbf{t})$  in the world coordinate system has to be calculated from the measured raw accelerations,  $\mathbf{a}_y(\mathbf{t})$  and  $\mathbf{a}_x(\mathbf{t})$ :

$$\mathbf{a}_{hor}(t) = \cos \theta(t) \mathbf{a}_y(t) - \sin \theta(t) \mathbf{a}_x(t) \quad (9)$$

The integration of the horizontal acceleration provides the horizontal velocity  $v_{hor}$ :

$$v_{hor}(t) = \int_0^{t_{end}} \mathbf{a}_{hor}(t) dt + v_{hor-gyr}(0) \quad (10)$$

Where  $v_{hor-gyr}(0)$  is the initial horizontal speed computed from gyrometer data at the start of the cycle:

$$v_{hor-gyr}(0) = \cos \theta(0) v_{tang}(0) \quad (11)$$

with  $v_{tang}(0)$ :

$$v_{tang}(0) = -\omega(0) D \quad (12)$$

and  $D$  the distance between the IMU and the ankle joint.

A velocity drift correction (ZVU) is then performed at the end of each cycle. The linear trend difference between the calculated velocity  $v_{hor}(t_{end})$  and the gyrometer based velocity  $v_{hor-gyr}(t_{end})$  at the stride end is added:

$$v_{hor-corrected}(t) = v_{hor}(t) + \frac{v_{hor-gyr}(t_{end}) - v_{hor}(t_{end})}{t_{end}} t \quad (13)$$

Once  $v_{hor-corrected}$  computed, a simple trapezoidal integration provides the horizontal displacement during a stride cycle:

$$StrideLength = \int_0^{t_{end}} v_{hor-corrected}(t) dt \quad (14)$$

#### d. 2D stride length: experimental validation

10 able bodied subjects, (5 male, 5 female; Age range: 23 to 61 years; Height range: 1.55 to 1.89 m) and 12 participants suffering from Parkinson's disease (9

male, 3 female; Age range : 63 to 82 years) participated to an experimental protocol to validate this first approach. The protocol was approved by the local ethical committee (international identification number NCT02317289). Participants were recruited at the Neurology (Chauliac Hospital) and Gerontology (Balme Center) departments of Montpellier hospital (CHU Montpellier). Subjects walked continuously for approximately 7 m along the GAITRite<sup>©</sup> electronic walkway with two Fox HikoB<sup>©</sup> IMU respectively strapped to the foot and the shank of each leg, as illustrated in Figure 17.

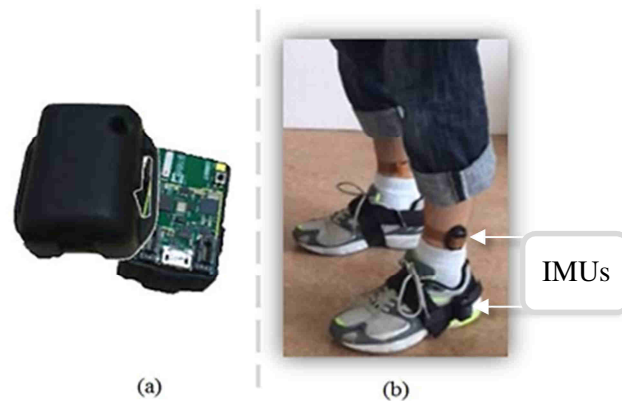


Figure 17. IMUs (a) were strapped to the foot and the shank of each participants' leg (b). The distance  $D$  between the IMU and the ankle joint was systematically measured.

The distance  $D$  between the IMU and the ankle joint was systematically measured once the subject equipped. Each subject from the healthy group performed two iterations of the walk at self-selected walking speeds ('normal' and 'fast'). Subjects from PD group only walked at their comfort speed. The IMU acquisition was remotely triggered. The sensors were synchronized each other via a radio beacon (phase shift  $<100 \mu\text{s}$ ) and the data were logged on micro SD cards inside each IMU. The GAITRite device provided a +5V trigger output for synchronizing data acquisition with the HikoB inertial sensors.

### e. 2D stride length: experimental results

For each subject in the two groups (Healthy / PD), data from inertial sensors were automatically segmented into stride cycles and the length of each stride was estimated. Each estimated stride length was compared to the corresponding stride length value computed from GAITRite (Figure 18). For each subject and for each of the 4 IMUs (shank and foot on each leg), we calculated the mean error and the standard deviation between considered IMU-based stride length estimation and corresponding stride length extracted from GAITRite (Table 1 and Table 2).

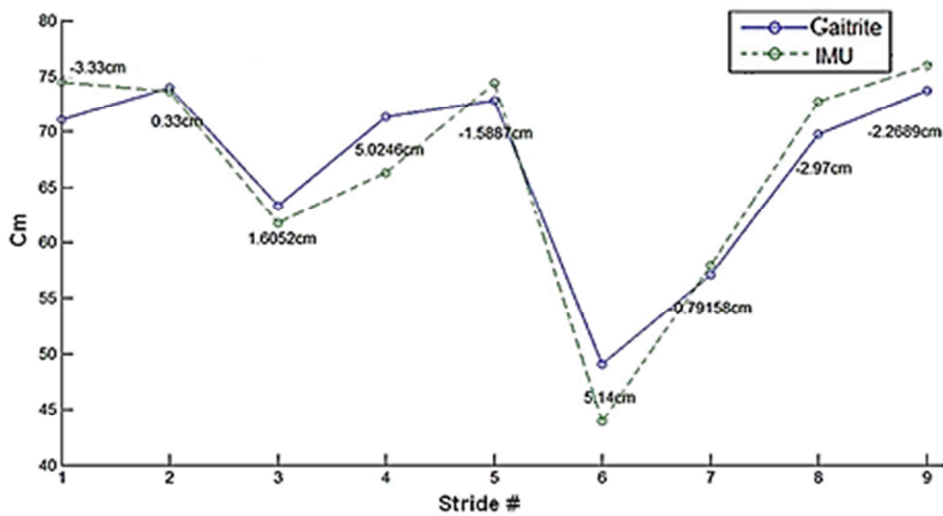


Figure 18. Error estimated between GAITRite data (blue line) and IMU-based stride length computation (green line) for each of the 9 strides of a considered trial.

399 stride lengths (229 in comfort walking, 170 in fast walking) from able bodied subjects were computed and compared to the reference system. For the shank mounted IMUs, mean errors of 5.9% for the 'normal' walk and 5.4% for the 'fast' one have been obtained. Standard deviation was lower than 10 cm in average. A slight difference between the foot and the shank location (the results are 3.2% better for shank mounted IMU) was observed.

Subject ID	Gait Type (Normal / Fast)	Nb of Strides	GAITRITE information				Error using IMU located on the foot			Error using IMU located on the shank		
			Speed (cm/s)	Cadence (step/min)	Stride length		Mean (%)	Mean (cm)	STD (cm)	Mean (%)	Mean (cm)	STD (cm)
					Mean (cm)	STD (cm)						
1	N	20	129.2	110	143.2	3.2	4	5.7	2.2	4.2	6.1	3.5
	F	15	203.8	142	174.4	3.4	3.9	6.8	1.7	4.2	7.2	3.9
2	N	20	143.8	116	150.1	5.4	3	4.6	3.0	5	7.5	4.4
	F	17	243.7	159	182.8	8.9	2.8	5.1	3.4	5.4	9.8	3.2
3	N	20	125.1	107	141.5	3.8	6.2	8.8	3.0	4.2	6	3.7
	F	13	240.9	145	198.7	10.6	5.7	11.4	5.0	4.2	8.3	5.3
4	N	24	115.5	106	131.3	7.1	6.4	8.3	2.5	6.3	8.3	4.3
	F	15	242.6	159	189	11.6	3.7	7.0	2.9	8.1	15.3	7.2
5	N	20	150	110	164	8.7	4.8	7.8	3.2	2.4	4	2.5
	F	15	227.3	138	199.6	7.2	3.8	7.5	4.1	1.6	3.3	3.4
6	N	17	163.9	114	173.1	4.7	6.7	11.7	3.4	6.4	11.1	5
	F	15	230.7	142	195.5	7.4	5.6	11.0	5.9	6.8	13.3	6.2
7	N	30	79.2	85	112.6	2.8	9.7	11.0	4.7	10.1	11.4	7.7
	F	20	148.9	111	162.4	7.4	7.3	11.8	3.8	8.9	14.4	5.9
8	N	25	127.5	117	131.1	4	18.2	23.9	4.6	6.3	8.2	3.8
	F	20	199.1	151	159	4.3	16.7	26.5	3.3	6.7	10.7	3.3
9	N	28	126.4	123	122.7	7.3	6.3	7.8	2.8	5.5	6.8	3.8
	F	25	160.9	138	140.1	3.4	6	8.4	3.1	4.6	6.5	3.3
10	N	25	97.9	94	126	6.3	13.4	16.9	6.0	8.5	10.8	10.5
	F	15	182.7	129	171.4	5.6	15.2	26.1	3.2	3.2	5.5	2.8

Table 1. Experimental results from able bodied subjects.

The stride lengths tended to be particularly variable over the subjects. 'Normal' strides going from 113 to 173 cm and from 140 to 200 cm for the 'fast' ones were recorded. Despite a huge speed increase between the two types of walks in some subjects (ex: subject 4, from 116 to 243 cm/s), the mean error remained under 10% in worst cases with a mean error of 5.6% (0.09 m) on both 'fast' and 'normal' walk using the shank mounted IMUs.

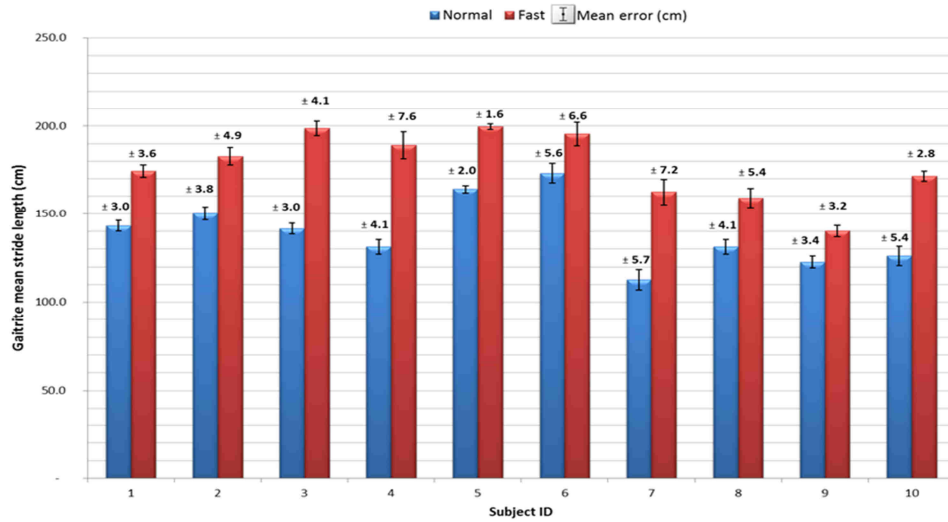


Figure 19. Stride lengths and mean errors for normal and fast gait from 10 able bodied participants.

In the Parkinson's Disease group, despite of consequently smaller and slower strides, a mean error of 9.5% for both legs using the shank mounted IMUs (Table 2) (8.6% for the left leg, and 10.3% for the right one) has been obtained. Standard deviation was lower than 5 cm in average.

Subject ID	Right leg					Left leg				
	GAITRITE information stride length		Estimation error using IMU located on the shank			GAITRITE information stride length		Estimation error using IMU located on the shank		
	Mean (cm)	STD (cm)	Mean (cm)	Mean (%)	STD (cm)	Mean (cm)	STD (cm)	Mean (cm)	Mean (%)	STD (cm)
1	58.6	6.7	6.8	11.7	4.2	58.6	6.3	3.6	6.3	2.6
2	37.5	5.0	3.8	10.2	2.8	37.8	4.5	4.2	11.1	3.5
3	102.3	6.2	6.12	5.98	2.9	102.7	5.8	4.2	4.2	2.9
4	95.7	7.0	8.2	8.6	5.2	95.9	7.4	8.0	8.3	5.9
5	92.1	7.6	6.5	7.0	5.4	93.2	7.1	4.6	4.9	3.1
6	42.7	6.7	6.9	16.1	4.9	42.1	5.1	5.7	13.6	5.6
7	112.6	8.7	8.5	7.4	4.2	112.1	9.9	10.5	9.4	5.6
8	107.8	6.0	14.9	13.8	6.1	107.5	5.8	7.5	7.1	5.5
9	101.9	5.7	8.5	8.3	5.4	102.1	5.5	7.6	7.5	4.6
10	99.8	7.1	5.8	5.9	3.8	100.3	5.2	8.5	8.5	5.1
11	91.3	5.2	17.05	18.67	6.9	91.4	4.7	10.2	11.2	6.6
12	79.4	9.8	8.1	10.4	4.1	79.5	10.1	9.2	11.8	3.3

Table 2. Experimental results from subjects with Parkinson's Disease.

The mean stride lengths were also very variable between each subject, going from 38 to 113 cm. In the worst case (subject 11) the mean error was 11.2% (0.102 m).

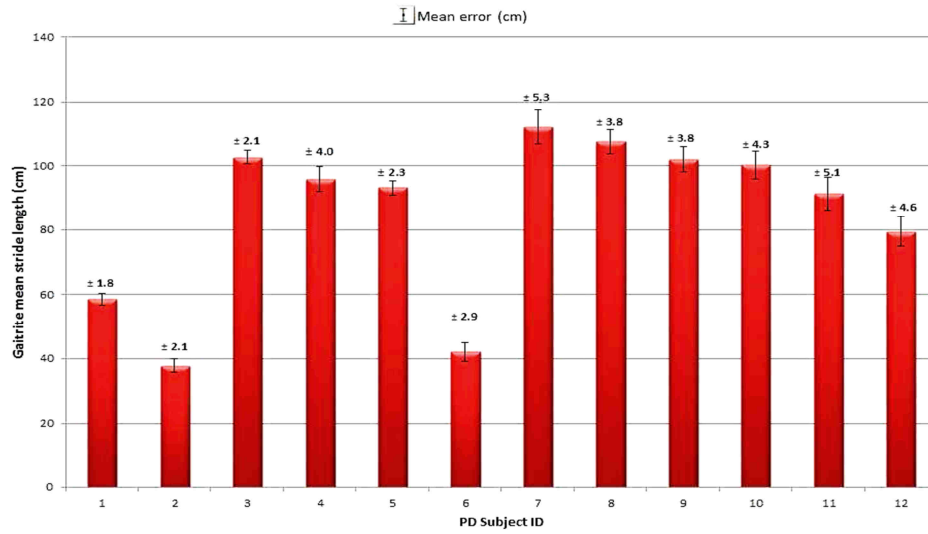


Figure 20. Stride lengths and mean errors from 12 participants with Parkinson's Disease.

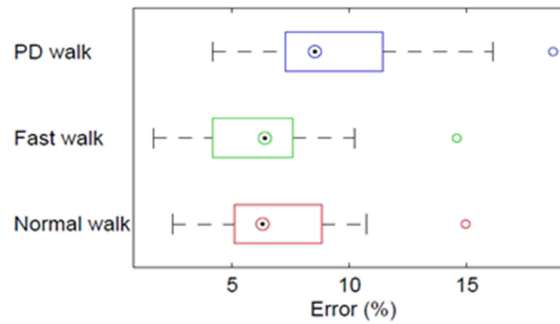


Figure 21. Box plots presenting all the errors (%) between all the trials and subjects, from both shank IMUs, for valid and Parkinson's disease gait.

The results emphasized the reliability of this first algorithm in the gait assessment of healthy volunteers, with variable lengths (113 to 200 cm) and speeds (79 to 244 cm/s) but also on patients suffering from Parkinson's disease, with consistently smaller stride lengths (38 to 113 cm). Gait partitioning and stride length estimation were accurate and robust enough to fit different morphology and type of gait patterns, with a mean error less than 9%.

The distance  $D$  between the sensor and the ankle joint has been systematically measured during the experiments and has been taken into account in the algorithm. However, the accuracy of this measure seemed to have a negligible impact on the performance of the results and could be approximately ( $\pm 2$ cm)

---

provided by the user. Two different sensors location were investigated. The results showed that the error was slightly increased ( $\approx 3\%$ ) for the foot mounted IMU. Indeed, at the mid-stance shank vertical event, the angular velocity reached a local maximum. At faster walking speeds, the impact of this estimated initial velocity based on the angular velocity becomes more important on the accuracy of the stride length computation. Because the shank IMU has a greater angular velocity than the foot one, the speed estimation is slightly underestimated. For some isolated cases, an important maximum error ( $\approx 30$  cm) generally due to a bad stride cycle detection (not properly detected because the gait pattern is too distorted). In most of the cases, PD gait presented a pattern similar to healthy gait. Nevertheless, some individuals showed huge difficulties to walk (outlier in Figure 20), thereby creating a hardly automatically and reliably segmentable pattern, which does not look as a step anymore. This underlines the influence of the gait partitioning process on the results. In the following sections, a more robust method will be presented to improve gait partitioning in these cases. The raw signals filtering also turned to be critical. Compared to other studies where a simple high pass filtering of the raw values is performed, using a zero-phase filtering enabled to keep a zero-phase distortion between accelerometer and gyrometer values.

Two different numerical integration methods were used for improving the results: the Simpson's and the trapezoidal one. The best compromise between efficiency and computational cost was obtained with the classical trapezoidal rule. Indeed, as the signals were integrated on single stride duration, the numerical drift due to the trapezoidal rule was not significant.

This first approach was designed for an offline processing. An online processing would require additional constraints, such as the filtering delay, the real-time gait partitioning (in this approach the algorithm would have a one stride delay because the current gait cycle has to be ended for being segmented) or the hardware limited real-time sampling rate (below 100 Hz an undersampled acceleration signal was found to cause major deterioration of the results).

---

Despite of an offline post-processing, being able to provide to the practitioner an accurate stride length measurement proves to be particularly useful in various contexts and clinical applications. The following section illustrates through a concrete example the use of such an algorithm in Parkinson's Disease assessment.

### **2.2.2 Application : FOGC criterion computation for FOG detection in Parkinson's Disease deficiency**

Parkinson's Disease is often associated to gait impairment and high risk of falls [142]. The small and variable stride lengths are typical characteristics of Parkinsonian gait. Their fluctuations can be directly associated with levodopa therapy efficacy, which already represents a major information for the practitioner [143] to follow the subject's recovery. Meanwhile, people suffering from this kind of disorder can also be subject to a more or less frequent and disabling event in their everyday life, difficult to assess in an ambulatory context and not always related to the dopamine level: the Freezing of Gait (FOG). This event is defined in literature as "an episodic inability (lasting seconds) to generate effective stepping in the absence of any known cause other than Parkinsonism or high-level gait disorders" [144]. This brief absence or marked reduction of forward progression of the feet despite the intention to walk can occur during initiation of the first step, turning phases [145], dual tasks, walking through narrow spaces, reaching destinations or passing through doorways [146]. FOG episodes are more often brief (1–2 s), but can also last 10 s. They are reported by the patient as a subjective feeling of "the feet being glued to the ground".

Among other symptoms related to Parkinson's Disease, festination while walking, is defined clinically as a tendency to move forward with increasingly rapid, but ever smaller steps, associated with the center of gravity falling forward over the stepping feet [147]. If the relation between festination and FOG is an important issue, it is not always well described in the literature and is often merged as a subtype of FOG.

Ambulatory monitoring FOG could significantly improve clinical management and quality of life of people with PD. Moore et al. have proposed a technique to identify FOG episodes [148] based on the frequency properties of leg vertical accelerations recorded via an IMU located on the shank. The approach is based on the hypothesis that FOG occurrences are associated to trembling motion, which affect limb acceleration signal. They have introduced the so-called freeze index (FI): the ratio between the signal (limb acceleration) power in the “freeze” band and the signal power in the “locomotor” band. The FI method was validated using one to seven accelerometers mounted on patients with satisfactory detection results. However, the FI method is not able to detect all the different FOG expressions, particularly the festination. In order to later propose an assistive solution based on FOG assessment, it was necessary to detect in a robust way every kind of FOG and related disorders. Taking advantage of the shank-mounted IMU sensor used by Moore et al., a complementary index was investigated as an illustration of the previously explained stride length estimation algorithm.

According to the festination definition and the continuous evaluation of two gait parameters: cadence and stride length, a criterion was proposed, based on the hypothesis that the cadence should increase whereas the stride length decreases when a FOG related to a festination should appear. The criterion called FOGC was defined as:

$$FOGC_n = \frac{C_n \cdot L_{min}}{C_{max} \cdot (L_n + L_{min})} \quad (15)$$

With for each detected stride  $n$ , its frequency (cadence) denoted  $C_n$ , its length  $L_n$  and  $C_{max}$  and  $L_{min}$  the expected maximal value for the cadence and minimal value for the length of strides. A minimum step length of  $L_{min} = 5$  cm was observed in the study presented in the previous section. Thus, in order to normalize the criterion to 1 when stride length tends to 0, the maximum cadence has been fixed to  $C_{max} = 5$  strides/s. The gait cycle segmentation used did not detect strides below  $1/C_{max}$  duration. A high value of the FOGC is associated to

a freezing of gait event. An increase in criterion value should indicate an imminent FOG episode.

Equipped with the same HikoB<sup>©</sup> Fox IMU synchronized to a video camera, 7 patients, (6 males, 1 female,  $70 \pm 5$  years old) participated to an experimental study (#NCT02317289, Gui de Chauliac University Hospital, Montpellier, France) where subjects were asked to walk along a 20 m corridor performing several dual tasks to maximize the number of FOG occurrences. The subjects' gait was analyzed offline based on the video recordings using a software (MovieFOG, see section 4.2.4) developed in this thesis. A practitioner spotted FOG events and classified them as follows: (1) slight modification of the gait - with no falling risk (green); (2) main gait modification with falling risk (orange); (3) FOG - gait is blocked with or without festination (red).

A total amount of 97 min of gait was recorded and analyzed. The neurologist identified and labelled 50 events (Table 3). IMU sensor data was processed in order to compute FI and FOGC indexes (Figure 22). The FI method detected 32 of these episodes and the FOGC method detected 41 of these episodes. Concerning the 31 main FOG events (labelled red and orange), FI “missed” 11 FOG events and FOGC missed only 5 of them.

FOG intensity	<i>Video</i>	<i>FI</i>	<i>FOGC</i>
Green	19	10	14
Orange	12	6	10
Red	19	16	17
False Positives	0	18	14

Table 3. FOG events labelled from video analysis and detected using FI and FOGC computation.

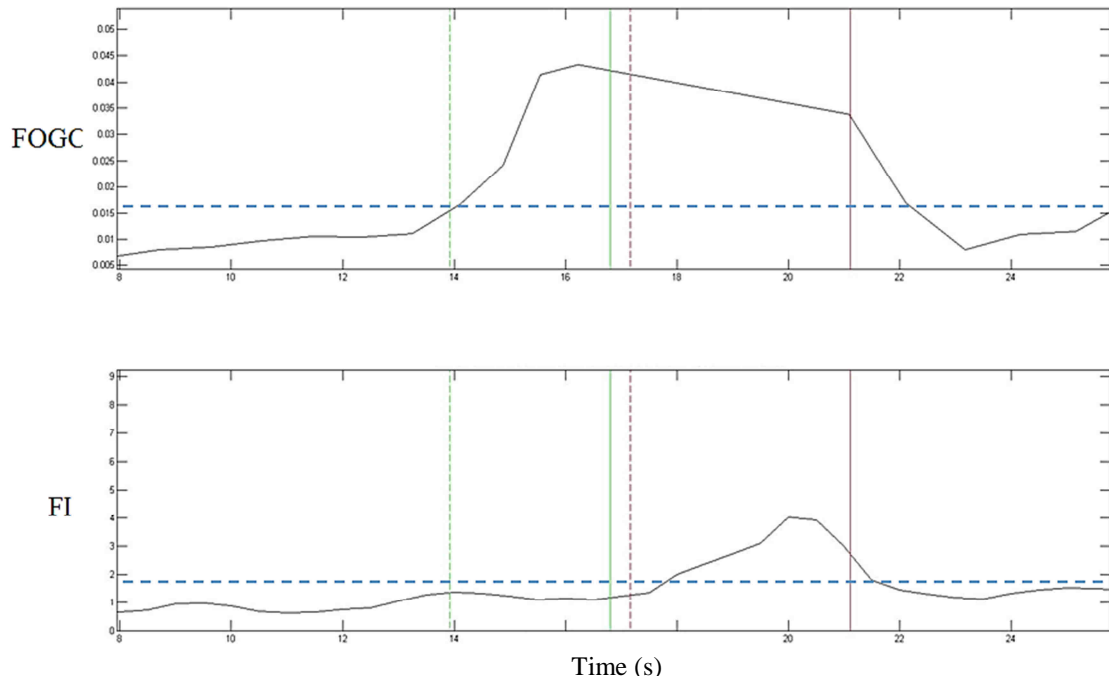


Figure 22. Example of detection performances using FI and FOGC computation. Around  $t = 16$  s, an important FOG event with tremors (Red) preceded by festination (Green) is detected by FOGC (Top). The FI increases beyond its threshold and detects also the FOG with tremors, but not the festination part (Bottom).

These preliminary results emphasized the FOG heterogeneous characteristics and the complementarity of monitoring both vertical acceleration frequencies (FOG with tremors) and stride lengths and cadence (FOG with festination). It also illustrated the advantages of using IMU in gait disorder assessment in a specific pathological context. In the next chapter, solutions will be presented to not only assess gait deficiency but to assist in real-time the subject with actuators (auditory and electrical stimuli) during his walk.

## 2.3 Pathological gait: a 3D approach

While the previous paragraphs highlighted the importance and the relevance of assessing lower limb motion in a particular clinical context, the algorithms were only applied on subjects with in most of the cases either a normal walk or with a slightly altered gait pattern (people suffering from PD).

However, this thesis aimed at addressing multiple kinds of lower limbs sensorimotor deficiencies, to propose assistive control strategies, including severely altered gait pattern (hemiplegia, cerebral palsy...).

Simple approaches previously presented suffered from various limitations in presence of impaired walk and required to go further by studying more complex solutions for assessing heavily impaired motion.

The following paragraphs will thus present different investigated approaches to provide a maximum of information (foot trajectory, joint angle...) coming from a body area network of IMUs, in order to be able to later specifically adapt the assistive solution in a maximum of pathological contexts.

All people with Parkinson's Disease, post-stroke individuals and people suffering from cerebral palsy show huge difficulties to walk, thereby compensating by a hardly automatically and reliably partitionable gait pattern, which sometimes does not look as a step anymore. In some cases, even through the use of data from the GAITRite instrumented mat does not allow to accurately recognize and identify stride cycles (Figure 23).

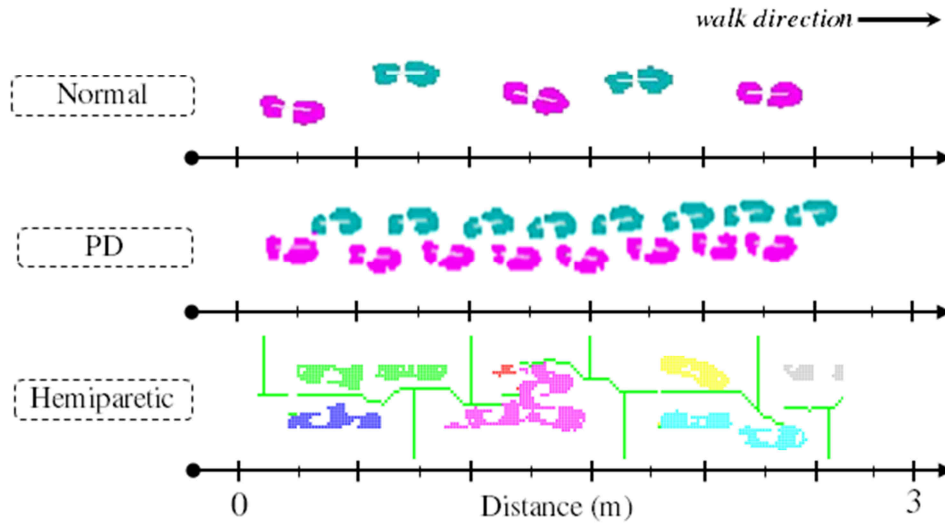


Figure 23. Gait patterns (normal, Parkinson's Disease and hemiparetic) from experimental data recorded through a GAITRite instrumented mat. The GAITRite software is not able to automatically segment hemiparetic gait. A manual identification (green lines) is not trivial and can lead to errors.

In these cases, a simple gait segmentation based on the sagittal angular speed as previously presented was not providing a sufficient accuracy and reliability.

In addition to a hardly partitionable gait pattern, post-stroke individuals often adapt compensatory strategies that lead to a direction of motion in swing phase which is no longer sagittal. Typical of cerebrovascular accident or any form of brain injury, this swing phase adaptation is called circumduction gait and is defined in literature as: “a gait in which the leg is stiff, without flexion at knee and ankle, and with each step is rotated away from the body, then towards it, forming a semicircle.” Leaning towards the unaffected side to create sufficient hip height on the affected side, the individual moves his/her foot through an arc, away from the body.

This leads to multiple major issues, particularly when segmenting gait based on a minimum number of IMUs located on lower limbs:

- the swing phase peak is sometimes missing because without any hip or knee flexion the angular velocity of the shank and/or the foot stay low (Figure 24).
- the gait pattern does not look as a cyclic or identifiable waveform anymore.

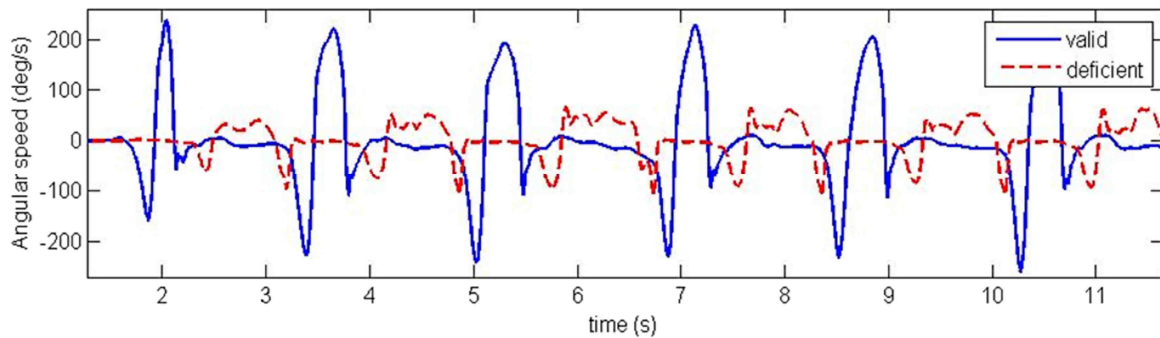


Figure 24. Sagittal angular velocity recorded from a gyrometer located on the shank of an hemiparetic individual. While on the valid side the swing phase peak can be easily identified, so as the IC and FO peaks, on the paretic side the gait pattern is considerably impaired.

Based on these observations, a new gait partitioning approach has been considered. As introduced in part 2.2.1.a, multiple existing algorithms also use acceleration data to segment gait cycle. Inspired by Moore et al. [143] work, a new partitioning method was proposed by combining angular velocity measurement with acceleration data to increase gait cycle detection robustness (Figure 25).

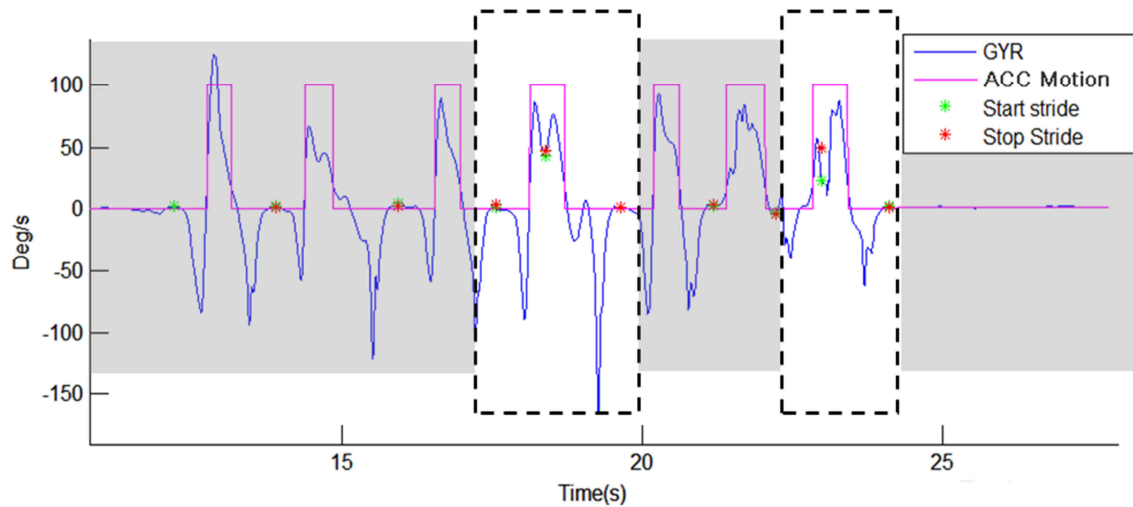


Figure 25. Example of the gait partitioning algorithm applied on data recorded from an hemiparetic gait. When gait pattern is too altered, swing phase angular velocity peak is no longer correctly detected or no peak is present because of a too slow motion. However, using the norm of the acceleration makes possible to discriminate between motion (swing) and no motion (stance). The pink curve (ACC Motion) represents the boolean result (i.e. norm of the acceleration above a preset threshold or not).

The magnitude of the accelerometer measured on the three axes (X-Y-Z) was combined with waveform initial detection from angular velocity in the sagittal plane. When the subject had a weak swing phase (e.g. circumduction gait, crouch gait in CP) and the gyrometer was not able to record any rotation, a simple threshold on acceleration magnitude was added to help increase partitioning accuracy.

In the previous parts, an important assumption was made considering the hypothesis that the lower limbs motion was assessed in a 2D plane (i.e. the sagittal plane or the heading direction plane). However, a quick observation in the field of a hemiparetic or CP individual gait highlights the strong limitation of this hypothesis. By definition, a circumduction gait leads to a 3D trajectory of the foot, for instance. This observation was a major and additional issue to gait partitioning problems when dealing with pathological motion assessment. While the first presented algorithm for stride length computation only used acceleration

---

and angular velocity, in the following paragraphs a novel method is described using an AHRS sensor fusion algorithm.

As previously introduced, not only step-by-step spatio-temporal (e.g. length, duration, clearance...) but also kinematic parameters have been shown to be clinically relevant markers of impaired walking performances [41]. Using AHRS sensor fusion algorithms could not only enable to accurately estimate sensor orientation for cancelling gravity and compute trajectory, but also to provide additional kinematics measurements, such as joint angles, for later artificially controlling motion.

In the following paragraphs, a novel approach is described to 1) compute 3D trajectory for each individual gait cycle and 2) compute joint angle (dorsiflexion angle) using two IMUs.

Experimentally validated in 26 participants with post-stroke hemiplegia (RCB 2015-A00572-47), the investigated method integrates three aspects:

- using a robust gait partitioning modality based on angular rate and acceleration combination.
- estimating the paretic foot attitude and heading in global frame based on an AHRS algorithm, for cancelling gravity and being able to integrate trajectory on each partitioned gait cycle (3D trajectory) and compute spatio-temporal parameters.
- using the same AHRS algorithm to estimate pathological joint angles (3D goniometer) to provide kinematics at different instants of the gait cycle.

### 2.3.1 Attitude based 3D Trajectory

Each quaternion representing the 3D orientation in global coordinate system was computed from 200 Hz sampled magneto-inertial data using Martin et al. [118] observer introduced in part 2.1.2. and calibrated using the same technique introduced in part 2.1.1.d.

Let us define  ${}^G\mathbf{p}$  and  ${}^G\mathbf{v}$ , the position and linear velocity of the feet sensors, respectively calculated by integrating twice and once the recorded acceleration without gravity  $\mathbf{g}$ . Given  $\mathbf{q}_B^G$  and unit quaternion properties:

$$\mathbf{q}_{acc}^B = (0, a_x^B, a_y^B, a_z^B) \quad (16)$$

we defined the following formula to rotate acceleration vector (Figure 26a) and remove gravity  $\mathbf{g}$  (Figure 26b), once the raw acceleration data filtered with a lowpass Butterworth filter (order 1,  $F_{cutoff} = 5$  Hz):

$$\mathbf{q}_{acc}^G = (0, a_x^G, a_y^G, a_z^G) = \mathbf{q}_B^G ** \mathbf{q}_{acc}^B ** \bar{\mathbf{q}}_B^G \quad (17)$$

with  $**$  the specific quaternion multiplication, known as Hamilton product [66] introduced in section 1.2.

Not only based on sagittal angular rate but also taking into account acceleration measurements, the gait partitioning method previously described was used to detect initial contact (IC).

To compute foot linear velocity, it is necessary to integrate linear accelerations on each gait cycle:

$${}^G\mathbf{v}(t) = \int_{t_{heel\ on}(n-1)}^{t_{heel\ on}(n)} (\mathbf{a}_G - \mathbf{g}) dt \quad (18)$$

where  $\mathbf{a}_G = (a_x^G, a_y^G, a_z^G)$

A ZVU (Zero Velocity Update) is then performed at each gait cycle to remove drift by adding a linear trend based on the difference between the end and the beginning of the gait cycle, making the hypothesis the linear velocity at these instants are supposed to be similar, and close to zero (Figure 26d):

$${}^G\mathbf{v}(t)_{corrected} = {}^G\mathbf{v}(t) + \frac{({}^G\mathbf{v}(t)_{end} - {}^G\mathbf{v}(t)_{start})}{N} \cdot t \quad (19)$$

Therefore, to compute foot trajectory on each strides  $n$  (Figure 26e):

$${}^G\mathbf{p}(t) = \int_{t_{heel\ on}(n-1)}^{t_{heel\ on}(n)} {}^G\mathbf{v}(t)_{corrected} dt \quad (20)$$

Stride length was then defined as the distance between two consecutive IC, computed in the transverse plane (Figure 26f):

$$SL(n) = \sqrt{(p_x[t_{ho}(n-1)] - p_x[t_{ho}(n)])^2 + (p_z[t_{ho}(n-1)] - p_z[t_{ho}(n)])^2} \quad (21)$$

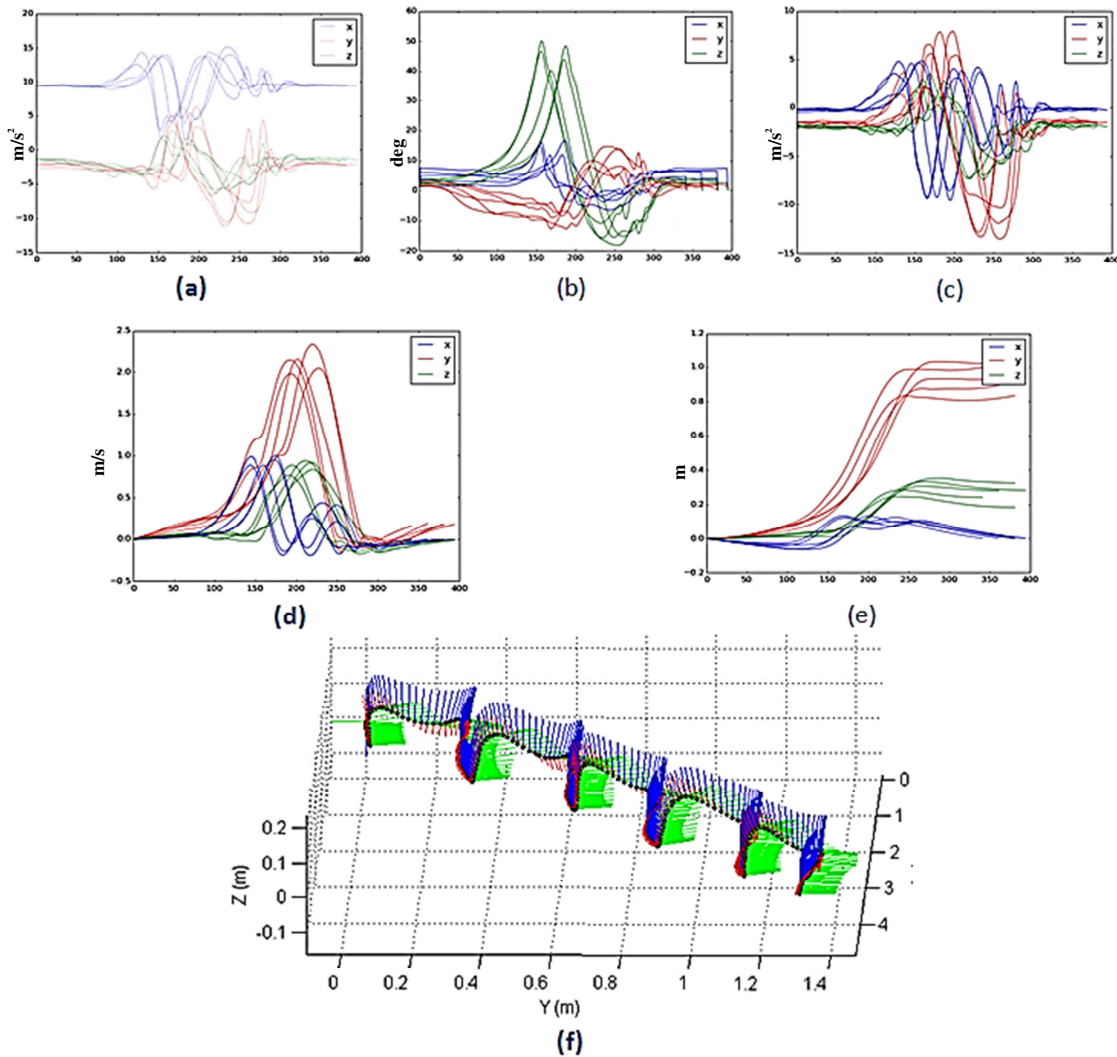


Figure 26. Processing of raw inertial data to compute 3D trajectory from a pathological gait. Illustration based on experimental data recorded from a foot mounted IMU. Raw acceleration is filtered (a). By using quaternion estimation providing the global attitude and heading of the sensor in the Earth frame (b), gravity is removed to obtain linear acceleration(c). Linear velocity is obtained by integrating the linear acceleration, and is corrected with a ZVU approach (d). By integrating linear velocity on each gait cycle, foot 3D trajectory can be estimated on each gait cycle (e,f).

### 2.3.2 3D Goniometer

By adding a second IMU and using the same quaternion estimation method, an algorithm to compute joint angles was designed and applied in the context of dorsiflexion angle computation (angle between the foot and the shank).

Let us defined  $q_{shank}^G$  and  $q_{foot}^G$  the orientation of the shank and foot sensors in the global (i.e. ground) reference frame. The dorsiflexion angle corresponds to  $q_{shank-foot}^{S_F}$ , the quaternion expressing rotations from shank to foot relative to the shank frame  $S_F$  and computed using the following formula, based on quaternion unit properties:

$$q_{shank-foot}^{S_F} = q_{dors} = \bar{q}_{shank}^G ** q_{foot}^G \quad (22)$$

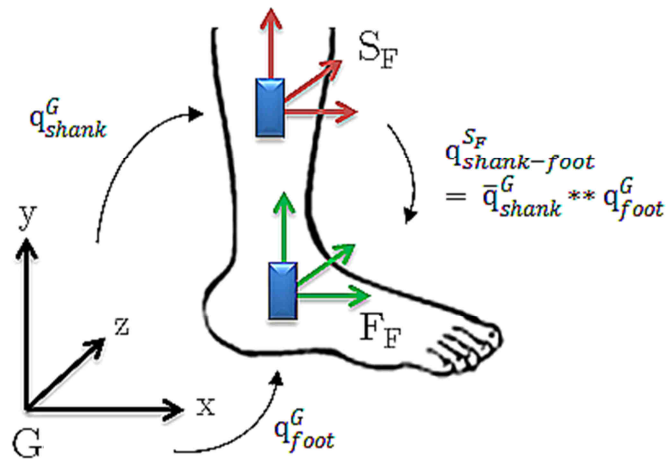


Figure 27. Dorsiflexion angle computation. The Hamilton product of the shank unit conjugate quaternion in global (Earth) frame by the quaternion of the foot also expressed in global frame gives the quaternion corresponding to the rotation of the foot relative to the shank.

### 2.3.3 Application: stroke and cerebral palsy

The two preceding methods have been validated by estimating 4 gait parameters initially defined as relevant by the practitioner to monitor rehabilitation progresses and to later adapt stimulation parameters: dorsiflexion angle at initial contact and at mid-swing instants, stride length and gait velocity.

Results were experimentally validated on 29 subjects (mean  $58.5 \pm 10.4$  years old; 9 females) after supratentorial ischaemic or hemorrhagic stroke, presenting a foot-drop, able to walk 10 meters without human help, with or without a walking stick. The protocol was approved by a national ethical committee (CPP) and by the local ethical committee of the University Hospital (CHU Nimes, France, RCB 2015-A00572-47), all subjects provided informed consent prior to the experiment.

Subjects were equipped with 2 IMUs (Fox HikoB<sup>©</sup>) on each leg strapped on a rigid support together with 4 reflective markers (Figure 28a) tracked by an optical motion capture system (OMCS, Vicon<sup>©</sup> Bonita MX) which cameras were installed along a GAITRite<sup>©</sup> walkway system (Figure 28b).

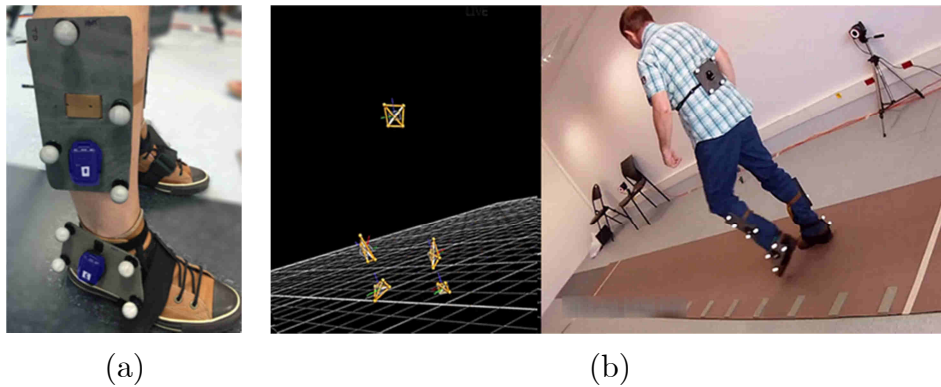


Figure 28. Each subject is equipped with IMUs strapped on rigid support together with 4 reflective markers (a) tracked by an optical motion capture system (Vicon<sup>©</sup>). Subject is instructed to stand still for 5 seconds and then walk five meters on an instrumented walkway mat (GAITRite<sup>©</sup>), turn at the end of the carpet and walk back to initial position (b). The reflective markers on the back were used for visualization only.

In order to facilitate walking and elicit measurable dorsiflexion angles, subjects were also equipped with a classical “foot drop” stimulator (Odstock<sup>©</sup> ODFS III) configured at the beginning of the experiment. Stimulation was triggered at heel off using a heel switch inside the shoe. Two electrodes of 23 cm<sup>2</sup> delivered the stimulation either to the peroneal nerve or directly to the tibialis muscles of the affected side.

In order to best match Emory Functional Ambulation Profile (E-FAP) test [149], participants were asked to walk 5 m at a comfortable self-selected speed on

the gait mat, to turn at the end of the carpet and walk back to their initial position. At the beginning of each trial, subjects were asked to stand still during 5 s for getting rid of potential biases while defining zeros between IMU system and VICON system and for enabling Martin et al. algorithm to converge to an initial attitude and heading.

In case of technical issues or data losses, each trial was repeated three times to record at least one set of data by subject. IMUs, OMCS and gait carpet were synchronized at a hardware level via a trigger sent by the GAITRite<sup>©</sup> to all the acquisition systems.

3 subjects were finally too weak to perform any trial. Therefore the analysis and results refer to 26 subjects. A total of 930 strides (457 on paretic side and 473 on healthy side) were recorded. For each stride, the spatio-temporal (stride length and velocity) parameters were computed from IMUs and compared to parameters estimated from gold standard devices. Dorsiflexion angles were compared between IMUs and Vicon<sup>©</sup> at mid-swing and heel-on, based on gait events instants extracted from GAITRite<sup>©</sup>. Table 4 shows the results for all the analyzed strides: a Root Mean Square (RMS) error between OMCS and IMUs estimations of dorsiflexion of  $5.51^\circ$  at initial contact and  $5.01^\circ$  at mid-swing and a Mean Absolute (MA) error of respectively  $3.39^\circ$  and  $3.74^\circ$ . The average dorsiflexion angle in all participants was  $8.76^\circ$  at initial contact and  $9.32^\circ$  at mid-swing. We observed a RMS error of 12.64 cm and a MA error of 9.84 cm regarding stride length estimations between GAITRite<sup>©</sup> and IMUs, and a RMS error of 6.17 cm/s and MA error of 5,06 cm/s for gait speed computation. The average stride length in all participants was 57.49 cm and the average gait speed 30.36 cm/s.

	<b>RMSE</b>	<b>MAE (<math>\pm</math>SD)</b>	<b>RMSE</b>	<b>MAE (<math>\pm</math>SD)</b>
<b>Dorsiflexion at heel on (initial contact)</b>			<b>Stride length (cm)</b>	
<b>All (S=930)</b>	5.51°	3.39° ( $\pm$ 3.37)	12.64	9.84 ( $\pm$ 7.94)
<b>Paretic side (S=457)</b>	4.89°	3.12° ( $\pm$ 3.17)	12.61	9.86 ( $\pm$ 7.87)
<b>Healthy side (S=473)</b>	6.06°	3.68° ( $\pm$ 3.56)	12.67	9.81 ( $\pm$ 8.02)
<b>Dorsiflexion at mid-swing</b>			<b>Speed (cm/s)</b>	
<b>All (S=930)</b>	5.01°	3.74° ( $\pm$ 3.83)	6.17	5.06 ( $\pm$ 3.45)
<b>Paretic side (S=457)</b>	4.89°	3.73° ( $\pm$ 3.72)	6.22	5.08 ( $\pm$ 3.47)
<b>Healthy side (S=473)</b>	6.10°	3.75° ( $\pm$ 3.95)	6.11	5.06 ( $\pm$ 3.43)

Table 4. Dorsiflexion angles RMS (root mean square) and MA (mean absolute) errors at heel on and mid-swing, between IMU computation and Vicon. Spatio-temporal parameters compared between GAITRite and IMUs computation.

The initial aim was to analyse the reliability and accuracy of using IMUs to analyse motion, for later considering them as FES-based assistive control inputs. The last sections showed how assessing pathological motion could be different from an healthy motion and challenging. It has required multiple non-optimal choices from the data collection to the algorithm design. In this last experimental protocol, OMCS data acquisition suffered from many data losses and artefacts due to VICON marker occultation by cane or markers breakage. As a result, we had to use rigid objects instead of a complete set of markers. Using a simple single strap, they were approximately positioned in sagittal plane, in order to improve visibility and ensure an eased installation time for the patient. An important advantage of the proposed approach was also the absence of specific procedure and preparation to locate sensors and use them. Except of a 5s static posture at the beginning of each trial, no specific calibration motions [47] were requested from the participants and no manual measurements of body dimensions had to be done nor individual adaptation. To estimate stride length and velocity for each step in each trial, feet trajectories had to be computed in a global frame. Usually, literature present solutions that consist in double integrating 2D linear

---

acceleration in sagittal plane with an angular rate based gait cycle segmentation and an angular rate integration to estimate orientation needed to gravity removal. In our approach, pathological gait was often associated to compensatory strategies (e.g. circumduction walk) and slow motions. As previously said, these existing methods were not applicable to assess the gait of post-stroke subjects with a complex forward swing. Therefore, we had to adapt algorithms to segment impaired gait cycle and to take advantage of Martin et al. quaternion computation to accurately remove gravity and compute joint angles. Only a few studies have been conducted in hemiplegic participants in the literature [122], thus we mainly compared our results with publications on healthy individuals [120]. They seem in accordance with a MA error less than  $4^\circ$  for the dorsiflexion angle and less than 10 cm for stride length estimation.

One challenge of this last study was also to estimate very small dorsiflexion angles (about  $10^\circ$  in all participants) in particularly constrained comparison conditions. Three different systems outputs (IMU, GAITRite<sup>©</sup> and Vicon<sup>©</sup>) were compared at different sampling rates but at a similar time mark (e.g. mid-swing). Synchronization had to be accurately done not to introduce additional error.

Computing dorsiflexion angle with an error of  $4^\circ$  has enabled to detect the dorsiflexion tendency to decrease in the presence of muscle fatigue and opens the way to adapt FES parameters for counteracting fatigue effects.

Even though the previous algorithms were applied offline for post-processing raw data, they have been designed to be straight forward implemented for online use, as intended to be used for FES control. To shorten calculation time and be able to track any orientations without singularities, the choice has been made to use a quaternion representation computed from a low-cost observer-based attitude and heading reference system in a patient-centered solution.

The results of this last study break new grounds towards adaptive online control of the dorsiflexion in post-stroke gait, such as adapting stimulation to fatigue based on dorsiflexion angle estimation. During this study, the subjects

were also asked to cross obstacles (Figure 29a). The complete knowledge of the trajectory (Figure 29b) has enabled to detect the crossed obstacles and estimate the foot clearance. These results could lead to a possible modulation of the stimulation parameters depending on the foot clearance, thereby helping the subjects to cross obstacles while limiting the compensatory strategies.

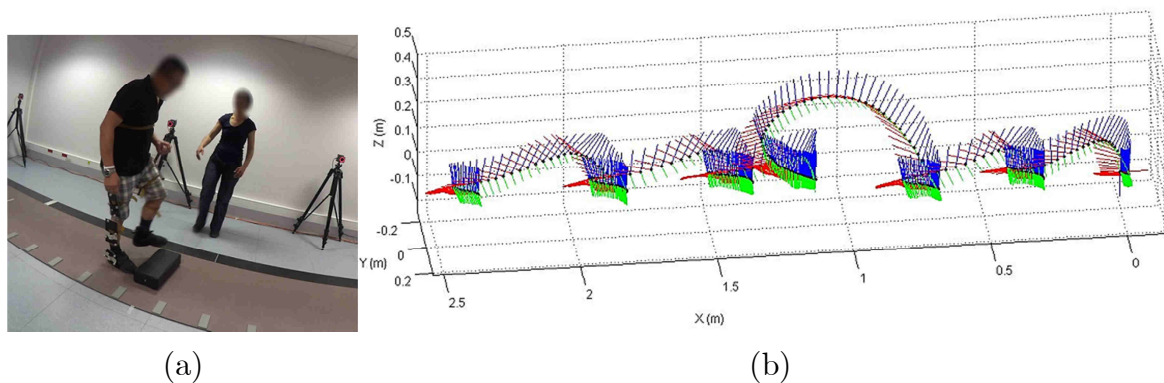


Figure 29. The participants were also asked to cross obstacles (a). The complete knowledge of the foot trajectory (b) could also enable to adapt the stimulation to obstacles and foot clearance. Illustration from experimental protocol.

The same algorithms were also applied on a set of data recorded as part of a collaboration with the Motion & Gait Analysis laboratory in Lucile Packard Children's Hospital in Stanford. Using the same sensors, different patterns characterizing the gait of children with cerebral palsy (toe walking, stiff knee gait, crouch knee gait, circumduction gait...) were assessed, in order to validate the feasibility of using the same approach on a different patient population.

---

The results presented through this thesis chapter aimed to investigate the ability of using IMUs to 1) observe and analyse pathological lower limb motions (joint angle, stride length, foot clearance, gait speed, FOG detection, etc...) 2) in order to use them as inputs to control an FES system, in a clinical context or for a personal use, considering only patient-centered solutions.

Several compromises had to be made between accessibility, usability and accuracy needed to go further into the achievement of efficient neurorehabilitation solutions.

In the following chapter, using the knowledge and algorithms performed on motion analysis, a particular focus is given to fulfill the main and initial goal of this thesis work: to offer adaptable, accessible and user-friendly FES-based assistive solutions in different pathologies affecting lower limb motions, based on a network of generic sensors and stimulators.

---

## 3 Controlling and acting on the motion

As introduced in section 1.1.3, FES systems need to provide a tailored but easy-to-use solution to efficiently restore motor functions following a CNS injury or disorder in lower limb neurorehabilitation. To ensure an appropriate control, these systems are often associated with different technologies in order to adapt the stimulation to the elicited action. Inertial sensors could offer a promising solution to answer to the different associated constraints (accuracy, portability, ease of use, cost...). Initially designed for aircraft navigation, to be able to use this technology in a clinical context, keeping in mind the different associated constraints of a patient-centered solution has required multiple studies. Addressed as an objective assessment tool in the previous chapter, the knowledge of ongoing lower limb motion can also be used as a feedback for closed-loop control or as an event to trigger the stimulation depending, for instance, on the voluntary motion.

This chapter presents the work done through this thesis around three patient populations (PD, SCI and post-stroke), combining with FES the knowledge and algorithms previously presented, from open-loop sensitive electrical stimulation to closed-loop motor stimulation of lower limbs.

*The results presented in this chapter have been published in the following papers: [61], [150], [159], [151]–[158].*

### 3.1 Open-loop control in Parkinson's Disease: triggering sensitive electrical stimulation at heel off

As previously introduced in part 2.2.2, the FOG (Freezing Of Gait) represents a major issue strongly affecting life quality of people suffering from Parkinson's Disease (PD).

Meanwhile, multiple existing solutions could be used to assist the gait of people with PD and some were investigated in this thesis, using IMUs to individually adapt the assistive approach.

Previous studies have shown that visual (e.g. rolling walker or cane with a laser beam visual cue on the floor) or auditory stimuli (e.g. using a metronome beeping at the gait pace) can help individuals with PD to reduce the occurrence and duration of FOG events [160]–[162] thereby improving their gait [163]. In a meta-analysis, Spaulding et al. [164] reviewed the numerous studies on visual and auditory cueing by comparing their efficacy on gait. They concluded to a benefit of auditory cueing on velocity, stride length and cadence; while visual cueing only resulted in stride length changes. Nevertheless, auditory and visual cueing modalities appear to be effective only in experimental and controlled conditions [165]. It has been also shown that variability in beat perception between subjects could differently affect gait when synchronizing footsteps to music or metronome cues [166].

The effects of sensorimotor cueing are not clearly established because this stimulation modality has received little attention comparatively to other ones. Numerous studies confirmed that Parkinson's disease motor deficits are associated with proprioceptive impairments. Vaugoyeau et al. [167] analyzed the postural adjustments of PD subjects standing on a platform executing small angular sinusoidal oscillations. Subjects were asked to maintain a vertical posture. In the absence of visual cues, subjects were clearly unable to use proprioceptive information as feedback to control their body verticality and stabilize their body

segments, resulting in blocking head and shoulders segments. The same strategies have been observed during gait [168]. The authors concluded that sensorimotor integration deficits partly account for the postural and locomotion impairments observed in PD. Other studies have shown that gait in PD patients could be improved by increasing somatosensory information from the plantar surface of the feet using textured insoles [169]. Rhythmic somatosensory cueing (RSC) has also been investigated [165] ; authors used a miniature-vibrating cylinder attached to the wrist as a cueing device in 17 patients. RSC improved the gait with lower stride frequencies and larger step lengths, while maintaining walking speed. This study showed that patients with PD could dynamically modify their stepping pattern to adapt to an external stimulus using somatosensory pathways. RSC seems to have a robust effect in gait pattern and to be resistant to visual interferences. Authors suggested that this technique could be a viable alternative to auditory or visual cueing.

Using muscle vibration during voluntary dorsiflexion movements of the ankle joint, Khudados et al. [170] showed that proprioceptive regulation of voluntary movement is disturbed in PD. El-Tamawy et al. [171] used augmented proprioceptive cues during gait on thirty levodopa-dependent PD subjects. They applied vibratory stimuli to the feet plantar surfaces (below the heel and forefoot) through miniature hidden vibrating devices that sent rhythmic vibrations to the skin in synchronization with the step at the push off-phase of the gait. Results demonstrated a significant improvement in gait kinematics and angular excursion of lower limb joints. Similarly, Kleiner et al. [172] applied mechanical stimulation (AMPS: Automated Mechanical Peripheral Stimulation Treatment) on four specific target areas in patient's feet while they were laying down and reported a 15% improvement in gait velocity after treatment.

To our knowledge, only three studies involving cutaneous electrical stimulation (ES) applied on patients with PD have been published. Mann et al. [173] studied the feasibility of functional electrical stimulation (FES) to assist gait in PD. During eight weeks they performed walking sessions under electrical stimulation

of the common peroneal nerve of the more affected leg in 6 subjects. Stimulation was triggered by a pressure-sensitive switch in the shoe and set to gain effective dorsiflexion and eversion of the foot during walking similarly to a drop foot stimulation modality. An immediate improvement was demonstrated with FES on distance and average stride length during a 3-min walk but not on the number of steps and walking speed. Fewer episodes of FOG occurred during the treatment period. Similarly, Popa et al. [174] used FES to assist dorsiflexion on 11 PD subjects during two weeks. They noticed a slight increase in step length and cadence. In the third study [175], the same motor stimulation approach was applied on 9 PD patients. Results showed a decreased duration of double support phase and variability of stride duration and stride length with FES. Two subjects did not experience FOG in a few situations where they previously experienced some. All of these protocols used the electrical stimulation (ES) at a motor level with a modality similar to the one used for correcting the foot-drop syndrome in post-stroke individuals (i.e. common peroneal nerve stimulation). To our knowledge, no protocol has investigated yet the use of ES at a sensory level in this context.

From these previous statements, we decided to design a protocol based on assessing the effects of somatosensory cueing by sensitive electrical stimulation.

### 3.1.1 Electrical Stimulation

Inspired by Spaich work on hemiparetic gait [11], we stimulated the arch of the foot as shown in Figure 31. A self-adhesive electrode (2.6 cm<sup>2</sup>) was placed as the cathode on the arch of the foot and a large common anode (45 cm<sup>2</sup>) was placed on the dorsum of the foot (Figure 31). The stimulation pattern consisted in five 500  $\mu$ s/phase charge-balanced biphasic pulses delivered at 200 Hz, repeated 4 times at 10 Hz.

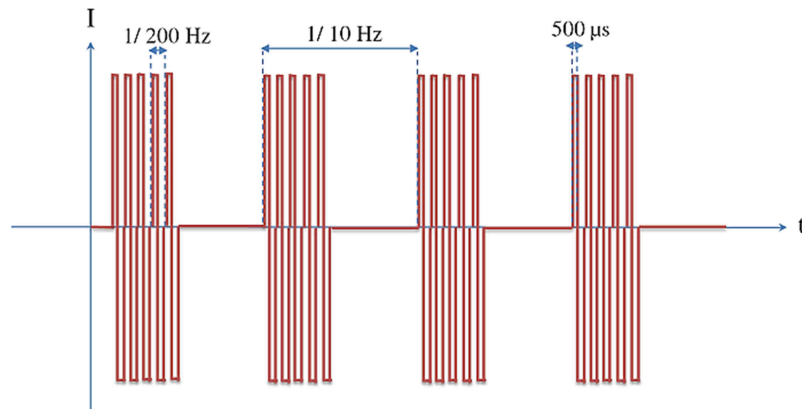


Figure 30. Nociceptive stimulation pattern consisted in five 500  $\mu\text{s}$ /phase charge balanced biphasic pulses delivered at 200 Hz, repeated 4 times at 10 Hz.

Current amplitude was adjusted in order for the subject to feel the stimulation without any discomfort ( $7 \leq I(\text{mA}) \leq 60$ ). Our initial hypothesis was to use a nociceptive stimulus to trigger a withdrawal reflex for helping to elicit gait at heel off. However the needed stimulation levels for enabling the reflex were too high and even at high intensities no withdrawal could be successfully triggered in some patients, thereby leading us to stay at a lower stimulation level. Subjects were equipped with one inertial measurement unit (Fox Hikob) strapped to the foot and a wirelessly programmable electro-stimulator (Phenix© Neo Usb, Montpellier, France) strapped around the shank (Figure 33).

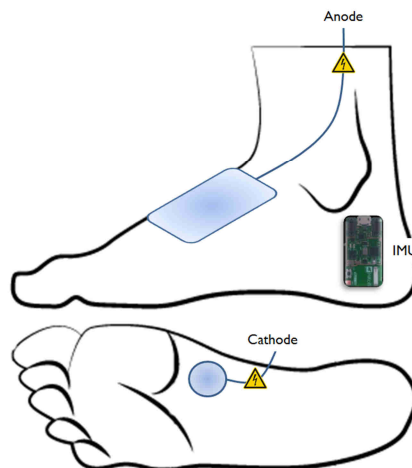


Figure 31. Electrodes and IMU locations. To deliver the stimulation, a self-adhesive electrode is placed as the cathode on the arch of the foot and a common anode is placed on the dorsum of the foot.

### 3.1.2 IMU based triggering

The stimulation was triggered thanks to the inertial information recorded from an IMU strapped to the foot. Compared to the previous sections, in this study the IMU data were processed online on a computer wirelessly collecting accelerometer and gyrometer data at a 100 Hz sampling rate.

The strategy was to determine the feasibility of using one inertial sensor as a heel switch alternative in order to trigger stimulation.

In addition to the advantages presented in section 2.2.1.a compared to a classical heel switch inside the shoe, the use of an IMU was motivated by the potential information available from the sensor to online modulate the stimulation depending on various parameters: FOG detection based on the methods presented in section 2.2.2, U-turn detection, gait cadence, obstacle detection, etc... The same sensor may also be used to monitor gait spatio-temporal parameters to assess functional improvement, based on the different algorithms presented in chapter 2.

While few studies investigated offline gait partitioning using IMUs in PD [143], [176], the challenge here has been to adapt the approach presented in section 2.3 and validated offline on able-bodied post-stroke and PD subjects, for an online use.

The triggering modality aimed at detecting stance and motion periods from the foot mounted IMU combining accelerometer and gyrometer measurements. In order to be the most sensitive and responsive to heel off velocity, the choice was made to attach the IMU under the lateral malleolus. For defining the lowest sensibility thresholds, acceleration and angular velocity raw data were firstly filtered with a low-pass filter to get rid of high frequency noises.

As the latency was a crucial parameter, we chose to use an Exponential Moving Average (EMA, low pass, Infinite Impulse Response - IIR) filter instead of the zero phase filters used in chapter 2. At any time, the output of the filter  $gX_{filt}$  was a weighted sum of the new sensor value  $gX_{raw}$  and the old filter output  $gX_{filt_{old}}$ . Filter coefficient  $\alpha$  controlled the filtering effects:

$$gX_{filt} = (1 - \alpha) \cdot gX_{filt_{old}} + \alpha \cdot gX_{raw} \quad (23)$$

with  $\alpha \in [0,1]$ .

The best filtering parameters were found to be an attenuation of 3 dB at a cutoff frequency of 5 Hz using  $\alpha = 0.1367$  with only one sample late. From gyrometer angular profile, we determined a magnitude threshold, which was the limit between foot flat phase and heel off phase ( $gyr_{th} \cong 30$  deg/s).

Combining accelerometer and gyrometer 3D norms of filtered data, we were able to successfully detect non-stationary periods on every PD subject. A maximum stimulation duration and a minimum successive stride time duration were also defined.

Based on the following equation, stimulation was triggered when a non-stationary period was detected.

$$if \left\{ \begin{array}{l} norm(acc_{filt}) \leq acc_{th} \\ \text{and} \\ norm(gyr_{filt}) \leq gyr_{th} \end{array} \right\} = \text{stationary/stance state} \quad (24)$$

To validate this approach on people suffering from PD, a preliminary offline analysis of experimental data recorded online from a foot mounted IMU was performed. The Start/End times of the stationary period as detected online through the previous equation were assessed. As an example, in Figure 32 is plotted the foot angular speed and the Start/Stop stimulation events triggered by the non-stationary period detection algorithm. Recorded from a real-time trial, it illustrates relatively to Terminal Stance (TS) sub-phase and Swing phase (Figure 14) that stimulation was actually initiated during TS and terminated during swing phase (depending on the preset stimulation duration), which was close enough of the sought stimulation event.

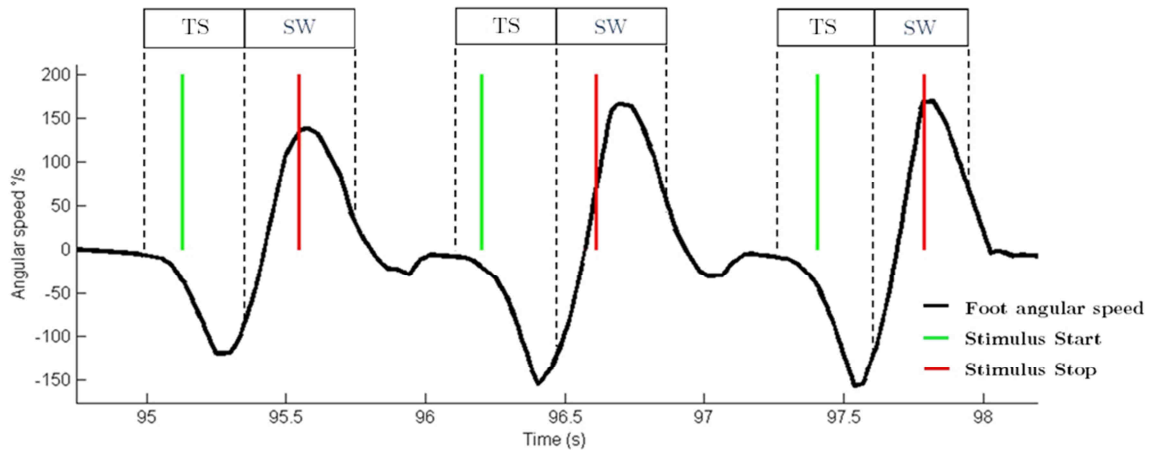


Figure 32. Example of real-time stimulation triggering based on accelerometer and gyrometer 3D norms of filtered data from an experimental record on PD individuals. Green and red lines are respectively the start and stop stimulation events triggered by the IMU-based detection algorithm. Terminal Stance (TS) sub-phase and swing (SW) phases were manually added to the figure for reference.

### 3.1.3 Experimental protocol

Most of the published studies have assessed the effect of cueing only during straight walking, in experimental conditions and with severe dopamine deficiency. However, FOG occurs in a random manner, in different environments, depending from the dopaminergic and emotional status.

In both ON and OFF conditions (under medication or not), turning phase has been demonstrated as the most frequent trigger of freezing of gait in Parkinson's disease. In their study, Schaafsma et al [177] found that FOG was mainly elicited by turns (63%), first step (23%), walking through narrow spaces (12%) and reaching destinations (9%). We also observed this predominance in some of our previous experiments [55]. Plotnik et al. tried to explain this occurrence by the asymmetric nature of these tasks, which would increase interlimb synchronization difficulties [178]. Crenna et al. showed this could possibly be related to a head rotation control. Indeed, patients in the early stage of the disease initiate head rotation later than controls while turning [179]. Nieuwboer et al. [145] chose to

focus their work on functional turning performance with different cueing modalities and observed it improved the turning speed in all subjects.

In order to increase FOG occurrence during experimentations and to be close to the daily life situations, we designed an experimental path including thus a maximum of turning phases.

13 subjects with Parkinson's disease (10 male, 3 female; Age range: 60 to 82 years) participated to the study (Table 5).

ID	AGE	DISEASE DURATION (years)	STAGE (H&Y)	AGE OF ONSET	*MDS-UPDRS			**MoCA
					3.11: FREEZING / 3.10: WALK / GLOBAL PART III	Freezing (Occasional / Frequent)	Falls (Y/N)	
1	71	5	2	66	1/1/28	O	N	26
2	63	7	3	56	1/1/28	F	Y	30
3	71	18	3	53	2/2/40	F	Y	30
4	74	22	3	52	1/2/23	F	Y	25
5	72	7	3	65	2/2/28	F	Y	27
6	74	8	3	48	3/3/na	F	Y	12
7	60	13	3	47	3/2/29	F	Y	25
8	66	3	4	63	2/1/30	F	Y	23
9	76	7	3	69	1/1/32	F	N	23
10	74	10	3	64	2/3/35	F	N	21
11	66	14	4	52	4/4/66	F	Y	na
12	74	13	3	61	2/2/41	F	Y	25
13	82	15	3	67	1/3/47	F	Y	26

Table 5. Clinical data of patients included in the study.

\*MDS-UPDRS: Movement Disorder Society-Unified Parkinson's Disease Rating Scale, from 0(normal) to 4(inability)

\*\*MoCA: MONTreal Cognitive Assessment, the maximum score is 30 points; a score of 26 or above is considered normal.

The protocol has been approved by local ethical committee (international identification number NCT02317289). Participants were recruited at the Neurology (Gui de Chauliac Hospital) and Gerontology (Balmes Center) departments of Montpellier hospital (CHU Montpellier). All subjects gave their informed written consent and were under the care of a neurologist also in charge of collecting clinical data.

The experimental protocol was divided into two parts: A) The first part consisted in recording the time needed for the subject to stand up, to walk three meters, to do a U-turn, to come back and to sit down. This task is also known as

‘Timed Up and Go’ (TUG) and described for the first time in Podsiadlo [180]. TUG task was repeated twice by the subjects. All trials were video-recorded. Using a software developed in this thesis (MovieFOG, see section 4.2.4) each event was manually labelled and timed. Part A was designed to evaluate TUG as a possible tool for measuring FOG occurrence, gait performances and motor disorders. The aim was to better characterize subject’s profile regarding responsivity to part B): this second and main part of the protocol consisted in assessing the use of electrical stimulation as a cueing method on the same population.

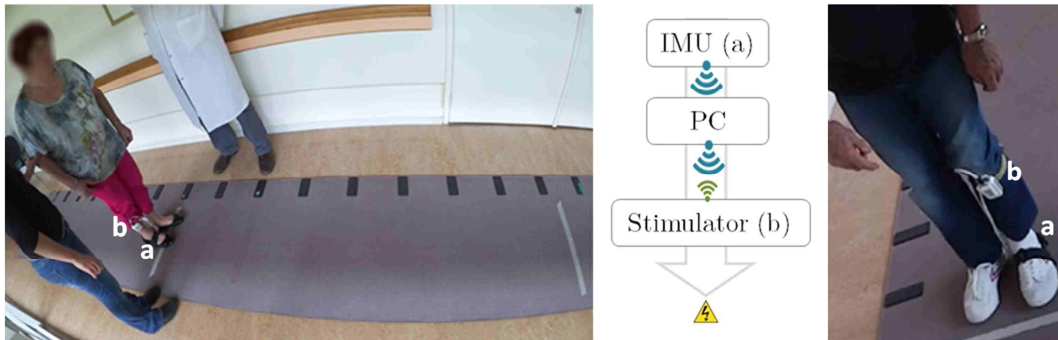


Figure 33. The participant is equipped with an inertial measurement unit (a) and a programmable stimulator (b) wirelessly connected through a PC.

Participants started from standing in the middle of a gait carpet. After a short familiarization to walk under stimulation, subjects were instructed to walk until reaching a line drawn on the ground, then do a U-turn, walk 5 meters, walk around a cone and keep walking to the start-stop line in the middle of the carpet (Figure 34). The test was repeated five times under the following conditions: no cueing pre-condition (C0), stimulation cueing (C1), no cueing post-condition (C0bis). C0 is considered as the baseline. For eliminating learning bias, we asked the participants to perform a 10 min ecological path without stimulation (random walk in the hospital) between C1 and C0bis conditions, to ensure in case of improvement in C1 that the performances went back to baseline level in C0bis.

In each condition (5 trials per condition) of the stimulation protocol, we analyzed the last three trials. Each FOG event, U-turn execution time, 5-meter

execution time and time to walk-around the cone were assessed from the video recording.

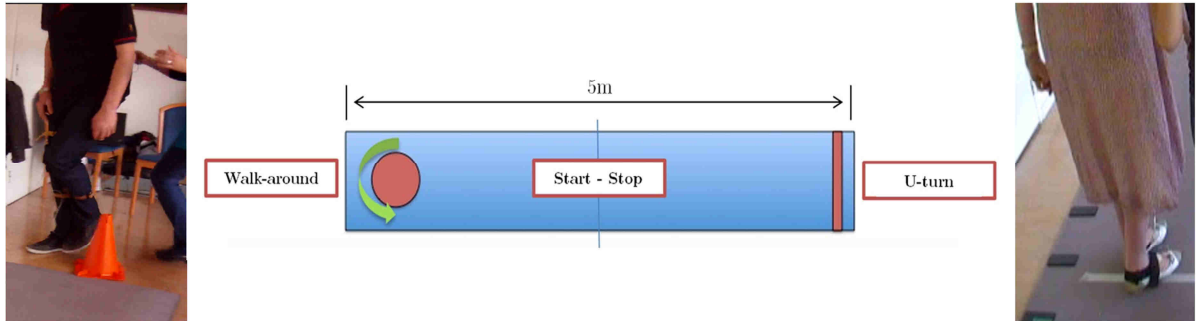


Figure 34. Five meters experimentation path. The subject starts in the middle of the walkway, walks 2,5 m, performs a U-turn at the line, goes back 5 m, walks around a cone, walks back 2,5 m then stops where he started.

### 3.1.4 Functional results and discussion

During the “Timed Up and Go” test, we assessed through video recording the total duration needed for the participants to accomplish the whole path, their cadence, average speed, and the FOG occurrences and durations (Table 6). Four participants over the 13 did not experience any FOG event during the TUG task. Twenty-six FOG events have been identified over the 2 TUG trials of these 13 participants (Figure 35).

ID	TUG 1					TUG 2				
	T.U.G. DUR. (s)	# FOG	FOG MEAN DURATION (s)	CADENCE (step/min)	AVG. SPEED (km/h)	T.U.G. DUR. (s)	# FOG	FOG MEAN DURATION (s)	CADENCE (step/min)	AVG. SPEED (km/h)
1	10.1	0		105	2.2	11.2	0		110	2.0
2	14.2	1	3.1	60	1.5	19.1	1	7.1	65	1.1
3	16.7	1	2.3	60	1.4	13.1	1	2.2	90	1.7
4	21.6	0		65	1.0	19.2	0		65	1.1
5	15.5	0		60	1.4	10.1	0		60	2.2
6	17.3	0		65	1.3	14.2	0		60	1.5
7	13.1	2	2.6	65	1.7	12.6	2	2.5	60	1.8
8	35.0	2	8.2	48	0.6	25.4	2	10.1	45	0.9
9	22.2	1	3.4	50	1.0	21.8	1	3.2	48	1.0
10	40.3	2	10.6	75	0.5	26.7	1	5.7	110	0.8
11	30.6	2	1.2	80	0.7	22.2	3	3.4	100	1.0
12	13.2	1	1.1	90	1.7	13.0	0		96	1.7
13	70.1	3	3.3	72	0.3					

Table 6. Timed Up and Go (TUG): Freezing Of Gait occurrence and gait performances

In the study presented in part 2.2.2 of this thesis, we observed that people with Parkinson's Disease scored with a high FOG-Q in daily life were not necessarily those who were prone to experience FOG during clinical experimental protocols. In Table 5, we can see that subjects ID 2, 3 and 4 reported as frequent freezers in their daily life did not freeze in C0 and only once during the TUG task for the patient ID2. Thus we chose to classify the studied population in two groups, whether subjects experienced FOG in C0 or not.

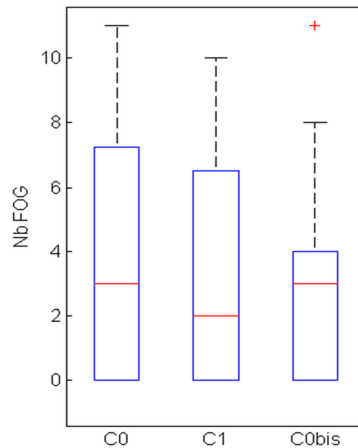


Figure 35. Number of Freezing of Gait events in baseline (C0), stimulation (C1) and control baseline (C0bis) on all subjects ( $n = 13$ ).

In the “freezers group” ( $n=9$ ), we observed that cueing globally decreased of 12% FOG occurrence compared to baseline without cueing. Table 7 shows cueing’s effects in relation to baselines for all the participants and in each subgroup during the different experimental path phases. Cueing improved gait performances in all the participants. A reduction of 15% in turning time, 14% in 5-m covering duration and 19% in time needed to walk-around the cone was observed. In “freezers group”, turning time was improved by 21%, time to walk-around the cone was reduced by 25% and the duration needed to cover the 5-m walk decreased by 18%. The entire path was completed 19% shorter than baseline.

	All (N=13)	Non Freezers (n=4)	Freezers (n=9)
U-Turn Time (s)			
Baseline 1 (C0)	3.0 (1.6)	1.9 (0.6)	4.1 (3.0)
<b>Stimulation (C1)</b>	<b>2.6 (1.1)</b>	<b>1.8 (0.6)</b>	<b>3.4 (2.7)</b>
Baseline 2 (C0bis)	3.2 (1.3)	2.2 (0.9)	4.1 (3.0)
Walk Around Time (s)			
Baseline 1 (C0)	4.7 (3.5)	2.2 (0.3)	7.2 (3.5)
<b>Stimulation (C1)</b>	<b>3.8 (2.3)</b>	<b>2.1 (0.4)</b>	<b>5.4 (4.1)</b>
Baseline 2 (C0bis)	4.7 (3.5)	2.2 (0.3)	7.2 (6.5)
5m Time (s)			
Baseline 1 (C0)	6.7 (1.8)	5.4 (1.3)	7.9 (4.2)
<b>Stimulation (C1)</b>	<b>5.8 (1.3)</b>	<b>4.9 (1.6)</b>	<b>6.7 (2.1)</b>
Baseline 2 (C0bis)	6.6 (1.6)	5.4 (0.8)	7.7 (3.3)

Table 7 Durations (standard deviation) of u-turn, 5-meters and Walk-around phases compared between baseline 1 (C0), stimulation (C1) and baseline 2 (C0bis) in all the subjects (n=13) and in the subgroups (freezers and non-freezers in C0).

FOG repartition on all trials was four times more frequent during turning phases than when walking in a straight line, and two patients who did not freeze doing TUG task, actually froze in C0 (Figure 36).

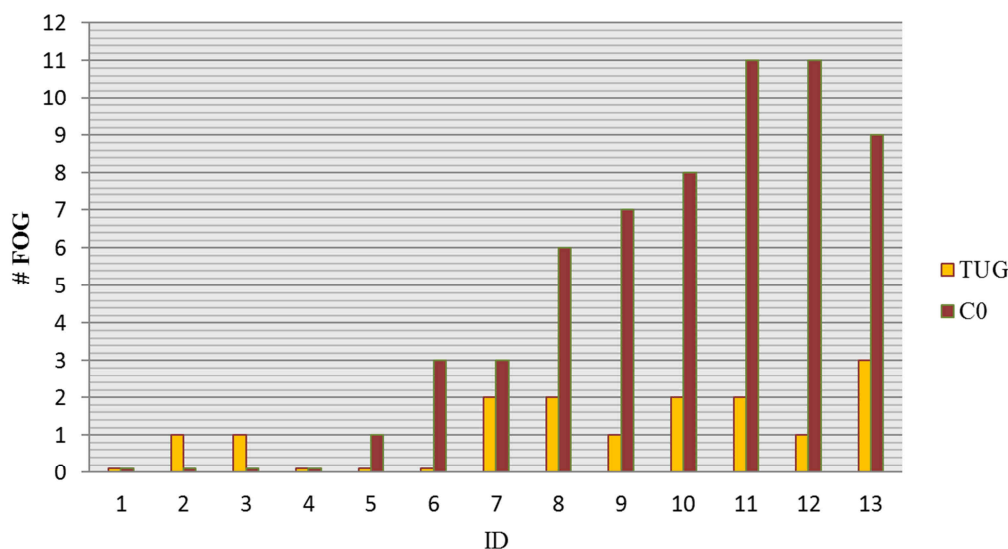


Figure 36. FOG events repartition between “Timed Up and Go” protocol and C0 condition (stimulation protocol baseline).

Two subjects (ID 7 and 13) showed a strong responsivity to the stimulation protocol and required to go further in analysing their results (Figure 37), subject ID13 was one of the slowest participants as he needed more than 13 s to perform

the 5 m path. This was reduced to 8 s with electrical stimulation based cueing in C1. Without stimulation he froze systematically doing the turning phase while he did not freeze at all in C1. Subject ID7 froze seven times during C0 protocol. With stimulation he froze only twice and the mean duration of his FOG events decreased from 5.5 s to 2.4 s. However, the time to perform the 5 m path remained unchanged in both conditions.

According to the preceding protocol presented in section 2.2, we considered as significant a change in stride length greater than or equal to 20 %. Using the stride length estimation algorithm presented in the same section, we computed the stride length and cadence of subjects ID7 and ID13 from IMU. While there were no significant changes in stride length (<10 % increase) for both participants, the cadence of subject ID13 increased of 41 % in C1 condition.

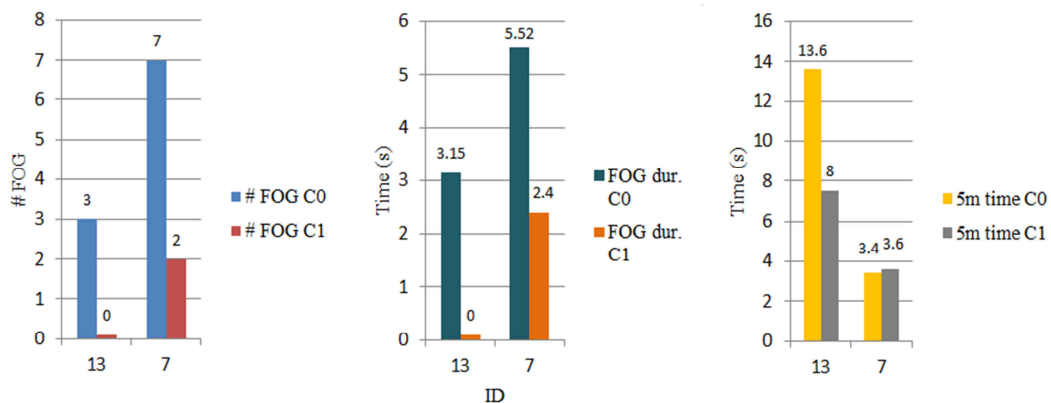


Figure 37. Subjects ID13 and ID7: FOG occurrence, FOG duration and time needed to walk 5 m. Comparison between C0 (baseline) and C1 (electrical stimulation)

Through this study, we investigated the feasibility of using electrical stimulation as a somatosensory cueing method of walking in Parkinson's disease. The aim was to investigate the capability of this cueing modality to prevent or at least reduce FOG events and to improve gait performances in this CNS disorder.

As partly related to environmental triggers, assessing freezing of gait during a clinical protocol was challenging. In accordance with other studies, our comparative results showed that there is some discrepancy between patient's self-

---

assessment and walking task measurements, which highlights the use of wearable sensors to better assess FOG in ecological conditions. The occurrence of freezing episodes is highly variable in mild freezers and depends on the emotional context and on the tasks repetitions. For instance, we noticed that some subjects could freeze repeatedly from the waiting room to the laboratory and rarely during the experiment. It has been hypothesized that people with PD use attentional strategies to compensate for their gait impairment. This cognitive engagement could be insufficient in a cognitive dual task but could be helpful in a challenging condition, like a research experiment. In the latter case, the participant (ID13) initially showing a strong responsivity to the stimulation protocol was asked to perform the same protocol one year later. During this past year, the participant had developed himself a strategy consisting in focusing on planning his walk trajectory and imagining each of his initiation step is done as if he was in a stair. At this point, neither the stimulation protocol or an auditory cueing triggered at HO could significantly improve his condition. This discrepancy raises questions about the specificities that would need each cueing method. The effect of auditory rhythm on gait would seem to be directly correlated to stimuli properties. It would be superior when using non isosynchronous rhythm [181]. When louder, auditory stimuli could improve force [182]. Rythmic auditory cueing seems also to be effective on improving perceptual and motor timing [183] and can be used as a gait rehabilitation method in people with PD [184]. The meta-analysis done by Spaulding et al. [164] conclude that auditory cueing is more effective that visual cueing. The former improved stride velocity while visual cueing only significantly improved stride length (Hedge  $g=.554$ ; 95% CI,  $.072-1.036$ ). However there is no gold standard for evaluating the effect of interventions on FOG, which limits considerably comparative studies.

Based on previous observations and literature, we designed a protocol with turning phases in order to increase FOG events occurrence. This hypothesis has been validated as FOG repartition on all trials was four times more frequent

---

during turning phases than when walking in a straight line and two patients who did not freeze doing TUG, actually froze in C0 (Figure 36).

Our results show a global positive effect on gait performances, as the time needed to achieve the protocol was considerably shorter with stimulation cueing. “Freezer” patients tend to be more responsive to cueing, with a turning time improved by 21%. We also observe a 12% decrease in FOG occurrence compared to baseline. However, the size of the studied population was too small for showing a statistically significant effect. Extra experiments should be done to include more participants.

None of the participants reported uncomfortable sensations induced by electrical stimulation. Some of them expressed an interest in such a possibility to be helped while walking in their daily-life and seemed to accept the additional technological equipment arising from it. In common with auditory and visual stimuli in other studies, sensitivity to the electrical cueing differs among the patients. We noticed that the electrical stimulation threshold needed for feeling the stimulus was highly variable between patients. Two of our 13 participants have been clearly improved by the stimulation (respectively 85% of FOG events reduction and a 5-m path 42% shorter compared to baseline for one), while it did not affect at all some others. In any cases, stimulation cueing never worsen performances or FOG occurrence.

In this protocol, the use of an inertial sensor based trigger did not offer much more functionality than a basic heel switch, except an eased installation on the subject and the ability to later assess motion with the practitioner. However, having access to gait kinematics data [58], [185] and to path information from only one sensor could be useful to real-time adapt cueing, when for example a turning phase or a FOG event [55], [186] is detected by the sensor. We could also modulate stimulation or dynamically change the trigger timing regarding walking rhythm or external events. Many other triggering strategies could be investigated to synchronize the stimulation with voluntary motion. Some technical aspects also need to be improved for getting rid of some latency problems experienced

---

during the trials (e.g. wireless data losses and radio disturbances, see section 4.2). Another approach could also consist in eliciting different responses by testing various electrode locations under the foot [187].

Due to technical constraints, only one leg of each subject was equipped. We asked them which direction of rotation was the most difficult for them and the most problematic limb was equipped. Considering the stimulation side may affect the observed effects in asymmetric tasks, upcoming experiments should also involve bilateral stimulation.

Through this study and this thesis section, the feasibility of using an IMU to trigger and adapt electrical stimulation in Parkinson's disease was investigated. While no closed-loop control have been performed yet, the command issued by the IMU-based algorithm provided an assistive aid by eliciting motion at HO.

This experimental protocol also validated the use of only one IMU, with no individual thresholds and no prior procedure, not only to trigger online electrical stimulation but to assess a pathological gait while designing a patient-centered solution.

The functional aim was to investigate the capability of this cueing modality to prevent or at least reduce FOG events and to improve gait performances, which was partly reached in some participants.

Meanwhile, the stimulation was sent at a sensory level of intensity and was based on a nociceptive approach. In the next section, a first step toward closed-loop control is presented through the use of FES at a motor level of intensity for cycling.

## 3.2 Open-loop control in SCI subjects: FES cycling

As briefly introduced in section 1.1.2, mobile and stationary cycling using FES have been widely investigated since the 1980s through many studies [17], [188]–[192]. It has been shown that FES-cycling of subjects with SCI results in physiological and psychological positive effects such as cardiovascular training, decrease in pressure sores occurrence and self-esteem improvements [16], [193], [194]. However, the use of this technology has often remained restricted to indoor and stationary ergometers in clinical contexts, partly due to the small amount (10–25 W) of power produced [36], [195], the requirement of experimented users and the lack of commonly available affordable FES outdoor bikes. The state-of-the-art highlights the need of improving the control strategies to increase the usability, the power output and the maximum covered distance [196]. In order to promote the research around this topic and more broadly the development of assistive technology for people with physical disabilities, the first Cybathlon event was launched by ETH Zurich in October 2016 [197]. Among six different disciplines (Brain computer interfaces, exoskeleton, instrumented wheelchairs, etc...) the FES-bike discipline consisted of a series of races between two spinal cord injured (SCI) participants propelling a cycling device by means of their lower limb muscular contractions elicited by FES. The participants had to face an endurance challenge by covering a 750 meters distance in less than 8 minutes, starting from a 10 degrees descending ramp (Figure 38).

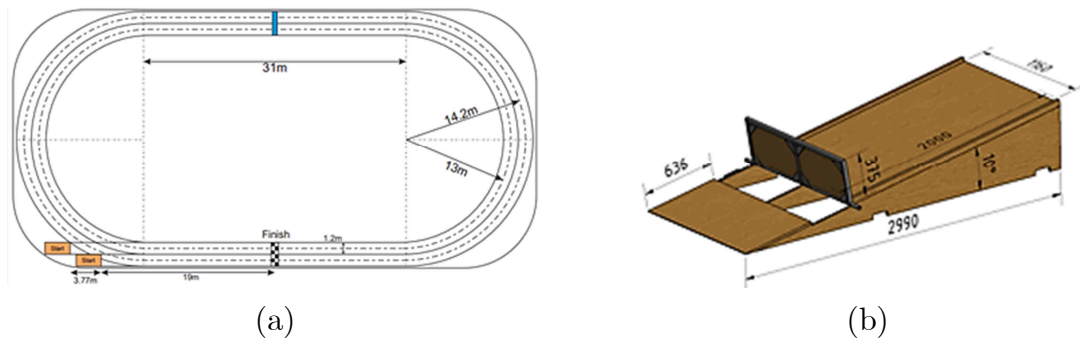


Figure 38. Race track (a) and starting ramp (b) used in FES-bike discipline (source: <http://www.cyathlon.ethz.ch>)

This section aims to present the upstream work and investigation done as part of this thesis to be able to participate in this competition with a SCI individual and above all to open the way to further control of FES in this specific context.

### 3.2.1 Participation to the Cyathlon: a longitudinal study

Participating to such a project within the framework of this thesis was an opportunity to study through a one-year longitudinal follow-up of a SCI individual, both technological and functional improvements needed for this lower limb neurorehabilitation approach.

Despite more than 14 years investigating on FES applications and more broadly in the field of neuroprostheses, using FES for cycling was a first for our research team and the opportunity to start developing a FES cycling solution from scratch.

Different objectives resulted in this protocol. From a clinical point of view, the objective of the study was to assess the physical, psychological and functional feasibility of training a paraplegic subject on a FES-assisted recumbent bike during one year and to assess the impact of this type of training on pain, cardiorespiratory function, muscle atrophy, body composition and bone metabolism. On the other side, to be able to reach the competition goal (750 meters in less than 8 minutes) has required multiple studies and improvements

---

aimed at enhancing the pedalling efficiency while keeping in mind the patient-centered approach described in this thesis.

The study was conducted in accordance with the principles of the Declaration of Helsinki and approved by the local Ethics Committee (CPP Dijon, RCB #2016-A00279-42), including the participant selection, physical preparation, training and participation into Cybathlon. One subject was included, the so-called pilot.

#### **a. Inclusion and exclusion criteria**

The Cybathlon competition rules constrained the participant to present an ASIA (American Spinal Injury Association) A or B spinal cord injury score, with a complete loss of motor function. The following inclusion criteria were furthermore defined: age  $\geq 18$  years and  $< 65$  years, complete traumatic lesion  $> 12$  months, neurological level T2 to T12, stable medical status, stimuable sublesional muscles and passive joint movement in the lower limbs. Exclusion criteria were defined as follows: BMI (body mass index)  $\geq 30$ , pressure ulcer, thrombophlebitis, neurogenic paraosteopathy, cardiovascular disease, muscle disease, DXA (Dual energy X-ray Absorptiometry) T-score (for measuring the bone mineral density)  $< -2.5$ , hip or knee arthroplasty, epilepsy, hypotension, lower limb fracture within the past 12 months, a pacemaker or other implant, and pregnancy. No beta-blocker treatment was authorized during the experiment.

#### **b. Pilot profile**

The pilot was selected in respect with the inclusion criteria listed in the previous section. He was 47 years old at the time of inclusion and presented a spinal cord lesion T3 (ASIA motor score = 50 and ASIA sensory score = 20) following a vertebro-medullary trauma in 1995.

A musculocutaneous flap was taken from the gluteus maximus as a treatment of a sacral pressure ulcer. This prevented us to consider this muscle group as a

candidate to electrical stimulation, whereas classically used in other FES cycling studies.

He presented spasms in the lower limbs spreading to the abdomen. He took no medication, did not verticalize, and did not follow any outpatient physiotherapy program. His BMI was estimated at 23. A prior venous Doppler ultrasound of the lower limbs was normal. The initial T-score with DXA was estimated to be -1.6.

The participant was practicing handbike at a competition level for several years before participating to the protocol.

### c. Tricycle description

Two distinct cycling devices were used during the study (Figure 39).

- the Berkelbike Pro<sup>©</sup>, previously introduced in section 1.1.2 and lended by BerkelBike company.
- the FreeWheels (team name) trike, an instrumented recumbent cycle adapted from a commercial device, the ICE Trike Adventure<sup>©</sup> designed for able bodied individuals.



Figure 39. Comparison of the two recumbent trike used during the initial training program (on the left, the Berkelbike Pro) and for the final training program and at the competition (on the right, the FreeWheels trike).

The Berkelbike Pro was chosen to allow the pilot to train before the FreeWheels competition device was finalized (3 months before the competition). No modification was done on the device.

The choice of the competition tricycle was based on several considerations. The first requirement concerned accessibility allowing for safe wheelchair/trike

transfers. In order to later facilitate diffusion of the approach we also wanted the device to be affordable, foldable and sufficiently light for transportation. We have selected the ICE Adventure 26 model (cost €3000, foldable steel frame, overall weight of 17.5 Kg and 2 m length). This product has a mesh seat, designed to provide an optimum back support and comfort. The tension in the back could be adjusted. The cover features is made on a breathable fabrics to maximize airflow. A VICAIR<sup>©</sup>-type pressure relief cushion was chosen by the team occupational and physiotherapists and then fixed on the seat to avoid sliding. Hase<sup>©</sup> pedals with calf support were adapted to ensure a sufficient lateral locking of the legs while holding the ankle joint at 90 °.

The ICE trike was initially equipped with a 26 ” rear wheel, we changed for a 24 ” one to tilt the bike and elevate the crank relatively to the pilot’s position (Figure 40). Low rolling resistance tires (Schwalbe<sup>©</sup> Kojak 24 x 1.35 ”) were also mounted instead of the original tires.



Figure 40. FreeWheels pilot during the Cybathlon final race.

A few weeks before Cybathlon competition we decided to modify the rear wheel transmission, initially a freewheel, to a fixed-gear. This decision was made in consequences of difficulties to pass the “dead points” during cycling phase (0° and 180°, full extension/full flexion). Our pilot could not succeed to complete the pedaling cycle once fatigue appeared and sometimes from the beginning of training. Furthermore, the co-contraction balance between hamstrings and

quadriceps muscle activations has a critical influence at these particular dead points and with time the equilibrium initially tuned is becoming less optimal (fatigue, movements on the seat...). The fixed-gear wheel was also supported by Szecsi 2007 et al. [196] results, where the force smoothing introduced by the use of a fixed-gear improved endurance.

The gear ratio was set to be equal to 1.22 (number of rear wheel spins for one complete crank spin, or ratio between the chainring and the rear sprocket). Calculated with the 24" rear wheel, we chose this ratio in order to best match between the optimal literature cadence [196] and the speed needed to reach 750 meters in 8 minutes, i.e. about 47RPM (5.6km/h).

As previously introduced, the classical approach of FES cycling is to predefine muscular activation patterns regarding the crank angle needed for the timing of the stimulation. The Berkelbike Pro is equipped with such a crank sensor that can be connected to a stimulator commercialized by the company. A similar crank angle encoder (Baumer MDFK08) has been adapted on the crank axis of the FreeWheels trike in order to provide pedaling angle as an input to the stimulator.

In addition, the device was instrumented with different kind of sensors used to monitor the performances. Two speedometers were set, one with the screen oriented towards the pilot and a second one oriented to be visible to a person walking aside the trike.

Finally, an ANT+ heart rate strap monitor was added to follow cardiac rhythm in response to effort.

#### **d. Electrical stimulation information**

During this study, the Berkelbike FES-Box stimulator, an 8-channel battery powered stimulator was used. In cycling mode, a pre-programmed pattern based on crank angle, triggered the stimulation on and off cycles (Figure 41a). Electrical stimulation was sent to each leg via three stimulation channels through three pairs of platinum stimulating electrodes, size 4.5 x 10 cm, respectively located

---

along the rectus femori/vastus lateralis muscles, the vastus medialis and the hamstrings (Figure 41b).

The stimulation pattern was designed with individualized quadriceps. On each leg, the first channel dedicated to the rectus femori/vastus lateralis muscles was set to be effective during the pushing phase (full flexion to vertical crank), meanwhile the second channel was meant to later activate the vastus medialis, from the time where the pedal was vertical to the full extension position. Hamstrings were respectively activated just before full extension and until the dead point was passed.

Each training sessions were initiated with a warm-up phase, either set on a home trainer or rolling on a flat surface, before proceeding to the endurance race. During the warm-up phase, stimulation frequency was set to a lower level (20 Hz) than during the race (30 Hz). In both cases, we used a rectangular charge-balanced biphasic pulse stimulation with a pulse width of 400  $\mu$ S per phase, an interpulse of 200  $\mu$ S and a maximum intensity set to 150 mA.

The pilot controlled the stimulation intensity based on the speedometer information in order to fit the desired cadence of 47 RPM. By pressing a button on the stimulator, he could gradually increase the level of stimulation on the quadriceps channels by 4.5 mA steps (2.4 mA for the hamstrings) when the speed tended to go below 5.6 km/h (see Figure 43).

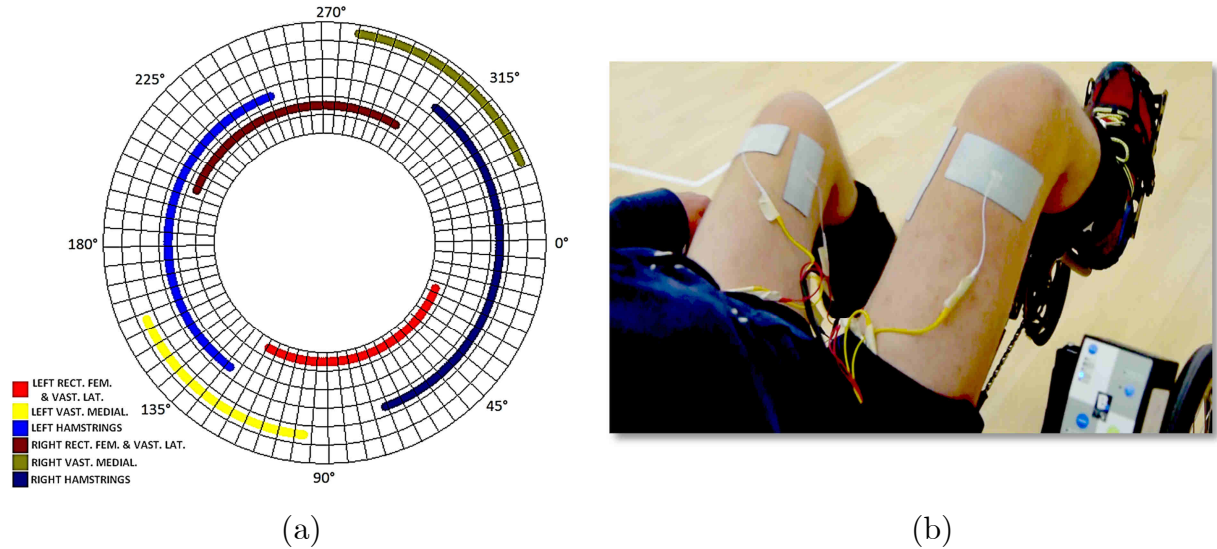


Figure 41. Stimulation pattern (a) designed with individualized quadriceps and hamstrings. On each leg (b), one channel is dedicated to the rectus femori/vastus lateralis muscles, a second channel to the vastus medialis and a third one to the hamstrings.

### e. Longitudinal study

A one year (12 mo.) training program was followed by the pilot, the program was divided into two stages preceding the competition:

- from months **M1 to M6**: home based, two to three times a week, stimulation program of the lower limb muscles during 30 minutes using CEFAR<sup>®</sup> Physio 4 stimulator and the following stimulation parameters: rectangular charge-balanced biphasic pulse stimulation with a pulse width of 300  $\mu$ S per phase and a ramp up, sent at 30 Hz during 10 s followed by 3 s of rest. At the start of each month, a mapping determined the intensity of stimulation needed to obtain contraction of the electro-stimulated muscle and the intensity needed to reach a 4/5 score on the MRC (Medical Research Council) scale.
- from **M7 to M11**: **FES-cycling training program**, two to three times a week, on an instrumented trike. Either set on a home trainer or rolling outdoor and indoor on a flat surface. Stimulations parameters were adjusted on the basis of progress.

From the beginning of the training, psychological and functional variables were also continuously monitored.

At M13, the pilot performed an endurance test in order to determine the maximum distance he was able to cover one month after the Cybathlon competition.

At M32, the pilot came back to the laboratory, more than one year and a half after having completely stopped the FES training protocol, and performed again an endurance test. The results are presented in the following section.

#### f. Performances and results

Our cyclist reached his best performance only one week before Cybathlon, when he succeeded to achieve a distance of 1820 m on the ICE trike in stationary mode and 760 m rolling outdoor on a flat surface (Figure 42).

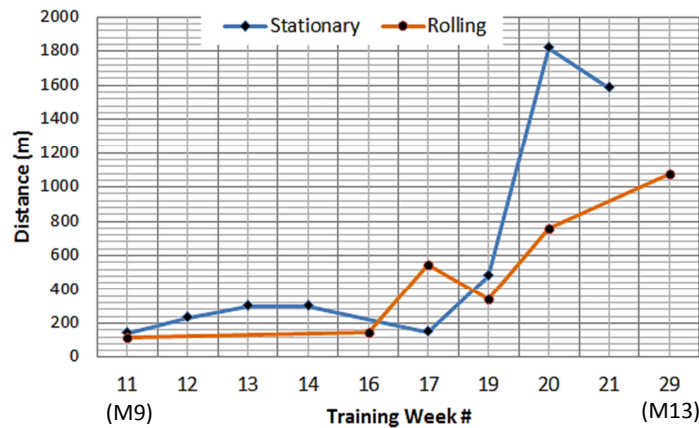


Figure 42. Maximum covered distance during the training sessions, from M9 to M13 (from week 11th to week 29th of the FES-cycling program)

Overcoming some technical issues, the functional performances dramatically and continuously increased starting from the last month before competition (Figure 42). Speed and endurance goals were successfully reached for the Cybathlon.

FES-bike race was divided into two main steps, a qualification race and a final race.

Our pilot was successfully qualified after a first race (670m in 430s, Figure 43) and could take part in the final race. The average speed during the final race was of 5.71km/h where he reached a maximal speed of 6.26km/h. He finished 6th out of 12, accomplishing the whole race in 467s.

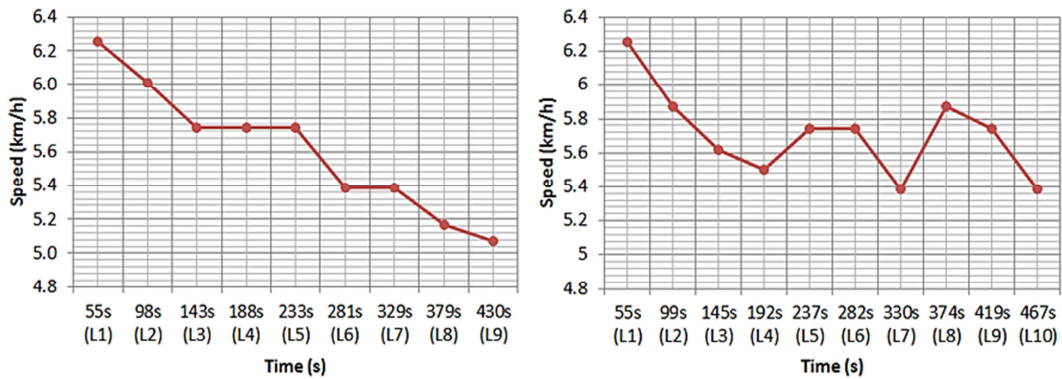


Figure 43. Average speed (km/h) computed on each lap (from L1 to L10) during the Cybathlon qualification (left) and final (right) races

At M13 his performances kept evolving as he was able to perform 1080 m in 14 min rolling on a flat floor (Figure 44).

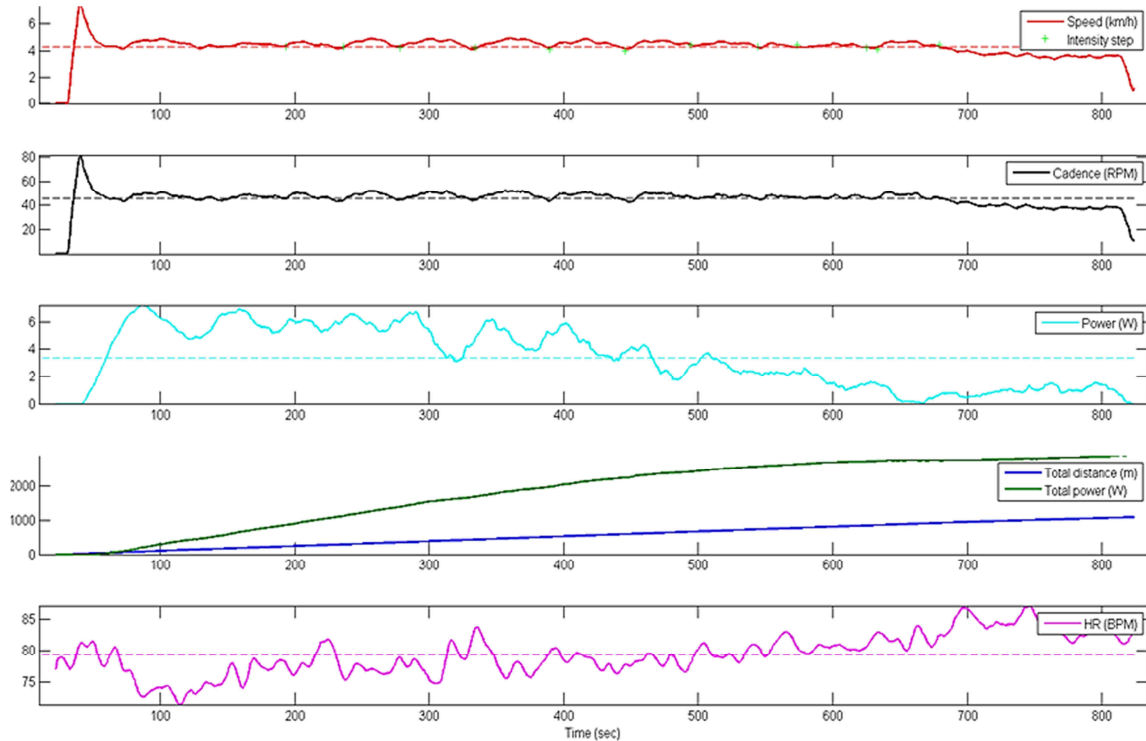


Figure 44. Data overview collected during a final evaluation race at M13.

---

At M32, he was successfully able to instantly cycle again and reached a maximum distance of more than 2500 m pedaling on the home trainer.

Our participation into this human adventure was a team success. Despite numerous practical issues the initial goal was reached.

Our pilot demonstrated a global acceptance of the participation into this 1 year protocol and an improvement along the experience of psychological variables such as life quality and self-esteem could be observed. Taking part in a competition as the final aim of the training program demonstrated a real benefit on training constraints tolerance.

### 3.2.2 Towards IMU based closed-loop control

Due to time and technological constraints, the work done through the Cybathlon participation and presented through the previous section did not use inertial sensors as an input to control the movement, but used a crank encoder installed on a generic recumbent bike. The solution has the advantage to be easily duplicated and the total cost of the device including the tricycle and the stimulator is estimated to €7650 (€4500 for the stimulator, €3000 for the tricycle, and the rest for mechanical adaptations).

However, the choices made on its adaptation were driven by the Cybathlon objective: to cover 750 m in less than 8 minutes. The stimulation patterns were designed through an individual manual tuning, making the procedure, at this stage, far from optimal and hardly feasible by an inexperienced user outside of a clinical environment. Moreover, the Cybathlon race conditions did not reflect outdoor reality as the track was completely flat with a low rolling resistance.

These conclusions highlight the need for a simpler automated stimulation pattern generator, able to adapt the stimulation to the environment, to the muscle fatigue or to the individual (e.g. position on the bike, number of stimuable muscles, etc...).

In order to further investigate control solutions, we first needed to be able to accurately quantify the influence of each parameter preliminarily used

(stimulation pattern, stimulation parameters, fixed-wheel or free-wheel, individualized quadriceps, pilot position, etc...) on power produced and endurance and observe if other variables could be used as an input instead of the crank angle.

#### a. Quantifying the FES system output

The results presented at M13 in Figure 44 were recorded using power pedals (Powertap P1<sup>©</sup>) initially designed for able bodied cyclists and adapted on the calf supports of the FreeWheels trike. Combined with IMUs located on the rear wheel and the crank, we were able to monitor speed, cadence, crank angle, distance and power (Figure 45).



Figure 45. Cycling instrumentation: power pedals and IMUs were mounted on the trike for monitoring the pilot's performances.

Meanwhile, no commercially available device could be successfully adapted to accurately measure the power produced by a SCI subject in this specific context at an affordable cost (e.g. SmartFit<sup>©</sup> and Sensix<sup>©</sup> pedal sensors  $\geq \text{€}10\,000$ ). The power pedals initially used have been intended to record powers higher than 250 W (e.g. an able bodied cyclist standing on the pedals) so as the instrumented home trainers commonly available-for-sale and were not accurate enough. As mentioned earlier, according to the literature the estimated power produced by a SCI subject should be between 10 and 25 W [36], [195]. Therefore, the decision was made to develop an instrumented home trainer specifically designed to record a weak power ( $< 200$  W) while ensuring a minimum accuracy of 0.5 %: a rotating torquemeter (Scaime<sup>©</sup> TSR 2300) was installed between the rear wheel and a

flywheel (Figure 46) thanks to a mechanical assembly built in collaboration with the National Engineering School of Saint-Étienne (ENISE, Loire, France).



Figure 46. The SCI participant is equipped with IMUs, surface electrodes, EMG sensors and a heart rate arm band monitor. The power produced is recorded at the rear wheel via a rotating torquemeter.

The different parameters modified during the Cybathlon protocol were then tested to accurately evaluate the influence of each change. EMG sensors (Delsys Trigno<sup>®</sup>) were additionally installed on the legs of the participant to monitor the quadriceps stimulation.

With the bike configured in fixed-wheel mode and using the Cybathlon stimulation pattern, first experimental trials were recorded to study the influence of the stimulation frequency. The 20 Hz warm-up, the usual 30 Hz stimulation and a trial at 40 Hz did not show any significant difference on power produced during a short 2-min recording (Figure 47).

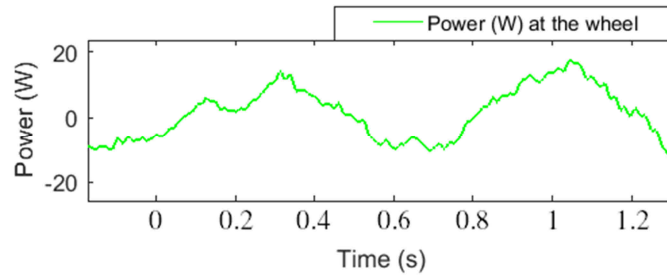


Figure 47. Power produced at the rear wheel by our SCI pilot over a crank revolution with the fixed-gear configuration. Recorded during an experimental trial using the Cybathlon stimulation pattern (individualized quadriceps plus hamstrings) via a rotating torque-meter.

The power produced was also compared between a stimulation pattern with individualized quadriceps (rectus femori/vastus during half of the pushing phase, then the vastus medialis is stimulated until reaching the full extension position) or with the entire quadriceps muscle group stimulated at the same time. No differences could be observed on short duration. Due to fatigue during the experimental protocol, the influence of this parameter could not be evaluated on a long duration recording.

During the Cybathlon competition, some pilots did not use hamstrings to propel the bike. In order to understand the influence of these muscles on the performances, this modality was also evaluated using the instrumented home trainer (Figure 48). The results obtained showed no difference in power produced with or without the hamstrings, with a similar power distribution over a crank revolution (green curve in Figure 48).

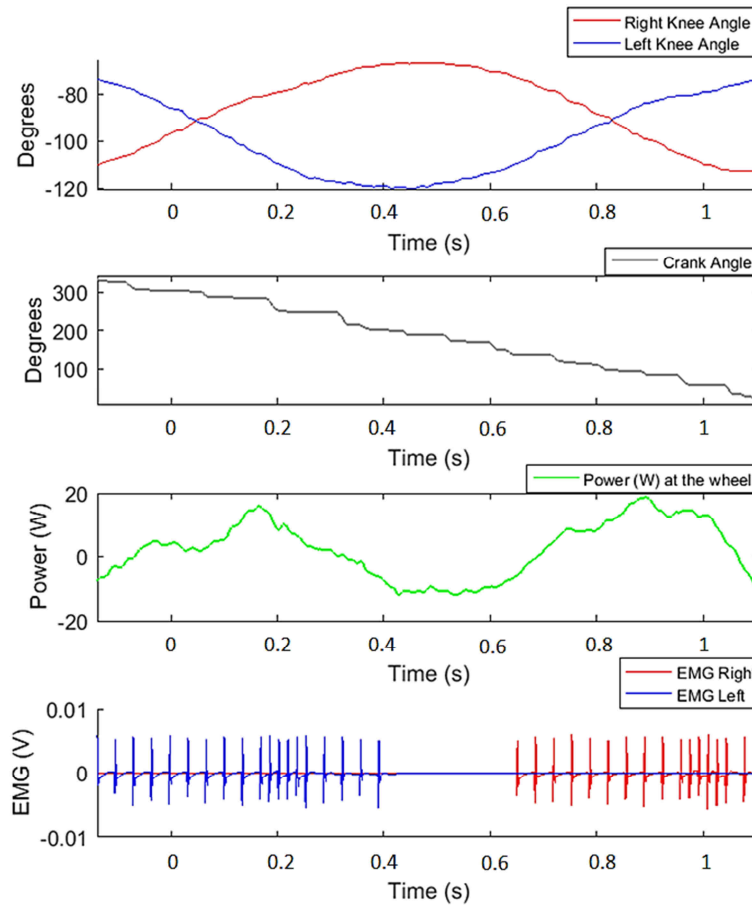


Figure 48. Knee angles, crank angle, power produced and EMG recording electrical activity of the quadriceps over one crank cycle with the fixed-gear configuration. Data recorded on a SCI participant without stimulating the hamstrings muscles.

As previously mentioned, one of the major issue associated to FES-assisted cycling on SCI subjects is the difficulty to pass the “dead points” during cycling phase ( $0^\circ$  and  $180^\circ$ , full extension/full flexion). At these specific points, a traction effort has to be produced by the participant to be able to complete the pedalling cycle. This effort should be produced by the hamstrings. However, in our case no appropriate stimulation timing of the hamstrings could be found to successfully complete the cycle and the hamstrings stimulation did not seem to bring a noticeable help. This last presented result confirms and underlines the poor influence of this muscle group on the power produced or the difficulty to accurately time the stimulation in order to produce an efficient contraction.

The fixed-gear wheel solution enabled our SCI subject to pass the “dead points” and competes to the Cybathlon. Szecsi 2007 et al. [196] proposed this approach to smooth the forces over a crank revolution thereby improving overall endurance on long duration FES-induced cycling. By mechanically bonding the bike inertia to the participant’s legs, this solution facilitates the design of the stimulation pattern by using the bike inertia to smooth the forces produced. However, smoothing the forces does not guarantee an optimal stimulation pattern and could hide an inadequate timing of the stimulation.

Using the instrumented home trainer, a further analysis was realized on the Cybathlon stimulation pattern. The fixed-gear wheel was removed and the power analyzed (Figure 49).

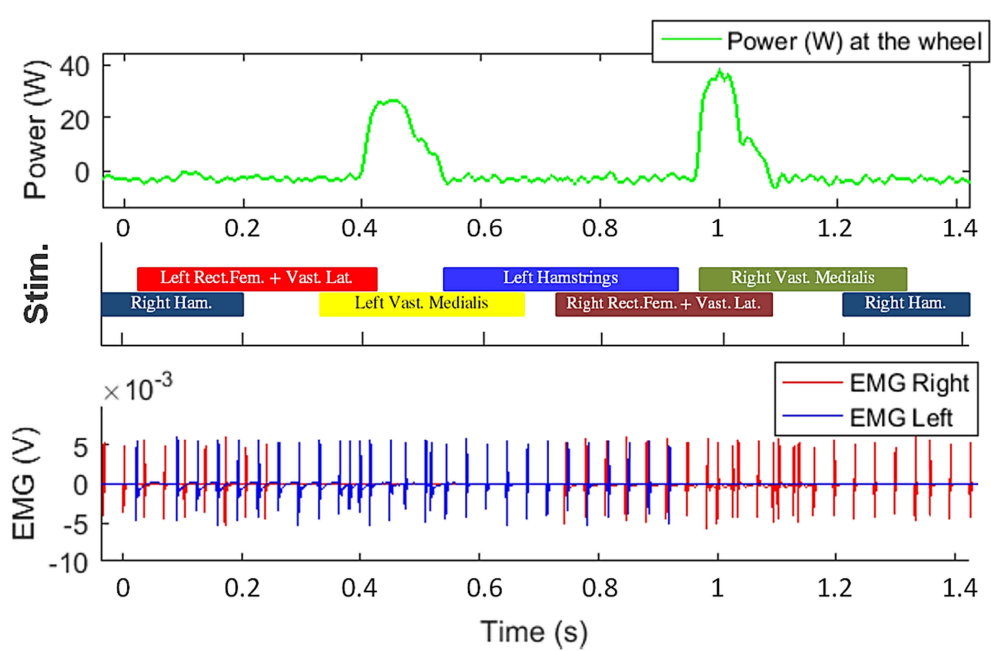


Figure 49. Power produced over a crank revolution without the fixed-gear wheel. The power is mainly produced by the quadriceps during the pushing phase.

Comparing Figure 48 (fixed-gear wheel) and Figure 49 (free wheel) power curves clearly highlights the distribution of the pushing forces due to the bike inertia enabling to pass the “dead points”. The results obtained highlight that on a complete crank revolution, most of the power is produced during the pushing

---

phase by the vastus medialis muscle. This allows to also offer this rehabilitation approach on SCI subjects with no stimuable hamstrings and glutei.

These different results confirm the important influence of the stimulation timing on the global effort produced and support the need to investigate innovative control strategies. By optimizing the pushing phase stimulation, a better efficiency and endurance could be achieved.

### **b. Future closed-loop control solutions**

The different figures illustrating speed during training and races (Figure 43 and Figure 44) show that the manual control of intensity level regarding cycling speed was really close to an automated control. The speed setpoint given to the pilot was to keep an average speed of 5.6 km/h. The actual average speed recorded during final race was of 5.71 km/h. This result shows the control of the stimulation amplitude over time does not require a complex control strategy, in opposite to other studies mentioned in section 1.1.3. A particular focus should be rather given to the study of the stimulation pattern which tends to play a key role in pedaling efficiency, usability and above all, fatigability.

Two original ideas emerged from the previous results as an alternative to the crank angle input. A simple automated process to finely tune the stimulation pattern could have been to accurately fit the stimulation timing to the power produced. We observed the quadriceps muscle, more specifically the vastus medialis activation, would provide most of the force produced over a crank revolution. In the initial stimulation pattern used through this study, this muscle was activated when the pedal crank is supposed to be vertical. This crank position is supposed to mechanically optimize the pushing effort. Meanwhile the actual muscle contraction and muscle response could happen earlier or later than this position. To monitor the actual power produced and adapt the associated stimulation timing could be a solution but would need to be able to accurately measure in real-time the power, which was a blocking point along the Cybathlon study and which does not seem an appropriate solution for an affordable and patient-centered solution.

---

Instead of using the crank angle, undergoing researches have also investigated the ability of using inertial sensors to automatically design a stimulation pattern on the bike depending on the knee angles [198]. Based on the joint angle computation presented in section 2.3.2 and experimentally validated, a similar control modality should have been studied and implemented to participate to the Cybathlon. However, due to technological limitations the strategy could not be tested on time. This approach could increase usability and genericity as no crank angle encoder or other instrumentation is required to be installed on the trike. It would also allow to adapt the pattern to the actual position of the pilot by using the knowledge of the knee angles.

In Wiesener et al. [198], the authors used a two-dimensional geometric model for the lower limbs, the knee and hip absolute angles were estimated from the IMUs and then transformed to a normalized range  $[0;1[$ . Instead of using the crank angle based stimulation pattern, a cycling percentage (CP) was used to define the stimulation pattern for each leg. The CP defines two ranges easily identifiable from the knee angles: flexion and extension. Depending on these two phases, different muscles contributions were activated to produce a positive torque. However, the method proposed in this work relies on a geometric model of the lower limbs and crank to estimate the real pedal position. Sliding in seat position and IMU placement could then disturb the output and no more guarantee a correct estimation even though several solutions have been investigated by the authors. A different method could be proposed and will be tested in further studies using the online peak knee flexion (PKF) algorithm presented in the section 3.3.2.a to continuously detect this event, in order to trigger the quadriceps stimulation at the beginning of the pushing phase. This would enable to take into account a possible sliding in seat position without requiring an accurate placement of the IMUs or a geometrical model of the individual. A study has been initiated with the University of Brasilia (UnB, District Federal, Brasil) to explore advanced control approaches [159]. A clinical protocol including several SCI individuals has been accepted. It will enable to

---

experimentally validate our different assumptions and will be realized in collaboration with the University of Brasilia in the coming months (autumn 2018).

The Cybathlon experience broke new grounds to innovative and generic FES-cycling based training programs for an important range of SCI subjects.

However, the constraints and the reality behind people with SCI daily lives are far from the Cybathlon FES bike context and require numerous improvements and further investigations to enable a safe recreational use of this activity in complete autonomy.

FES-induced cycling in the context of this thesis work has enabled to study the different aspects of a lower limb neurorehabilitation system based on a motor activation of preserved sublesionnal muscles. A complete FES cycling solution was developed from scratch and has enabled our research team to gain experience in this research field and to successfully reach the Cybathlon objectives.

Despite technological constraints did not allow to further investigate on time a closed-loop control strategy, several results have been transposed to another lower limb neurorehabilitation approach: gait restoration.

### 3.3 Closing the loop: online FES knee control in central neurological pathologies for stance phase improvement

As introduced in section 1.1.2, numerous stimulation strategies have been investigated over the past thirty years to assist or restore gait. The studies using FES to restore gait have been mostly conducted in post-stroke individuals and focused on correcting the drop foot syndrome by supplementing the absence of dorsiflexion. The state-of-the-art reflects a real lack of interest in using FES to improve the paretic knee rehabilitation, which however plays a key role in post-stroke gait recovery. In post stroke individuals, using FES on a stiff knee decreases spasticity of the knee flexors and extensors and increases their range of motion [199]. A preliminary evidence of a positive therapeutic effect on balance and mobility was observed using FES based knee control in early stroke rehabilitation [25], [200].

Multiple studies suggested that preventing hyperextension (*genu recurvatum*) and enabling a small knee flexion of the paretic limb during the stance phase would be helpful to improve gait recovery. In able bodied individuals, the knee flexion during the stance phase is lower than  $10^\circ$  when walking at a slow gait pace, similar to an FES assisted walk ( $< 0.5$  m/s) [201]. Meanwhile, in diplegic gait the individuals walk with their knee considerably flexed. This crouch gait (Figure 50) leads to an important joint overload. Perry et al. [202] showed that a knee flexed at an angle of  $30^\circ$  required to the quadriceps a force to stabilize the knee equals to 210 % of the load on the femoral head, while a flexion of  $15^\circ$  decreased the force to 75 % of the load.



Figure 50. Crouch gait leading to an important joint overload in children with cerebral palsy. (source: thebiomechanist.wordpress.com)

Chantraine et al. [203] proposed to extend the timing of the common peroneal nerve stimulation during the stance phase in order to tilt the tibia forward and limit the knee hyperextension.

On the other hand, to prematurely stimulate the quadriceps just after IC (Initial Contact) leads to a knee hyperextension that would prevent shock absorption by a too early joint locking [204].

During mid-stance, stiff limb restricted to the sagittal plane by the use of a knee orthosis creates a compass type gait causing excessive vertical center of mass motion and requiring excessive effort to carry the body over the stance limb [204].

A stiff knee at the end of the stance phase prevents to easily go forward in swing phase. Reinbolt et al. study [205] showed a late deactivation of the knee extensors decreases the maximum knee flexion angle in swing phase. Meanwhile, in absence of voluntary control Kobetic et al. [204] observed that a premature deactivation of the knee extensors at the end of the stance phase before the leg is fully unloaded can lead to collapse.

These different results reflect the importance and the need of an appropriate and accurate timing to control the knee stimulation in stance phase while ensuring a safe and efficient support. These studies also highlight the need to accurately monitor the knee angle in both swing and stance phase to adapt the assistive control to multiple patient profiles. Different thigh muscle activations

---

can be used on individuals with a CNS disorder to correct an identified knee problem throughout the gait cycle [206]:

- **Crouch gait** (increased knee flexion during the stance phase): quadriceps stimulation from 87 % of the first gait cycle to 50 % of the next gait cycle.
- **Reduced knee extension during the swing and stance phase**: quadriceps stimulation from 87 % of the first gait cycle to 12 % of the next gait cycle.
- **Reduced knee flexion during the swing phase**: hamstrings stimulation from 50 % to 70 % of the gait cycle.
- **Stiff knee gait** (excessive knee extension throughout the gait cycle): hamstrings stimulation from 95 % of the first gait cycle to 70 % of the next gait cycle.
- **Genu recurvatum** (knee hyper-extension during the stance phase): hamstrings stimulation from 95 % of the first gait cycle to 55 % of the next gait cycle.

This previous information highlights, in addition to an accurate timing and knee angle monitoring, the need of studying a solution able to provide an individualized and specific control of the stimulation depending on the patient's gait features. Based on promising preliminary evidences from literature, the potential of this neurorehabilitation paradigm motivated to further investigate assistive closed-loop control of the knee in post-stroke subjects. The use of inertial measurement units and of the knowledge previously addressed in this thesis has enabled to go further and to face the multiple constraints of an online closed-loop stimulation protocol in this specific context.

### 3.3.1 Experimental Protocol

An experimental protocol (#RCB 2017-A03611-52, CRF La Chataigneraie, Menucourt, France) was then designed with the main purpose of proposing a novel approach using a FES-based control of knee joint to reduce stance phase asymmetry and study the feasibility of using such FES systems in clinical rehabilitation, compared to classical knee orthosis. Secondary objectives aimed at improving gait quality, walking range and comfortable speed using the same modality.

The main hypothesis was to prove that using FES to real-time control the knee angle could reduce the time needed to recover a normal balance while providing a secure stance phase. To monitor weight bearing and stance time asymmetry the participants were equipped with Bluetooth instrumented insoles (FeetMe<sup>©</sup>, Versailles, France) able to monitor at a 100 Hz sampling rate the pressure distribution through 70 sensors located inside the device. A collaboration with the FeetMe<sup>©</sup> company enabled to develop a specific software to access the pressure data in real-time. The subjects were also equipped with 2 inertial measurement units (IMU Bosch<sup>©</sup> BNO055) located on the thigh and the tibia, wired to a Raspberry Pi3<sup>©</sup>. Each IMU embedded a high speed ARM Cortex-M0 based processor and a Kalman Filter directly providing quaternion estimation needed to compute knee angles at a 100 Hz sampling rate, using the goniometer computation explained in section 2.3.2. One IMU (Fox HikoB<sup>©</sup>) was installed in the back of the participants at the second sacral vertebra level to estimate vertical trunk displacement. Stimulation was sent via a two-channel wireless stimulator (Phenix Neo<sup>©</sup>) to the quadriceps (channel #1) and hamstrings (channel #2) via surface electrodes (Figure 51). A further description of the hardware architecture specifically developed for this protocol is given in section 4.2.

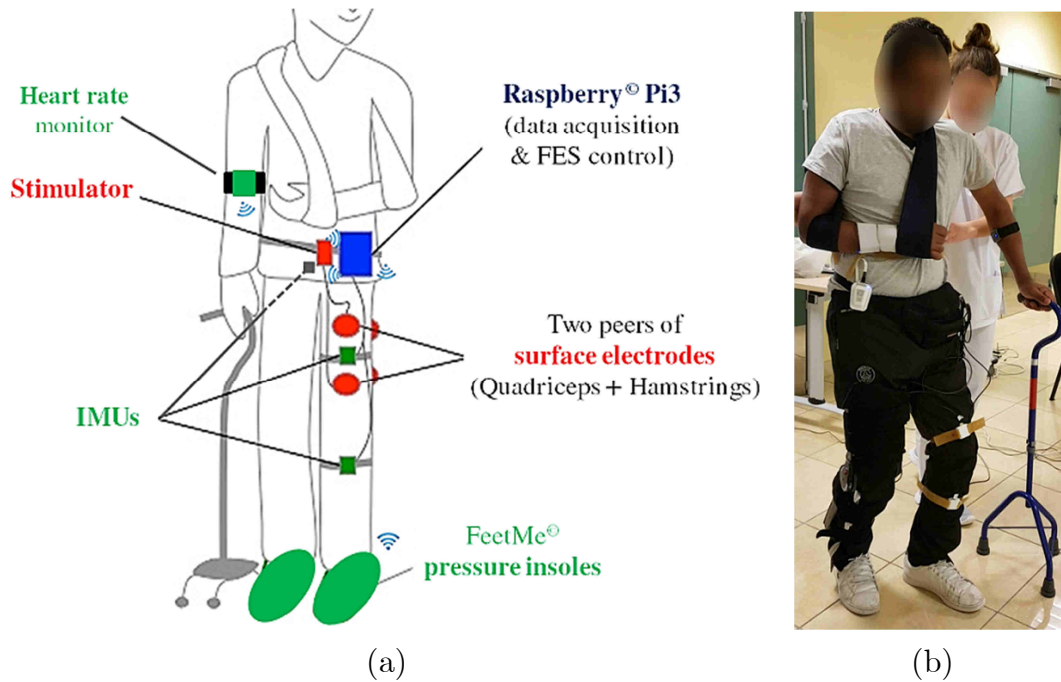


Figure 51. Experimental setup diagram (a) and picture (b). The participants are equipped with Bluetooth pressure insoles, 2 wired IMU on the leg and 1 wireless IMU in the back. A Raspberry records and processes the sensors data to send an appropriate command to a wireless stimulator to stimulate the quadriceps and hamstrings via surface electrodes

### a. Evaluation criteria

Main and secondary evaluation criteria were defined with the practitioner. The first main criterion was computed following the method described in Patterson et al. [207] as the **symmetry ratio of stance time** between paretic and non-paretic limbs. The second main criterion was computed as described in Mizrahi et al. [208] as the **asymmetry in weight bearing** during the stance phase, expressed in percentage of the total weight. These two main criteria aimed at quantifying both in time and magnitude the gait asymmetry using the foot pressure insoles. The secondary criteria aimed at measuring the comfortable walking speed and quantifying **gait quality** and physiological cost through a series of different markers:

- **Perceived exertion of walking** using a Borg scale [209] from 6 (no exertion) to 20 (maximum exertion).

- **Physiological Cost Index (PCI):** calculated as the ratio of the difference in working and resting mean heart rates (bpm) and the self-selected (comfort) walking speed (m/min). The PCI value reflects the increased heart rate required for walking and is expressed as heartbeats per meter by formula:

$$PCI = \frac{\overline{HR_{work}} - \overline{HR_{rest}}}{Walk_{speed}} \quad (25)$$

In order to accurately and automatically compute the PCI between each experimental trial, two infrared systems were installed at the beginning and at the end of a 10-meters experimental path and synchronized with a heart rate monitor armband.

- **Vertical displacement of the center of mass:** several studies demonstrated the correlation between the vertical displacement of the trunk during gait and the associated physiological cost in able bodied and SCI individuals [210]. Enomoto et al. [211] showed the vertical movement of an inertial sensor mounted on sacrum is equivalent to the vertical movement of the center of mass. For this protocol, the vertical displacement of the center of mass was then computed by double integrating filtered acceleration recorded on the vertical axis of the IMU located in the back of the subject. The considered value corresponded to twice the standard deviation around the mean estimated displacement (Figure 52) along a 10-meter experimental path.

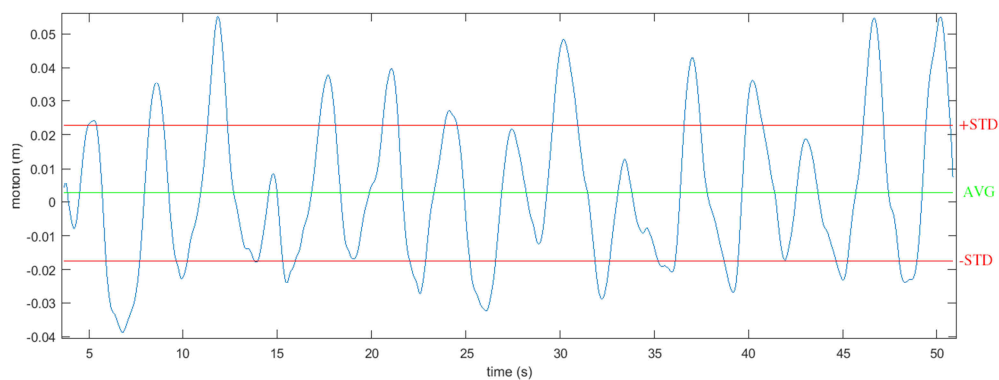


Figure 52. Vertical displacement of the center of mass during walking estimated by double integrating filtered acceleration data from an IMU located at the second sacral vertebra level during an experimental trial.

### b. Balance training

In order for the participants to get used to apply their weight on their paretic limb, a balance training was performed prior to the FES based gait protocol. Standing on their feet equipped with the pressure insoles, the participants were asked to maintain their body sway to less than 7 % of asymmetry (expressed as a percentage of their total weight measured by the insoles) with the help of a visual feedback (Figure 53a) specifically developed for this application (see section 4.2). The  $\pm 7\%$  range was measured in Mizrahi et al. [208] on able bodied subjects and was considered here as a reference value to reach for a normal body balance. The total time spent in the  $\pm 7\%$  range was computed on a 180 s exercise in order to monitor the participant's progresses and ability to follow the FES assisted gait protocol.

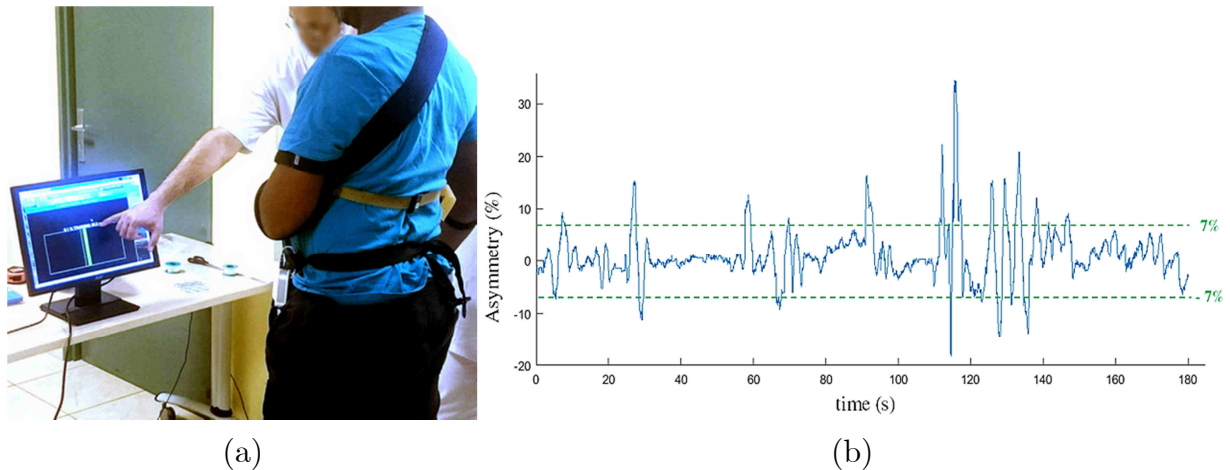


Figure 53. Balance training protocol: each participant was asked to maintain his balance to an asymmetry below 7 % (b) of their total weight during 180 s with the help of a visual feedback (a).

### c. FES assisted gait protocol

Participants started from standing. They were asked to walk on a flat floor on a total distance of 16 meters. The first 3 meters aimed at achieving a steady state gait on the following 10 meters. The last 3 meters enabled the participants to slow down and stop. Only the 10 meters of steady state walking were considered for post-processing and results. An oral instruction was given at the beginning of

each trial to encourage the participants to transfer their weight onto the paretic leg.

The experimental path was performed under three different conditions:

- C1: no assistance, the participants walk at a self-selected speed.
- C2: the paretic limb is equipped with a knee orthosis limiting the knee flexion angle and the knee extension angle around  $5^\circ$ .
- C3: the paretic limb is stimulated following the control modality presented in section 3.3.2.

The three conditions were successively repeated in a random order, in order to avoid a possible learning effect, until at least three trials of each condition were successfully recorded or until the participant's fatigue prevented him to further continue the experimental protocol.

### 3.3.2 Control modality

#### a. Pre-stance event

As mentioned previously, a CNS disorder can be associated with different impairments at the knee level. A crouch gait leads to an increased knee flexion during the stance phase, while a genu recurvatum leads to a hyper-extension.

Multiple studies investigated the delay between the muscle force response and the time of the stimulation [212]. The order of the magnitude usually considered is around 100 ms [180]. In addition, the global hardware latency should be added to this physiological latency in order to take into account the delays between the actual stimulation event (e.g. the foot reached the ground), the time to process data, the detection algorithm, and the triggering of the stimulator (addressed in section 4.2).

In severe cases of crouch gait or genu recurvatum, starting the control of the stimulation on the detection of IC (Initial Contact) seemed too late to reach on time an efficient motor response and counter the knee problem over the stance phase.

To minimize the motor response delay and obtain a rapid and forceful response, Andrews et al. [213] applied a relatively high frequency stimulation (up to 100 Hz) to the thigh muscles to progressively reduce the frequency to 20 Hz with automatic compensation of pulse width.

The stimulator used in our protocol did not enable to online modulate the frequency and apply this strategy.

Therefore, a pre-stance event detection algorithm was studied and developed to be able to anticipate the stance phase in some participants with a given type of gait and compensate the delay. Inspired by the different motion analysis works previously mentioned in Chapter 2, two main events have seemed to be relevant and easily detectable in real time on these heavily impaired gait patterns: the peak knee flexion angle during swing phase and the negative zero crossing of the sagittal angular speed recorded from the gyrometer output signal located on the tibia (Figure 54).

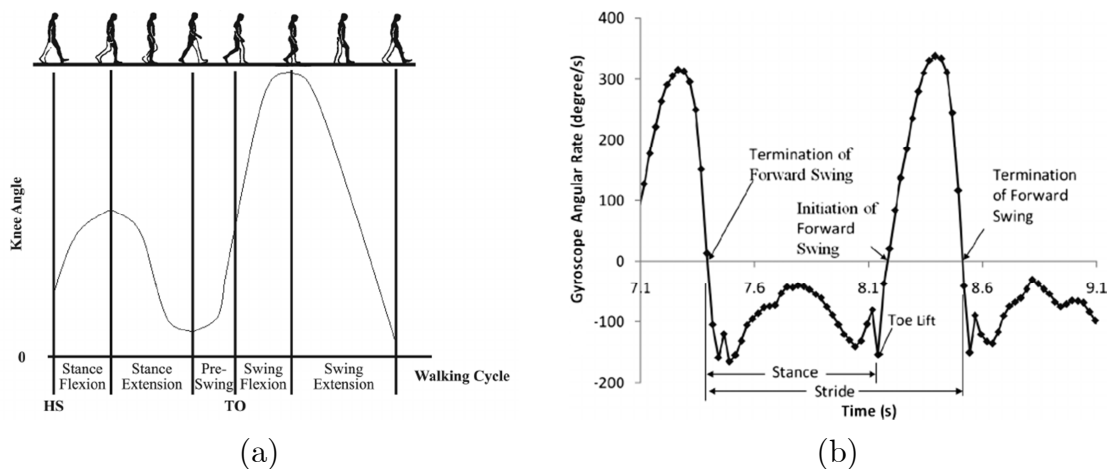


Figure 54. The peak knee flexion angle during swing phase (a) and the negative zero crossing of the sagittal angular rate (b) turned out to be two relevant and easily detectable events prior to the stance phase. (adapted from: [176], [214])

Used in Parkinson's Disease gait assessment [215] to reliably detect the gait cycle from inertial data, the zero crossing event corresponds to the termination of forward swing time. As observed in Figure 24 in section 2.3, this gyrometer characteristic waveform is in most of the cases still present in highly impaired

---

gait. In addition, the zero crossing detection algorithm is easily implementable by monitoring the sign and magnitude of the angular speed in swing phase. Above a minimum motion threshold, if two consecutive gyrometer samples changed from a positive to a negative sign, the zero was crossed.

Meanwhile, this pre-stance event is not adapted to all pathological gait patterns and can lead to false positives when the gyrometer waveform does not show any detectable characteristics or when the dynamic range of the gyrometer is not adapted to a slow gait pattern. As an alternative, the knee flexion angle is usually a smoothed signal over the gait cycle, less sensitive to noise, vibrations or dynamic of motion and presents an interesting waveform characteristic: the peak knee flexion (PKF) angle. The PKF angle corresponds to an event about 14% earlier than the TS (Terminal Swing) [216]. In order to reliably detect in real time this event from the knee angle, a specific algorithm was developed and is explained in the following flowchart (Figure 55).

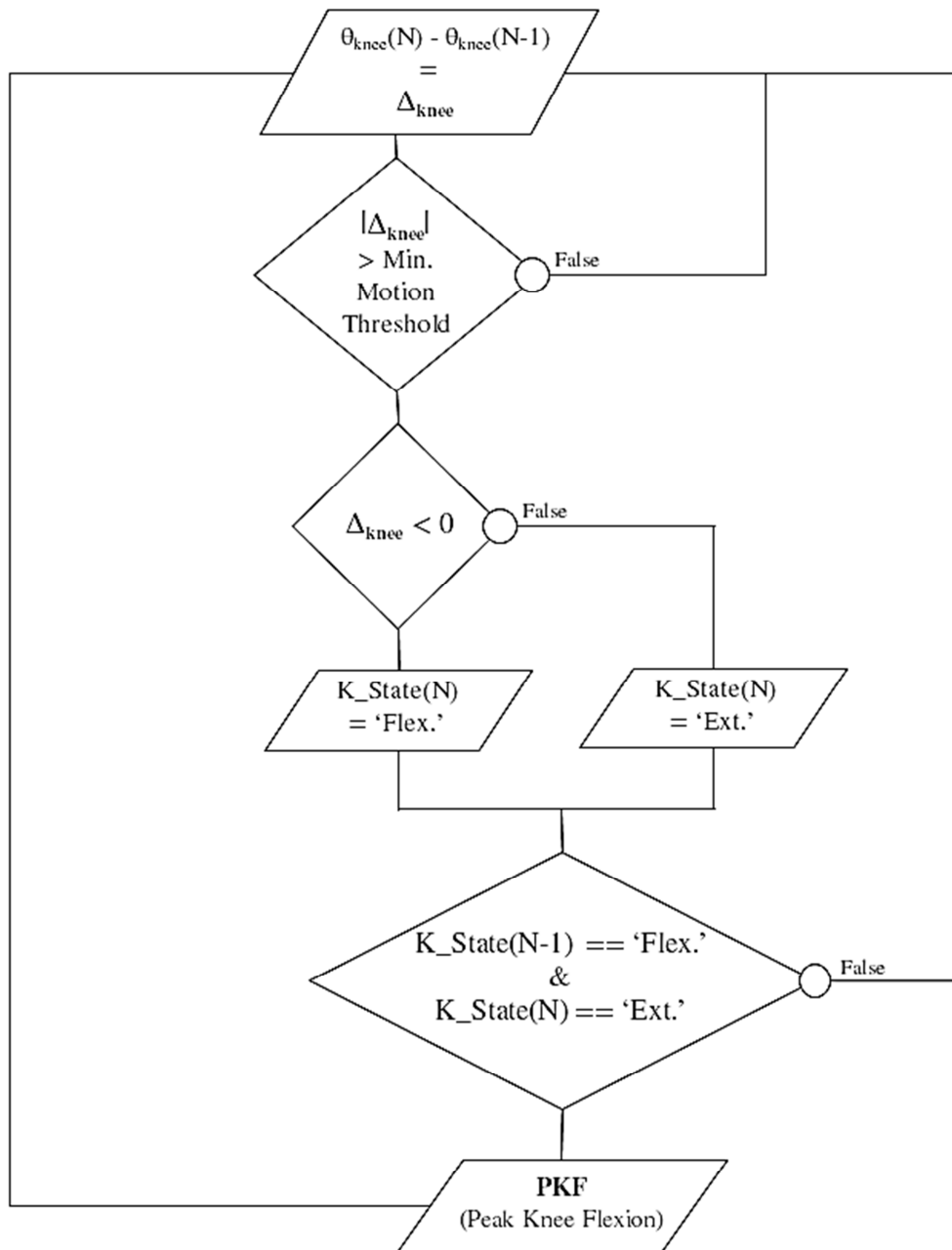


Figure 55. Flowchart illustrating the real-time detection algorithm of the 'peak knee flexion' (PKF) as a pre-stance stimulation event.

---

**b. Knee control**

The pre-stance event was investigated for eventually compensating the motor response delay and counteracting before the stance phase a hyper-flexed or hyper-extended knee in some participants. This section describes the global closed-loop control applied over the gait cycles.

A knee angle setpoint (KAS) was defined by the practitioner as the optimal knee flexion during stance phase (around  $5^\circ$ ). The stance phase was detected using a simple threshold on the foot pressure insoles, already used to compute the main evaluation criteria. Stimulation was sent either to quadriceps or hamstrings, depending on the actual paretic knee angle (PKA) compared to the desired KAS in stance phase. A knee too flexed leads to the closed-loop control of the quadriceps, while a knee too extended leads to the control of the hamstrings.

An initial pulse width value  $PW_i$  was defined for each participant and each muscle (quadriceps and hamstrings) as the first value to elicit an efficient motor response of the muscle (manually assessed by the practitioner while the participant was standing up). This initial stimulation level was used 1) as a pre-stance stimulation, to start to lock the knee before initial contact; 2) as the initial level of stimulation used in the proportional (P) controller of the closed-loop (Figure 56). Once the frequency and the intensity of the stimulation set ( $f = 30$  Hz,  $I = 50$  mA), only the pulse width was modulated. The P controller adjusted the pulse width depending on the error  $\varepsilon$  between the estimated PKA (ePKA), computed from the IMUs quaternions, and the desired KAS.

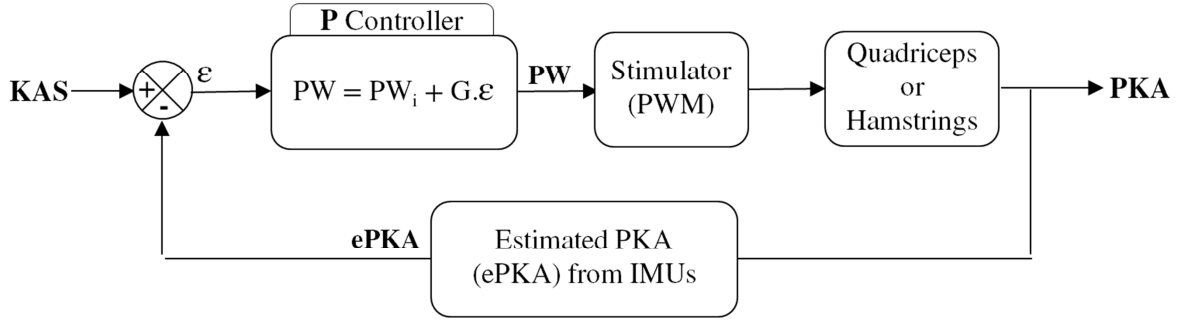


Figure 56. Closed-loop control of the thigh muscles. A P controller modulates the pulse width of the stimulator depending on the error between the knee angle setpoint (KAS) and the estimated parietic knee angle (ePKA) from the IMUs quaternions during stance phase. An initial pulse width ( $PW_i$ ) and a gain  $G$  are set for each participant depending his knee issue.

A maximum pulse width  $PW_{max}$  was determined as the maximum bearable level of the stimulation before pain.

A maximum range of motion  $ROM_{max}$  was defined in extension (hamstrings) and in flexion (quadriceps) around the KAS (e.g.  $KAS - ROM_{max-quadri} < KAS < KAS + ROM_{max-hamstrings}$ ).

The controller gain  $G$  was automatically computed for each participant and each muscle group depending on  $PW_i$ ,  $PW_{max}$  and  $ROM_{max}$  in order to bind the stimulation pulse width to  $PW_{max}$  when the maximum range of motion is reached:

$$G = \frac{PW_{max} - PW_i}{ROM_{max}} \quad (26)$$

The flowchart in Figure 57 summarizes the IF-THEN rules regulating the knee stimulation throughout the control cycle.

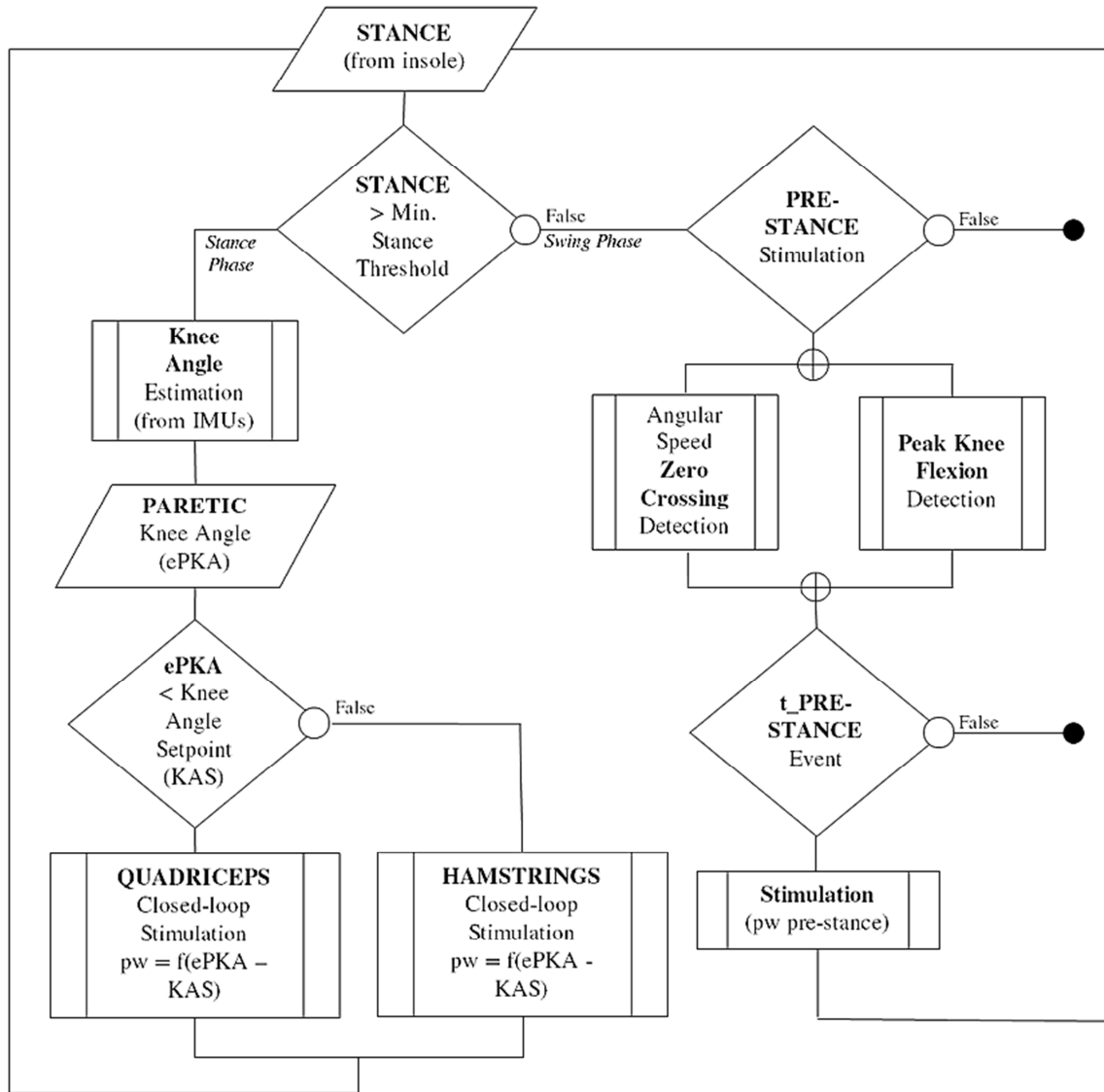


Figure 57. Flowchart of the IF-THEN rules regulating online the stimulation control.

### 3.3.3 Preliminary results and discussion

The protocol will include 15 participants. 2 subjects have been included so far, the inclusions will end in September 2018. This section presents preliminary results obtained on these 2 participants.

From a technical point of view, despite a complex hardware and software architecture (see section 4.2) needed to embed this wearable custom-made FES system on the participant, the control strategy successfully sent the stimulation

as intended during the gait, depending on the decisional algorithm executed in real-time (Figure 58).

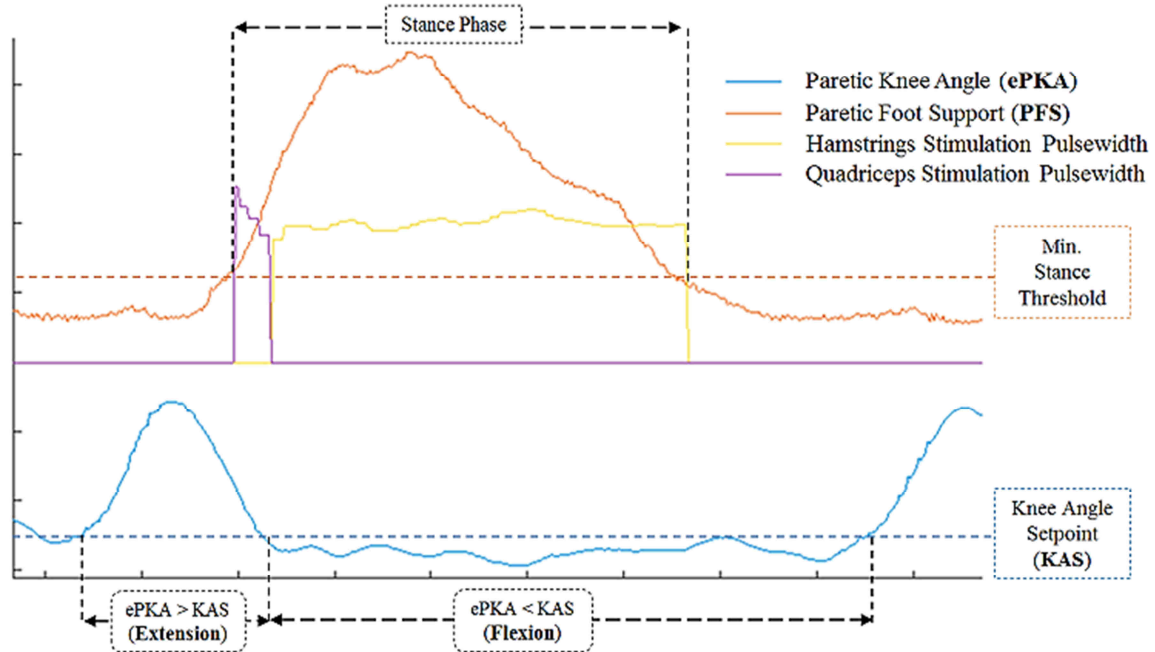


Figure 58. Example of recorded data during one gait cycle. During stance phase, defined when PFS data (orange) goes above a preset threshold, stimulation of hamstrings (purple) is delivered when ePKA is higher than KAS and stimulation of quadriceps (yellow) delivered when ePKA lower than KAS.

At this stage, the evaluation criteria (main and secondary) show that in most of the cases the condition C3 (stimulation) lead to unsatisfactory results. The two main criteria (asymmetry in weight bearing and the stance time symmetry ratio) were globally degraded by the use of FES (Figure 59). The perceived exertion of walking was however minimized in C3 so as the physiological cost index (PCI). The vertical displacement of the center of mass was globally lower with FES (C3) than with the knee orthosis (C2), but the walking speed was the slowest in C3 condition (Figure 60).

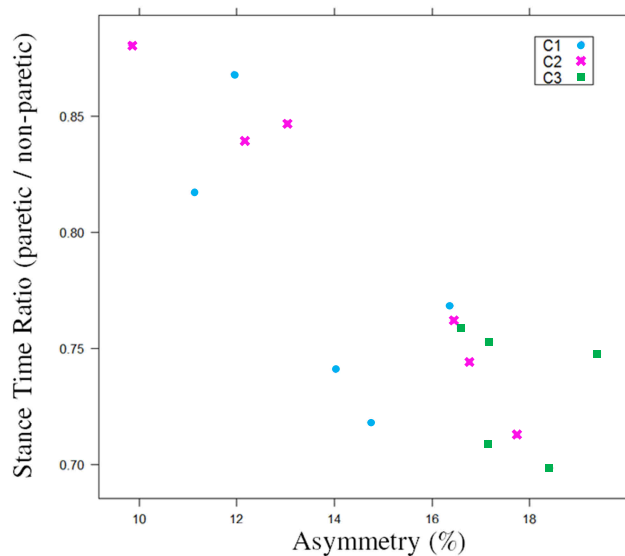


Figure 59. Main evaluation criteria computed from the two participants under the three experimental conditions (C1 no assistance, C2 knee orthosis, C3 stimulation). On the abscissa axis is represented the force asymmetry between the two legs, expressed in percentage of body weight. On the ordinate axis, the stance time symmetry ratio (paretic/non-paretic) is plotted. Optimal results correspond to a stance time ratio close to 1 and to the lowest asymmetry (upper-left corner).

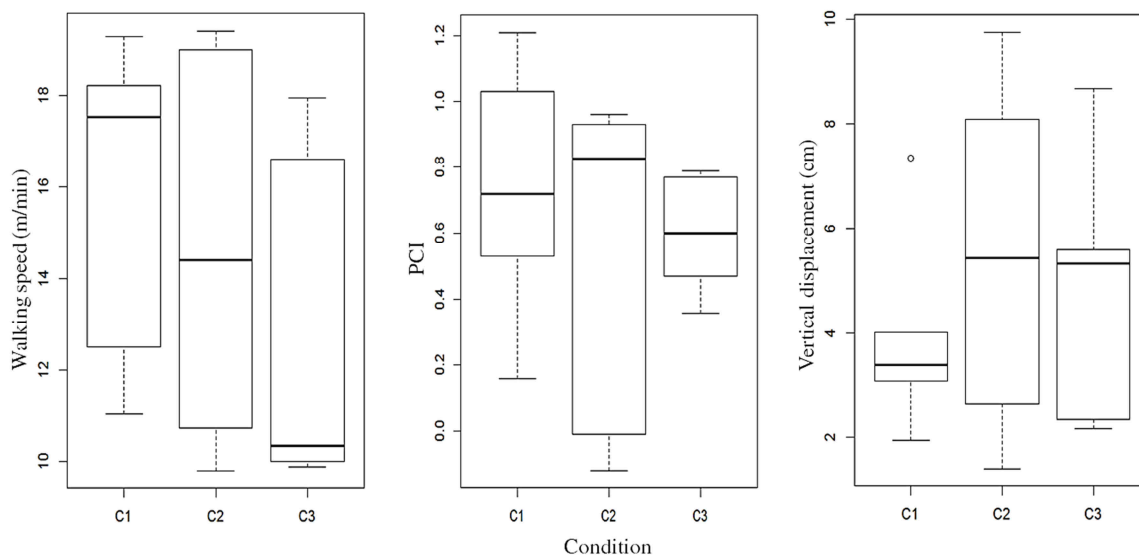


Figure 60. Boxplots representing secondary evaluation criteria. The walking speed, the PCI and the vertical displacement of the center of mass reflect the gait quality under the three experimental conditions.

Despite unsatisfactory clinical results associated to the main evaluation criteria and the use of FES, the results obtained in C3 condition remain promising. The initial aim of the protocol has been to study the feasibility of using such FES systems in clinical rehabilitation compared to classical knee orthosis commonly used by the physical therapists. The main hypothesis relies in the fact that the use of FES could improve stance phase support symmetry recovery in acute post-stroke individuals and enable a faster rehabilitation compared to knee orthosis. However, the experimental protocol conducted on these two preliminary participants did not able to compare the learning speed between C2 and C3. Indeed, each condition was randomly changed at each trial, thereby preventing the subject to get used to the stimulation or to the knee orthosis (Table 8).

	Trial #	Condition	Asymmetry (% Weight)	Stance Time Ratio
<b>P1</b>	1	C1	14.03	0.74
	2	C2	16.78	0.74
	3	C2	16.45	0.76
	4	C3	18.42	0.70
	5	C3	17.15	0.71
	6	C1	14.75	0.72
	7	C3	16.58	0.76
	8	C2	17.75	0.71
<b>P2</b>	1	C1	16.39	0.77
	2	C3	17.17	0.75
	3	C2	13.05	0.85
	4	C1	11.14	0.82
	5	C3	19.40	0.75
	6	C2	12.16	0.84
	7	C1	11.94	0.87
	8	C2	9.84	0.88

Table 8. Order of the different trials and main evaluation criteria associated.

Meanwhile, the three repetitions of the C3 condition in P1 demonstrate a significant increase in performance compared to C2. Under C3 condition, between the first trial (#4) and the third repetition (#7) the estimated value in weight bearing asymmetry decrease of about 10 % compared to the first trial, whereas in

C2 condition (knee orthosis) the third trial value degraded of about 6 % the first trial performances.

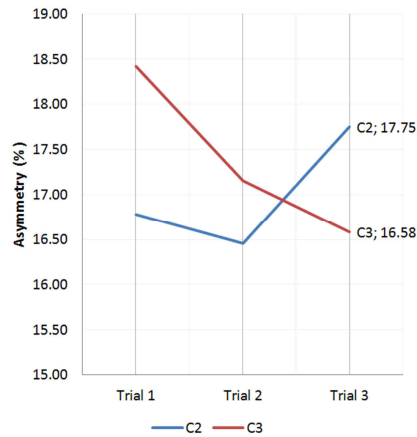


Figure 61. Learning curves representing the asymmetry in weight bearing measured on the first participant (P1) under C2 (knee orthosis) and C3 (stimulation) conditions. The C3 condition significantly improves the asymmetry over the repetitions, while the knee orthosis degrades the results.

The learning curves suggest a promising improvement of the FES approach compared to a classical orthosis. However, these preliminary results highlight a wrong initial distribution of the different conditions of the experimental protocol. More repetitions should be performed for each condition and each repetition should be done consecutively under the same condition. The participants should perform 6 times each condition C2 and C3. Needed to properly parameterize the stimulation depending on the gait pattern, the C1 condition should be performed at least one time at the beginning of experiment. The order between the C2 and C3 conditions could be randomly alternated between the participants (e.g.: P1 – C1 – C2 (x6) – C3 (x6) and P2 – C1 – C3 (x6) – C2 (x6)). This will be followed for the next 13 participants to be included.

---

Despite no clinical results have been clearly observed yet, this last experimental protocol represents a major result arising from this thesis work, thereby successfully supporting all the different approaches addressed through this document. A wearable FES system has been developed for an online closed-loop control of the knee, keeping in mind the initial constraints of a patient-centered solution, merging and validating all the different steps gradually investigated through this thesis. A real-time assessment of pathological motions was successfully performed from low-cost inertial sensors and was used to feed a P controller able to modulate the stimulation signal depending on the desired joint angle.

---

## 4 Discussions – Conclusions

Each of the studies presented in this thesis was initiated by a clinical need expressed by the practitioner and a possible solution to deepen from the academical side. Multiple steps were needed to start a collaboration between these two worlds, to materialize a theoretical hypothesis, to investigate the feasibility of a proposed approach and adapt it for validation in experimental conditions.

From the clinical protocol design, the clinical data processing, the numerous hardware and software developments and constraints associated to the study of patient-centered solutions, this following section underlines the **cross-functional work** accomplished to face these challenging points in parallel with the scientific work conducted.

## 4.1 Clinical Protocol: design, follow-up and data processing

The conduct of an experimental protocol to validate scientific hypotheses and prototypes intended for a medical use has required following different steps, in accordance with the directions of the practitioner. Multiple documents had to be written in collaboration with the practitioner in order to respect the safety and ethical regulations associated to a clinical protocol. For each protocol, an official document (in French, CPP: Comité de Protection des Personnes) had to be written and submitted to a medical board and to the ANSM (National French Agency for the Safety of Health Products) in order to be able to experiment on people with disabilities, in a clinical environment and to publish the results. The document had to accurately describe all the devices used on the patient (active and passive, in contact with the patient or not, etc...), evaluate the potential incurred risks, the objectives, the innovative nature of the protocol and the different evaluation criteria and steps relative to its conduct. Each clinical protocol needs to be also reported to the CNIL (National Commission on Informatics and Liberty) and covered by the subscription to an insurance.

To elaborate an experimental protocol in a clinical environment, the academic research laboratory needs to collaborate with at least one university hospital and one practitioner in charge of the inclusion and the follow-up of the patients.

Through this thesis, experiments were conducted on multiple pathologies in different clinical environments (rehabilitation centers, university hospitals, motion analysis laboratories, etc...). 4 CPP documents were submitted and accepted, 1 international collaboration grant was written and accepted (FIN279 - France Stanford Collaboration Grant, Lucile Packard Children's Hospital, Department of Orthopedic Surgery, Stanford, USA, Prof. Jessica ROSE) to support the cost of two weeks of experiments. Table 9 gives an overview of the number of subjects included in each associated protocol.

Description	Thesis Section	Number of Patients included	Location	ID (International Identification Number or RCB)
Stride length estimation based on 1 IMU	2.2.1	10 able bodied & 12 with Parkinson's Disease (PD)	Gui de Chauliac University Hospital and Antonin Balmes Gerontology Center, Montpellier, France  Dr Christian GENY	NCT02317289
Detection of Freezing of Gait based on 1 IMU	2.2.2	7 PD		
Electrical stimulation as a somatosensory cueing in PD triggered with 1 IMU	3.1	13 PD		
Inertial sensors based analysis of pathological gait	2.3.3	29 Post-Stroke (PS)	Nîmes University Hospital, Le Grau du Roi, France  Dr Jérôme FROGER (Medicine thesis : Dr F.Feuvrier)	RCB 2015-A00572-47
FES-assisted cycling of a SCI individual	3.2	1 Spinal Cord Injured	CRF COS Divio, Dijon, France Dr Charles FATTAL	RCB 2016-A00279-42
FES-based control of knee joint to reduce stance phase asymmetry	3.3	2 / 15 PS (ongoing)	CRF La Chataigneraie, Menucourt, France Dr Charles FATTAL	RCB 2017-A03611-52

Table 9. Overview of the different clinical protocols and subjects included.

---

Depending on the protocol, a variable amount of data was recorded for each participant. While in some cases the number of sensors used was relatively low (e.g. 1 IMU on the feet for the electrical stimulation based cueing in PD), other protocols required a high number of sensors and devices and led to a considerable quantity of data to process over time (e.g. inertial sensors, gait mat, videos, OMCS data, stimulation log, pressure insoles, heart rate sensor, etc...). For instance, the inertial sensors based analysis of gait in post-stroke participants led to more than 7400 files (22 GB size), 930 analyzed strides for 29 participants included over two years. To respect anonymity, generic IDs were generated for each subject.

If the clinical experimental data processing required numerous software developments to automatize it and be able to manage a high number of data, multiple hardware and software implementation were also needed to make the experiments possible.

## 4.2 An hardware and software architecture challenge

### 4.2.1 Problematic

Most of the clinical experimental protocols published in literature are usually conducted in controlled conditions, inside a restricted environment (e.g. a gait analysis laboratory, in a hospital corridor, etc...) with a person in charge nearby.

One of the major challenges of this thesis was to investigate and design realistic patient-centered solutions.

In addition to the previously mentioned constraints of functionality and ease of use, to meet this requirement the considered solution had to be usable outside the experimentation room, with maximum autonomy and portability.

However, the different studies addressed through this document highlighted the need for computing power, speed and reliability to design a generic FES controller able to process input data (e.g. filtering raw inertial data), execute algorithms (e.g. joint angle estimation, gait event detection...) and generate a command signal for the stimulator in real time.

How to design a hardware and software solution able to answer all of these specifications?

Through the implementation of different experimental protocols, multiple technological iterations have enabled to converge to a generic solution, achieved by means of a scalable architecture decentralized on the subject.

### 4.2.2 Iterations: toward a decentralized solution

In order to be able to experimentally validate the assumptions made through this thesis, numerous hardware and software developments had to be done, often combining devices initially conceived for a different intended use.

Chapter 2 of this thesis gives an overview of how to use an inertial sensor to assess motion in an ambulatory context. The first experiments were realized with generic low-cost IMU (HikoB<sup>©</sup> FOX) able to work either offline or online.

Configured in offline mode, these inertial sensors are able to record data at a high sampling rate (up to 800 Hz for the gyrometer) on a  $\mu$ SD card embedded on each IMU. The start and stop of the data acquisition is managed by a master node sending a radio beacon when a button is pressed by the user.

In case the IMUs are combined with a gait instrumented mat, it is necessary to synchronize the gait mat acquisition with the IMU data. This has been achieved by modifying one of the IMU to be able to record a trigger output signal emitted by the gait carpet on first IC (Initial Contact).

For the protocol presented in section 2.3.3, an OMCS (Optical Motion Capture System) was additionally used. To synchronize the OMCS with IMUs and the gait mat, the trigger output from the carpet was recorded on an acquisition board and logged on a computer (Figure 62).

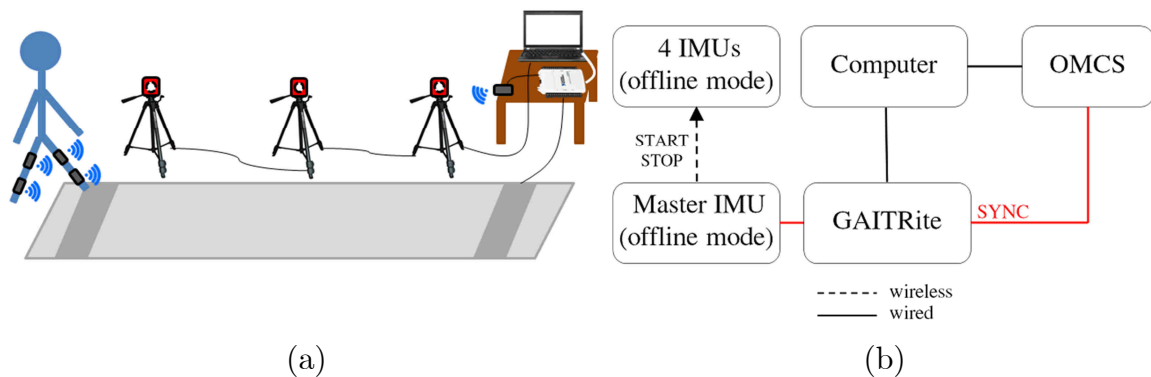


Figure 62. Illustration of the experimental setup (a) and architecture associated (b) implemented for an offline analysis of gait based on inertial sensors in post-stroke individuals (section 2.3.3).

In chapter 3, our low-cost sensors had to be configured in an online mode in order to use the data flow to perform an associated action in real-time. A computer nearby was used to collect the inertial data via a sink node, process them and send the adequate stimulation command.

The FOX wireless inertial sensors have been chosen for their low-cost and genericity, meanwhile this kind of IMU is designed as Wireless Body Area Network (WBAN) sensors. A WBAN is a network of mobile and compact

---

computing devices. Either wearable or implanted into the human body, the sensors are able to monitor human body vital parameters, activity and have been recently used for other purposes such as monitoring traffic, crops, infrastructure...

BAN sensors have to respect defined standards: low power, short range, and extremely reliable communication.

In our case, the radio transceiver and microcontroller embedded inside the FOX sensor and the sensor network management limited the overall performances compared to powerful Bluetooth or Wi-Fi inertial sensors with high data rates. Depending on the number of sensors communicating inside the WBAN and on the type of data to process (raw inertial data only, raw inertial data + AHRS, AHRS only) the sampling rate could go from 20 Hz up to 100 Hz at a maximum transmission range of about 10 meters between the IMUs and the sink node connected to the computer.

Among the different experimental protocols conducted through this thesis, some did not required a high number of sensors or a powerful processing. For instance, the experimental requirements presented in section 3.1 (i.e. electrical stimulation as a cueing in PD) needed one IMU and the access to raw inertial data only (gyrometer and accelerometer). Therefore a 100 Hz sampling rate could be reached from the WBAN to successfully trigger the stimulation at heel on (Figure 63), via the sink node connected to a computer processing the inertial data and sending the stimulation command via the stimulators' network manager unit. In this case, the subject had to stay nearby the computer to prevent wireless transmission losses with the stimulator and the IMU.

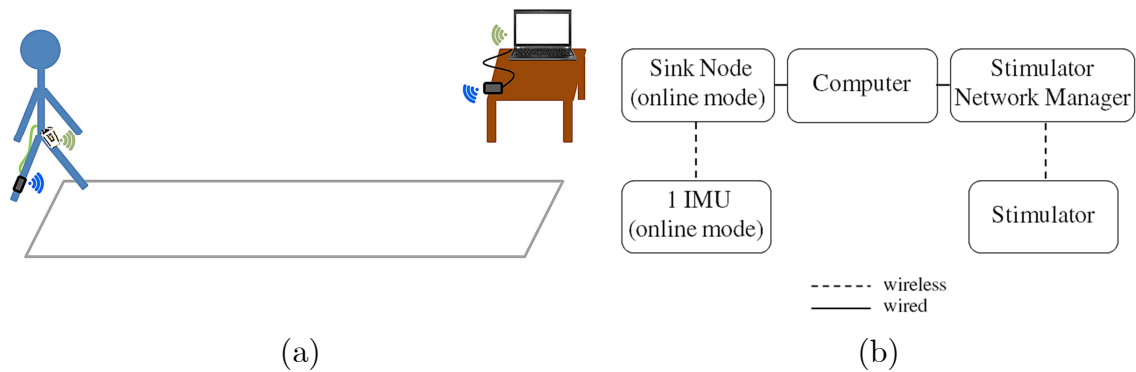


Figure 63. Illustration of the experimental setup (a) and architecture associated (b) implemented for an online triggering of wireless stimulator based on a wireless inertial sensor mounted on the foot of a PD individual.

At least two inertial sensors are needed to compute a joint angle. As mentioned in section 2.1.2, to obtain an optimal accuracy and preventing error accumulation over time, the angle should be computed via an AHRS method and the error should be reset when a zero velocity event is detected (ZVU). This requires getting both quaternion and raw inertial data for each IMU (i.e. 4 sensors if two joint angles to be computed) in case of knee angles computation while walking.

Two online solutions were first implemented. The first one consisted in getting only raw inertial data from the 4 FOX sensors, then computing Martin et al. [118] AHRS method and ZVU detection on a computer nearby. The second one consisted in embedding the AHRS algorithm directly on each IMU and transmitting directly the quaternion instead of the raw inertial data. Meanwhile, none of these solutions were able to successfully and reliably broadcast the needed data at a sampling rate higher than 50 Hz with the wireless FOX inertial sensors. As introduced in section 2.1.2, a normal gait leads to frequencies around 25 Hz [107], thereby requiring a data rate of at least 50 Hz. Munoz et al. [217] demonstrated that the lowest usable sampling frequency lies between 100 Hz and 200 Hz to analyse walking from a foot mounted IMU without impacting the results. We also experimentally observed that to monitor joint angles, a rate of 50 samples per second was too low for a fine control of motion (e.g. missing peak

knee angles). In addition, as mentioned in section 2.1.1.c, inertial data have to be integrated to be able to obtain velocity or trajectory from an initial position. The higher the sampling is, the lower the integration drift will be. At 50 Hz, the accumulated error was considerable and gave inconsistent results. Moreover, numerous data losses were due to wireless transmissions between the sensors, the computer and the stimulator.

In order to solve these issues, a new hardware and software architecture has been elaborated.

### 4.2.3 A scalable solution

The decision was made to decentralize the controller (i.e. the computer) directly on the participant, thereby relocating the essential wireless links around the user (Figure 51b). For this purpose, a mini low-cost computer (Raspberry Pi3<sup>®</sup>) was embedded in a 3D-printed case strapped around the waist of the subject.

Using the wireless inertial sensors connected as a WBAN, the sink node was in charge to get the data from all the IMUs, therefore highly decreasing the data flow when multiple IMUs were transmitting inside the network. To get rid of this limitation and guarantee an overall 100 Hz sampling rate no matter the number of IMUs, the FOX wireless inertial sensors were replaced by wired ones, low-cost with a high speed ARM Cortex-M0 based processor and a Kalman Filter directly providing quaternion estimation at 100 Hz for each IMU. The use of a multiplexer connected through an I2C interface (Inter Integrated Circuit) enabled to keep a 100 Hz rate using 4 IMUs.

The stimulator used in the experiments was a wireless programmable and controllable device (Phenix Neo<sup>®</sup>). Latency issues and communication losses were observed when the computer sending the command to the stimulator was too far or if an obstacle was present between the computer and the participant wearing the stimulator. Taking advantage of the FES controller located on the subject to control the stimulator nearby has enabled us to solve this issue.

---

In this configuration, this autonomous FES controller is able to acquire the data, process them, execute control algorithms and send the appropriate stimulation command to the stimulator.

For safety reasons, in order to access to the FES controller and to enable a remote access to the stimulation from a computer, an ad-hoc Wi-Fi network is automatically provided by the Raspberry on start-up. The ad-hoc network enables to be independent of a network infrastructure where the connection is not always possible (e.g. Wi-Fi network from the hospital).

The closed-loop control of the knee presented in section 3.3 used this last architecture combined with additional wireless sensors (heart rate monitor, foot pressure insoles)(Figure 64). A careful selection and configuration of the wireless technologies had to be respected in order to not create radio disturbances between the frequencies ranges used. The heart rate arm band monitor used an ANT+ communication protocol, the foot pressure insoles a Bluetooth 4.0 BLE protocol, the stimulator a proprietary protocol and the ad-hoc network relied on a standard secured Wi-Fi protocol. Additional FOX wireless sensors could be also added on demand. In this case, more than five different wireless protocols were spread in the same location using the same frequency range: 2.4 – 2.5 GHz. To limit radio interferences different channels were chosen between the stimulator, the ad-hoc Wi-Fi network, and the ANT+ protocol.

The stimulator and the FOX inertial sensors are part of their own scalable network [218]. In these distributed architectures, the respective network managers (i.e. the stimulators' network manager unit and the IMUs' sink node) can pilot a set of stimulation and acquisition units and modify dynamically stimulation and acquisition parameters. This major advantage enables the user to add several stimulators and several wireless IMUs, depending on the considered therapeutic rehabilitation application. If needed, the I2C multiplexer can also manage up to 8 IMUs without decreasing the 100 Hz acquisition rate.

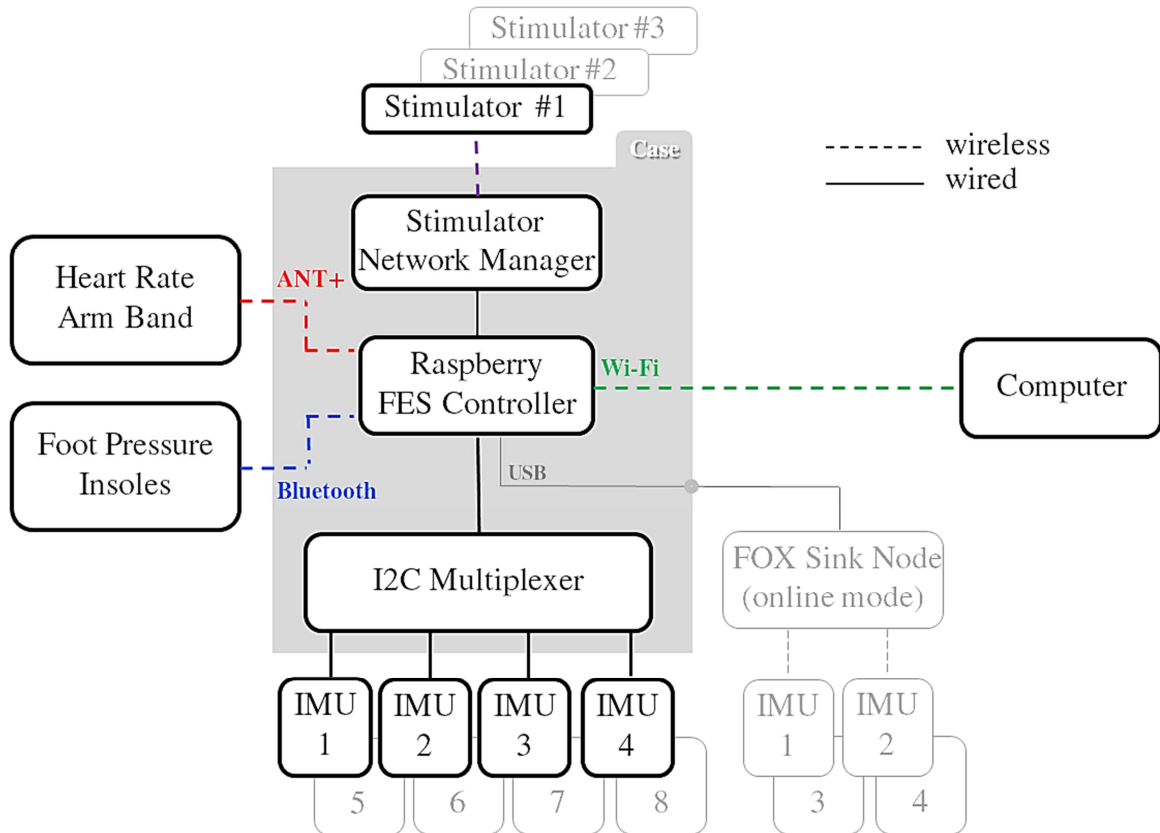


Figure 64. In bold, the hardware architecture developed for the FES based knee control protocol presented in section 3.3. Wireless and wired sensors feed the Raspberry running a P controller, wirelessly connected to the stimulator. A computer can be used to remotely start, stop and configure the closed-loop process. The scalable architecture (light grey) enables to add additional inertial sensors (wired or wireless) and stimulators.

Powered by a commercial USB power bank, a dedicated case was designed to host the Raspberry card, a loudspeaker (for audio feedback), the stimulators' network manager unit and the I2C multiplexer (Figure 65). With up to 8 hours of battery life provided by the USB power bank, the FES controller case weighs less than 130 g and measures 9 (length) x 6 (width) x 4 (depth) cm.

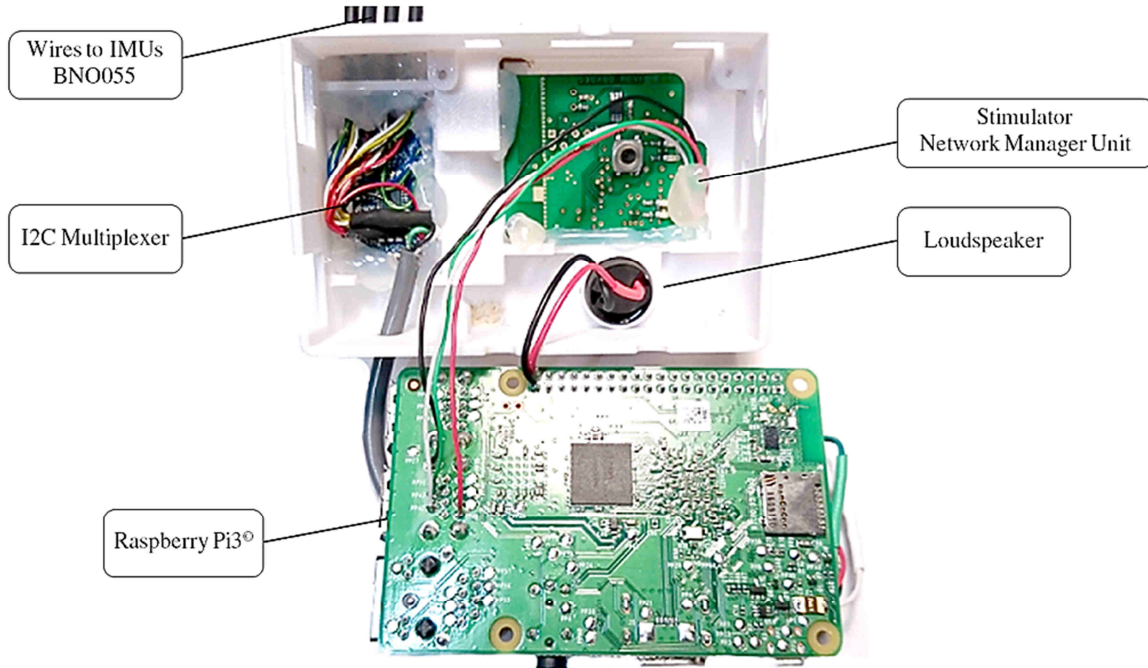


Figure 65. A FES controller based on a Raspberry Pi3, including a multiplexer I2C wired to Bosch BNO055 IMUs, a loudspeaker and the stimulators' network manager unit were embedded on the participant inside a custom-made 3D-printed case. Bluetooth, ANT+ dongle and USB FOX sink node could enable to add multiple sensors running different radio protocols.

Through this open architecture, an evolutive hardware solution has been achieved, adaptable to the needs of different FES applications, environments and pathologies. It is now used by our research team for other applications, enabling clinicians to explore novel directions and study new hypotheses.

#### 4.2.4 Software implementation

In addition to the development of hardware architectures, several software developments had to be performed in order to allow the practitioner (Figure 67) and the investigator to interact with the sensors, to visualize data or to control and follow the level of assistance (Figure 66). Used during clinical experiments, the graphical user interfaces (GUIs) had to be reliable and had to offer a maximum of functionalities, such as a patient-centered approach.

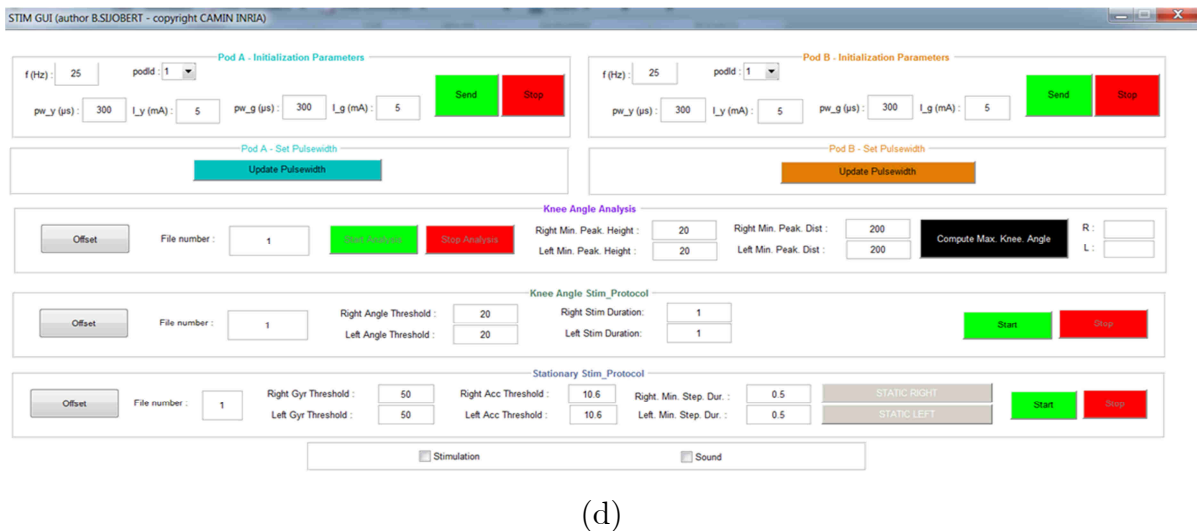
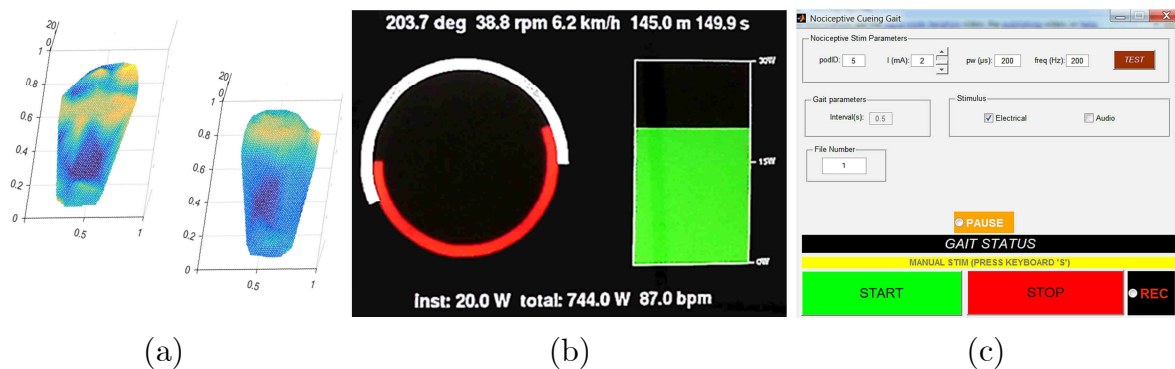


Figure 66. Examples of graphics displays and GUI (Graphical User Interfaces) created through this thesis. a) 3D mesh plot of pressure distribution based on raw matrix data from FeetMe<sup>©</sup> insoles b) Live plotting of power, crank angle, bike speed and heart rate to follow online FES cycling protocol performances and monitor the subject's health. c)d) GUIs for online setting and controlling stimulation and triggering modality in FES protocols.

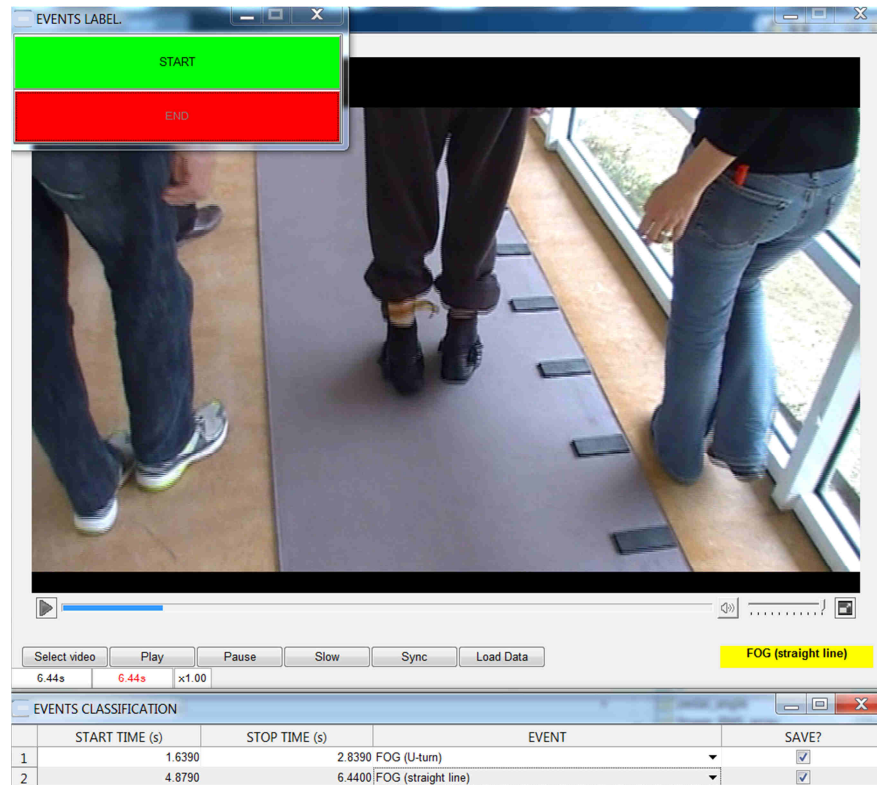


Figure 67. MovieFOG: software intended for the practitioner to label FOG events from video recording.

Most of the algorithms developed through this thesis were systematically written using Python programming language. As an open source programming language being available for many operating systems (i.e. multi-OS), Python turned out to be an appropriate choice to promote genericity and usability for future users.

An open-source toolbox containing most of the IMU related algorithms presented in this document was developed and published on a participative software development platform (<https://github.com/sensbio/sensbiotk>) to enable a maximum of users to implement the algorithms and solutions on any generic inertial sensor.

In addition to open-source, multi-OS and genericity requirements, the scalable architecture and the integration of several technologies being executed in parallel have required a programming language able to manage multithreading and object-oriented programming. In section 3.3, the closed-loop control of the knee is

based on a master Python script generating multiple threads for each specific parallel task: reading values from insoles and IMUs, computing knee angles from quaternion, detecting the pre-stance events, sending the stimulation command... The script was executed and managed online via a SSH (Secure Shell) remote access from the computer connected to the ad-hoc Wi-Fi network (Figure 68).

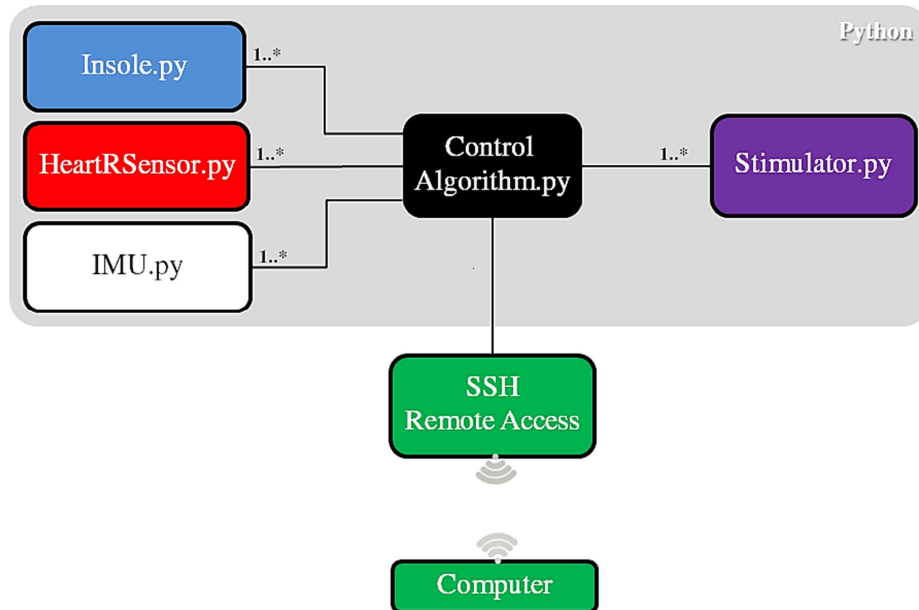


Figure 68. Python based software architecture executed on the FES controller. Multiple threads enable in parallel to read and process data while controlling the stimulation. A secure shell (SSH) remote access enables the user to manage the master script from the computer.

The ad-hoc network could be also used to display the remote desktop of the Raspberry and above all to check and download the data files recorded on the FES controller directly on the PC via a FTP (File Transfer Protocol) communication. This last point is a major advantage compared to previous experimental setups (e.g. data logging on  $\mu$ SD cards) where checking the data was impossible before the end of the clinical experiment.

### 4.3 Patient-centered solutions for an ambulatory use in a clinical context: a constrained challenge

This thesis aimed at investigating innovative assistive solutions based on FES of lower limbs and intended to be used by people with disabilities. As part of a neurorehabilitation program in a clinical environment, the proposed approaches could be also considered for a personal use at home. In addition, the solution undertaken had to be usable in an ambulatory context (e.g. gait restoration, cycling...). These aims led to major constraints that conditioned from the beginning the whole research process of this thesis.

A patient-centered approach prevented to consider numerous approaches where a technological overload or a complex procedure to operate the FES system would not have been realistic to investigate. To study pathological motions on different people often requires to finely parameterize individual thresholds. To optimize a proposed approach, literature often proposes mathematical solutions based on motion repetitions, on geometrical modelling or on simulation. In this thesis context, to ask a participant with a physical disability to stay still during more than 5 s or to perform 20 repetitions in order to optimize the calibration of an algorithm could not be reasonably considered. Similarly, asking a practitioner or a disabled user to accurately align a sensor in order to respect a precomputed geometrical model, or to test different thresholds to correctly parameterize the solution, did not meet the needs for a maximum usability, functionality and ease of use.

All the presented results of this thesis have been obtained with the objective of studying algorithms also answering to genericity, in terms of sensors used and pathology considered. Better results could have been obtained by designing a very specific solution for a given pathology or user regarding motion assessment. Moreover, the low-cost sensors used all along this work could not concurrence the performances of costly 3D motion tracking products.

Meanwhile, the results obtained at the end of this work fulfilled each of the initial objectives set at the beginning of this thesis, ensuring to study realistic, scalable and adaptable neurorehabilitation solutions to be later used by a patient or a practitioner in different environments and applications.

## 4.4 Conclusion – Perspectives

Major advances in neurorehabilitation engineering have led to a deeper knowledge of the control of motion. Following many years of research in the field of motor control and rehabilitation technology and despite outstanding technological development capabilities (microelectronics, biocompatible materials, micromachining, etc...), FES-based neurorehabilitation however still remains confined to punctual clinical uses, reflecting the slow acceptance of rehabilitation technology. Despite a substantial need expressed by both the practitioners and patients, the design and implementation of an efficient FES system still remain a complicated process which often results in unusable or inaccessible devices.

Considerable improvements of the quality of life of a person with disabilities could be however provided using these technologies, by enhancing autonomy and mobility.

Challenged by this paradoxical observation, this thesis aimed at investigating convenient and accessible neurorehabilitation solutions to promote their usability and allow human with sensorimotor disability to participate in activities beneficial to the overall health.

Using functional electrical stimulation for neurorehabilitation of lower limb movements, several approaches and algorithms were studied through this thesis and experimentally validated in different clinical and pathological contexts, using low-cost wearable sensors combined to programmable stimulators to successfully assess and control motion. Through an open architecture, an evolutive hardware solution has been achieved, adaptable to the needs of different FES applications, environments and pathologies. It is now used by our research team and clinicians

---

to explore novel directions and study new hypotheses. Promising clinical results were also obtained on several individuals with sensorimotor impairments.

Assessment is necessary to objectively measure functional impairments, to evaluate a rehabilitation treatment and to provide a customization of a neurorehabilitation solution. Meanwhile, only clinical studies and the feedback from the users can provide a measure of the quality of the proposed neurorehabilitation technology.

Following the work initiated through this thesis, the closed-loop control of the knee presented in section 3.3 performed on post-stroke subjects should be transposed to individuals suffering from cerebral palsy. Few alternatives to major surgeries exist to correct a crouch or a stiff-knee gait. The use of FES could represent a promising solution. Using a similar closed-loop control modality of the knee joints in the context of FES cycling could open the way to exciting perspectives and will be investigated in the coming months as well.

In the coming years, the development of innovative implantable devices and the technological progresses in neural engineering should open new horizons from where the success is likely to come, by directly interfacing the central and peripheral nervous system.

Meanwhile, a comprehensive work around motor control and technology integration could be achieved using external FES as a first step toward implantable solutions. This should maximize the usage and open the way to pioneering FES neurorehabilitation solutions, combining for instance wearable sensors and mechanical actuators to design advanced hybrid FES-based neuroprostheses.

## 5 References

### Publications

#### Journals

C. Azevedo, **B. Sijobert**, R. Pissard-Gibollet, M. Pasquier, B. Espiau, and C. Geny, “Detection of Freezing of Gait in Parkinson Disease: Preliminary Results,” *Sensors*, vol. 14, no. 4, pp. 6819–6827, Jan. 2014.

**B. Sijobert**, M. Benoussaad, J. Denys, R. Pissard-Gibollet, C. Geny, and C. Azevedo, “Implementation and Validation of a Stride Length Estimation Algorithm, Using a Single Basic Inertial Sensor on Healthy Subjects and Patients Suffering from Parkinson’s Disease,” *Health (Irvine, Calif.)*, vol. 7, no. June, pp. 704–714, 2015.

M. Benoussaad, **B. Sijobert**, K. Mombaur, and C. Azevedo, “Robust Foot Clearance Estimation based on Acceleration Integration of Mounted Inertial Measurement Unit,” *Sensors*, no. October 2015, pp. 1–13, 2015.

**B. Sijobert**, C. Azevedo, D. Andreu, C. Verna, and C. Geny, “Effects of sensitive electrical stimulation based cueing in Parkinson’s disease: a preliminary study,” *Eur. J. Transl. Myol.*, vol. 26, no. 2, p. [1] P. Lorenzi, R. Rao, A. Suppa, A. Kita, R. Pari, 2016. **1<sup>st</sup> prize Vodnovnik Award**

A. Daubigney, C. Azevedo, **B. Sijobert**, J. Parent, and C. Fattal, “Stimulation électrique fonctionnelle et vélo couché : un apport rééducatif et récréatif dans la prise en charge du blessé médullaire,” *Kinésithérapie, la Rev.*, vol. 17, no. 184, p. 88, Apr. 2017.

**B. Sijobert**, C. Azevedo, D. Andreu, C. Verna, and C. Geny, “Effects of sensitive electrical stimulation-based somatosensory cueing in Parkinson’s disease gait and Freezing of Gait assessment,” *Artif. Organs*, 2017.

**B. Sijobert**, C. Fattal, A. Daubigney, and C. Azevedo, “Participation to the first Cybathlon: an overview of the FREEWHEELS team FES-cycling solution,” *Eur. J. Transl. Myol.*, vol. 27, no. 4, p. 7120, 2017.

S. D. Bella, **B. Sijobert**, V. Cochen De Cock, F. Puyjarinet, C. Azevedo, and C. Geny, “Capacités rythmiques des patients parkinsoniens avec freezing,” *Rev. Neurol. (Paris)*, vol. 174, p. S114, 2018.

F. Feuvrier, **B. Sijobert**, C. Azevedo, A. Dupeyron, I. Laffont, and J. Froger, “Inertial measurement unit compared to motion optical capturing system in post stroke patients with foot-drop syndrome.” *Ann. Phys. Rehabil. Med.*, *accepted under minor revisions*, 2018.

C. Fattal, **B. Sijobert**, A. Daubigney, E. Fachin-Martins, and C. Azevedo, “Training with FES-assisted cycling in a subject with spinal cord injury: psychological, physical and physiological considerations,” *J. Spinal Cord Med.*, 2018.

## Conference

**B. Sijobert**, J. Denys, C. Azevedo, and C. Geny, “IMU based detection of freezing of gait and festination in Parkinson’s disease,” in *2014 IEEE 19th International Functional Electrical Stimulation Society Annual Conference, IFESS 2014 - Conference Proceedings*, 2014.

**B. Sijobert**, C. Lebrun, V. Begel, C. Verna, G. Castelnovo, S. Dalla Bella, C. Azevedo, and C. Geny, “Interest of the task of ‘Stepping in place’ in the assessment of freezing in Parkinson’s disease patients,” *Ann. Phys. Rehabil. Med.*, vol. 58, pp. e71–e72, Sep. 2015.

**B. Sijobert**, R. Pissard-Gibollet, J. Froger, and C. Azevedo, “Validation of inertial sensor fusion algorithms in the context of hemiparetic gait assessment,” in *7th International IEEE/EMBS conference on neural engineering*, 2015.

C. Azevedo, **B. Sijobert**, J. Froger, and C. Fattal, “Preliminary developments towards closed-loop FES-assistance of posture and gait,” in *IFAC-PapersOnLine*, 2015, vol. 28, no. 20, pp. 333–337.

**B. Sijobert**, A. Daubigney, E. F. Martins, C. Azevedo, C. Fattal, “Longitudinal feasibility study of a SCI subject one-year training based on sublesional muscles FES assisted cycling,” in *International FES Society Conference*, London 2017, p. 2017.

F. Feuvrier, **B. Sijobert**, C. Azevedo, A. Dupeyron, I. Laffont, and J. Froger, “Assessment of the metrological qualities of inertial sensors compared to the reference system for adaptive trigger functional electrical stimulation to correct dropfoot in poststroke hemiplegic patients,” SOFMER 2017, Nancy. *Ann. Phys. Rehabil. Med.*, vol. 60, p. e42, Sep. 2017.

C. Azevedo, **B. Sijobert**, C. Geny, J. Froger, and C. Fattal, “The Potential of Inertial Sensors in Posture, Gait and Cycling FES-Assistance,” ICNR: International Conference on NeuroRehabilitation, Oct 2016, Ségovie, Spain. *Biosystems and Biorobotics*, vol. 15, 2017, pp. 699–704.

C. Azevedo, **B. Sijobert**, and J. Froger, “FES-Drop-Foot Correction: From Pre-programmed Patterns to Online Modulation,” ICNR: International Conference on NeuroRehabilitation, Oct 2016, Ségovie, Spain. Springer, Cham, 2017, pp. 971–974.

C. Fattal, **B. Sijobert**, A. Daubigney, B. Lucas, and C. Azevedo, “The feasibility of training with FES-assisted cycling: Psychological, physical and physiological consideration,” SOFMER 2017, Nancy. *Ann. Phys. Rehabil. Med.*, vol. 60, p. e15, Sep. 2017.

- 
- B. Sijobert**, F. Feuvrier, J. Froger, and C. Azevedo, “A Sensor Fusion Approach for Inertial Sensors Based 3D Kinematics and Pathological Gait Assessments: Toward an Adaptive Control of Stimulation in Post-Stroke Subjects.,” in *40th Annual International Conference of the IEEE Engineering in Medicine and Biology Society*, 2018.
- R. Baptista, **B. Sijobert**, C. Azevedo, “New approach of cycling phases detection to improve FES-pedaling in SCI individuals,” in *International Conference on Intelligent Robots and Systems (IROS)*, Madrid, Spain, 2018.
- B. Sijobert**, F. Charles, J. Pontier, and C. Azevedo, “FES-based control of knee joint to reduce stance phase asymmetry in post-stroke gait: feasibility study,” in *International Conference On Neurorehabilitation (ICNR)*, Pisa, Italy, 2018.

---

**Bibliography**

- [1] J. Chae, K. Kilgore, R. Triolo, and G. Creasey, “Functional neuromuscular stimulation in spinal cord injury,” *Physical Medicine and Rehabilitation Clinics of North America*, vol. 11, no. 1. pp. 209–226, 2000.
- [2] D. B. Popović and T. Sinkjær PhD, *Control of Movement for the Physically Disabled*. Springer London, 2000.
- [3] W. T. Liberson, H. J. Holmquest, D. Scot, and M. Dow, “Functional electrotherapy: stimulation of the peroneal nerve synchronized with the swing phase of the gait of hemiplegic patients,” *Arch. Phys. Med. Rehabil.*, vol. 42, pp. 101–105, 1961.
- [4] F. Gracanin, A. Kralj, and S. Rebersek, “Advanced version of the Ljubljana functional electronic peroneal brace with walking rate controlled tetanization.,” *Adv. Extern. Control Hum. Extrem.*, p. pp 484-500, 1969.
- [5] R. Kobetic, R. J. Triolo, J. P. Uhler, C. Bieri, M. Wibowo, G. Polando, E. B. Marsolais, J. A. Davis, and K. A. Ferguson, “Implanted functional electrical stimulation system for mobility in paraplegia: a follow-up case report.,” *IEEE Trans. Rehabil. Eng.*, vol. 7, no. 4, pp. 390–8, Dec. 1999.
- [6] U. Stanic, R. Acimović-Janezic, N. Gros, A. Trnkoczy, T. Bajd, and M. Kljajić, “Multichannel electrical stimulation for correction of hemiplegic gait. Methodology and preliminary results.,” *Scand. J. Rehabil. Med.*, vol. 10, no. 2, pp. 75–92, 1978.
- [7] N. J. Postans, J. P. Hasler, M. H. Granat, and D. J. Maxwell, “Functional electric stimulation to augment partial weight-bearing supported treadmill training for patients with acute incomplete spinal cord injury: A pilot study.,” *Arch. Phys. Med. Rehabil.*, vol. 85, no. 4, pp. 604–10, Apr. 2004.
- [8] T. Yan, C. W. Y. Hui-Chan, and L. S. W. Li, “Functional electrical stimulation improves motor recovery of the lower extremity and walking ability of subjects with first acute stroke: a randomized placebo-controlled trial.,” *Stroke.*, vol. 36, no. 1, pp. 80–5, 2005.
- [9] D. Popović, M. Popović, L. Schwirtlich, M. Grey, and N. Mazza, “Functional Electrical Therapy of Walking: Pilot study,” in *10th Annual Conference of the International Functional Electrical Stimulation Society*, 2005, vol. 8, p. 86.
- [10] R. Dai, R. B. Stein, B. J. Andrews, K. B. James, and M. Wieler, “Application of tilt sensors in functional electrical stimulation,” *IEEE Trans. Rehabil. Eng.*, vol. 4, no. 2, pp. 63–72, 1996.
- [11] E. G. Spaich, N. Svaneborg, H. R. Jørgensen, and O. K. Andersen, “Rehabilitation of the hemiparetic gait by nociceptive withdrawal reflex-based functional electrical therapy: a randomized, single-blinded study.,” *J. Neuroeng. Rehabil.*, vol. 11, p. 81, 2014.
- [12] M. H. Granat, B. W. Heller, D. J. Nicol, R. H. Baxendale, and B. J. Andrews, “Improving limb flexion in FES gait using the flexion withdrawal response for the spinal cord injured person,” *J. Biomed. Eng.*, vol. 15, no. 1, pp. 51–56, Jan. 1993.
- [13] S. Gervasio, C. B. Laursen, O. K. Andersen, K. Hennings, and E. G. Spaich, “A

- Novel Stimulation Paradigm to Limit the Habituation of the Nociceptive Withdrawal Reflex,” *IEEE Trans. Neural Syst. Rehabil. Eng.*, vol. 26, no. 5, pp. 1100–1107, May 2018.
- [14] E. G. Spaich, J. Emborg, T. Collet, L. Arendt-Nielsen, and O. K. Andersen, “Withdrawal reflex responses evoked by repetitive painful stimulation delivered on the sole of the foot during late stance: site, phase, and frequency modulation,” *Exp. Brain Res.*, vol. 194, no. 3, pp. 359–368, Apr. 2009.
- [15] T. Bajd, A. Kralj, R. Turk, H. Benko, and J. Šega, “Use of functional electrical stimulation in the rehabilitation of patients with incomplete spinal cord injuries,” *J. Biomed. Eng.*, vol. 11, no. 2, pp. 96–102, 1989.
- [16] J. PL and N. MS, “Modes, benefits, and risks of voluntary electrically induced exercise in persons with spinal cord injury.,” *J Spinal Cord Med*, vol. 24(1). pp. 10–18, 2001.
- [17] R. P. Wilder, E. V Jones, T. C. Wind, and R. F. Edlich, “Functional electrical stimulation cycle ergometer exercise for spinal cord injured patients,” *J. Long. Term. Eff. Med. Implants*, vol. 12, no. 3, pp. 161–174, 2002.
- [18] T. W. J. Janssen, R. M. Glaser, and D. B. Shuster, “Clinical efficacy of electrical stimulation exercise training: effects on health, fitness and function,” *Top. Spinal Cord Inj. Rehabil.*, vol. 3, no. 3, pp. 33–49, 1998.
- [19] H. Berry, C. Perret, N. Donaldson, and K. J. Hunt, “Cardiorespiratory and Power Adaptations to Stimulated Cycle Training in Paraplegia,” *Med. Sci. Sport. Exerc.*, vol. 40, no. 9, pp. 1573–1580, Sep. 2008.
- [20] A. Frotzler, S. Coupaud, C. Perret, T. H. Kakebeeke, K. J. Hunt, N. de N. Donaldson, and P. Eser, “High-volume FES-cycling partially reverses bone loss in people with chronic spinal cord injury,” *Bone*, vol. 43, no. 1, pp. 169–176, Jul. 2008.
- [21] L. D. Duffell, N. de N. Donaldson, T. A. Perkins, D. N. Rushton, K. J. Hunt, T. H. Kakebeeke, and D. J. Newham, “Long-term intensive electrically stimulated cycling by spinal cord-injured people: Effect on muscle properties and their relation to power output,” *Muscle Nerve*, vol. 38, no. 4, pp. 1304–1311, Oct. 2008.
- [22] C. L. Sadowsky, E. R. Hammond, A. B. Strohl, P. K. Commean, S. A. Eby, D. L. Damiano, J. R. Wingert, K. T. Bae, and J. W. McDonald, “Lower extremity functional electrical stimulation cycling promotes physical and functional recovery in chronic spinal cord injury,” *J. Spinal Cord Med.*, vol. 36, no. 6, pp. 623–631, Nov. 2013.
- [23] R. S. Gibbons, C. G. Stock, B. J. Andrews, A. Gall, and R. E. Shave, “The effect of FES-rowing training on cardiac structure and function: pilot studies in people with spinal cord injury,” *Spinal Cord*, vol. 54, no. 10, pp. 822–829, Oct. 2016.
- [24] K. J. Hunt, J. Fang, J. Saengsuwan, M. Grob, and M. Laubacher, “On the efficiency of FES cycling: A framework and systematic review,” *Technol. Heal. Care*, vol. 20, no. 5, pp. 395–422, 2012.
- [25] J. Kojovic, “Sensors driven functional electrical stimulation for restoration of walking in acute stroke patients,” *European Journal of Neurology*, vol. 16, no. S3.

- p. 312, 2009.
- [26] G. D. Wheeler, B. Andrews, R. Lederer, R. Davoodi, K. Natho, C. Weiss, J. Jeon, Y. Bhambhani, and R. D. Steadward, “Functional electric stimulation–assisted rowing: Increasing cardiovascular fitness through functional electric stimulation rowing training in persons with spinal cord injury,” *Arch. Phys. Med. Rehabil.*, vol. 83, no. 8, pp. 1093–1099, Aug. 2002.
- [27] R. Davoodi, B. J. Andrews, and G. D. Wheeler, “Automatic Finite State Control of FES-Assisted Indoor Rowing Exercise after Spinal Cord Injury,” *Neuromodulation Technol. Neural Interface*, vol. 5, no. 4, pp. 248–255, Oct. 2002.
- [28] N. M. Yusoff, N. A. Hamzaid, N. Hasnan, N. Ektas, and G. M. Davis, “Automatic stimulation activation for a sliding stretcher FES-rowing system,” in *2014 IEEE 19th International Functional Electrical Stimulation Society Annual Conference (IFESS)*, 2014, pp. 1–3.
- [29] J. Arnin, T. Yamsa-Ard, P. Triponywasin, and Y. Wongsawat, “Development of practical functional electrical stimulation cycling systems based on an electromyography study of the Cybathlon 2016.,” *Eur. J. Transl. Myol.*, vol. 27, no. 4, p. 7111, Dec. 2017.
- [30] C. Wiesener and T. Schauer, “The Cybathlon RehaBike: Inertial-Sensor-Driven Functional Electrical Stimulation Cycling by Team Hasomed,” *IEEE Robot. Autom. Mag.*, vol. 24, no. 4, pp. 49–57, Dec. 2017.
- [31] K. J. Hunt, C. Ferrario, S. Grant, B. Stone, A. N. McLean, M. H. Fraser, and D. B. Allan, “Comparison of stimulation patterns for FES-cycling using measures of oxygen cost and stimulation cost,” *Med. Eng. Phys.*, vol. 28, no. 7, pp. 710–718, 2006.
- [32] P. J. Sinclair, G. M. Davis, R. M. Smith, B. S. Cheam, and J. R. Sutton, “Pedal forces produced during neuromuscular electrical stimulation cycling in paraplegics,” *Clin. Biomech. (Bristol, Avon)*, vol. 11, no. 1, pp. 51–57, 1996.
- [33] P.-F. Li, Z.-G. Hou, F. Zhang, Y.-X. Chen, X.-L. Xie, M. Tan, and H.-B. Wang, “Adaptive Neural Network Control of FES Cycling,” *2010 4th Int. Conf. Bioinforma. Biomed. Eng.*, pp. 1–4, 2010.
- [34] J. J. Chen, N. Y. Yu, D. G. Huang, B. T. Ann, and G. C. Chang, “Applying fuzzy logic to control cycling movement induced by functional electrical stimulation,” *IEEE Trans. Rehabil. Eng.*, vol. 5, no. 2, pp. 158–169, 1997.
- [35] M. Bellman, T.-H. Cheng, R. Downey, C. Hass, and W. Dixon, “Switched Control of Cadence During Stationary Cycling Induced by Functional Electrical Stimulation,” *IEEE Trans. Neural Syst. Rehabil. Eng.*, vol. 4320, no. c, pp. 1–1, 2015.
- [36] P. C. Eser, N. de N. Donaldson, H. Knecht, and E. Stüssi, “Influence of different stimulation frequencies on power output and fatigue during FES-cycling in recently injured SCI people,” *IEEE Trans. Neural Syst. Rehabil. Eng.*, vol. 11, no. 3, pp. 236–240, 2003.
- [37] M. J. Decker, L. Griffin, L. D. Abraham, and L. Brandt, “Alternating stimulation of synergistic muscles during functional electrical stimulation cycling improves

- endurance in persons with spinal cord injury,” *J. Electromyogr. Kinesiol.*, vol. 20, no. 6, pp. 1163–1169, 2010.
- [38] A. J. Van Soest, M. Gföhler, and L. J. R. Casius, “Consequences of ankle joint fixation on FES cycling power output: A simulation study,” *Med. Sci. Sports Exerc.*, vol. 37, no. 5, pp. 797–806, 2005.
- [39] S. C. Abdulla and M. O. Tokhi, “Optimization of indoor FES-cycling exercise assisted by a flywheel mechanism using genetic algorithm,” *2014 IEEE Int. Symp. Intell. Control*, pp. 1867–1871, 2014.
- [40] S. M. Woolley, “Characteristics of Gait in Hemiplegia,” *Top. Stroke Rehabil.*, vol. 7, no. 4, pp. 1–18, 2001.
- [41] C. K. Balasubramanian, R. R. Neptune, and S. A. Kautz, “Variability in spatiotemporal step characteristics and its relationship to walking performance post-stroke,” *Gait Posture*, vol. 29, no. 3, pp. 408–414, 2009.
- [42] K. E. Webster, J. E. Wittwer, and J. A. Feller, “Validity of the GAITRite® walkway system for the measurement of averaged and individual step parameters of gait,” *Gait Posture*, vol. 22, no. 4, pp. 317–321, 2005.
- [43] A. J. Nelson, D. Zwick, S. Brody, C. Doran, L. Pulver, G. Rooz, M. Sadownick, R. Nelson, and J. Rothman, “The validity of the GaitRite and the Functional Ambulation Performance scoring system in the analysis of Parkinson gait,” *NeuroRehabilitation*, vol. 17, no. 3, pp. 255–62, 2002.
- [44] P. Merriaux, Y. Dupuis, R. Boutteau, P. Vasseur, and X. Savatier, “A study of vicon system positioning performance,” *Sensors (Switzerland)*, vol. 17, no. 7, pp. 1–18, 2017.
- [45] A. I. Cuesta-Vargas, A. Galán-Mercant, and J. M. Williams, “The use of inertial sensors system for human motion analysis,” *Phys. Ther. Rev.*, vol. 15, no. 6, pp. 462–473, Dec. 2010.
- [46] R. Caldas, M. Mundt, W. Potthast, F. Buarque de Lima Neto, and B. Markert, “A systematic review of gait analysis methods based on inertial sensors and adaptive algorithms,” *Gait Posture*, vol. 57, pp. 204–210, Sep. 2017.
- [47] T. Seel, J. Raisch, and T. Schauer, “IMU-Based Joint Angle Measurement for Gait Analysis,” *Sensors*, vol. 14, no. 4, pp. 6891–6909, 2014.
- [48] P. Angeles, M. Mace, M. Admiraal, E. Burdet, N. Pavese, and R. Vaidyanathan, “A Wearable Automated System to Quantify Parkinsonian Symptoms Enabling Closed Loop Deep Brain Stimulation,” Springer, Cham, 2016, pp. 8–19.
- [49] J. Jovic, C. Azevedo Coste, P. Fraise, S. Henkous, and C. Fattal, “Coordinating Upper and Lower Body during FES-Assisted Transfers in Persons with Spinal Cord Injury in Order to Reduce Arm Support,” *Neuromodulation*, vol. 18, no. 8, pp. 736–743, 2015.
- [50] C. Azevedo Coste, J. Jovic, R. Pissard-Gibollet, and J. Froger, “Continuous gait cycle index estimation for electrical stimulation assisted foot drop correction,” *J. Neuroeng. Rehabil.*, vol. 11, no. 1, p. 118, 2014.
- [51] J. Malešević, S. Dedijer Dujović, A. M. Savić, L. Konstantinović, A. Vidaković, G. Bijelić, N. Malešević, and T. Keller, “A decision support system for electrode

- shaping in multi-pad FES foot drop correction,” *J. Neuroeng. Rehabil.*, vol. 14, no. 1, p. 66, Dec. 2017.
- [52] R. Williamson and B. J. Andrews, “Gait event detection for FES using accelerometers and supervised machine learning,” *IEEE Trans. Rehabil. Eng.*, vol. 8, no. 3, pp. 312–9, Sep. 2000.
- [53] R. Williamson and B. J. Andrews, “Sensor systems for lower limb functional electrical stimulation (FES) control,” *Med. Eng. Phys.*, vol. 22, no. 5, pp. 313–25, Jun. 2000.
- [54] B. Sijobert, J. Denys, C. A. Coste, and C. Geny, “IMU based detection of freezing of gait and festination in Parkinson’s disease,” in *2014 IEEE 19th International Functional Electrical Stimulation Society Annual Conference, IFESS 2014 - Conference Proceedings*, 2014.
- [55] C. Coste, B. Sijobert, R. Pissard-Gibollet, M. Pasquier, B. Espiau, and C. Geny, “Detection of Freezing of Gait in Parkinson Disease: Preliminary Results,” *Sensors*, vol. 14, no. 4, pp. 6819–6827, Jan. 2014.
- [56] B. Sijobert, R. Pissard-Gibollet, J. Froger, and C. Azevedo, “Validation of inertial sensor fusion algorithms in the context of hemiparetic gait assessment,” in *7th International IEEE/EMBS conference on neural engineering*, 2015.
- [57] B. Sijobert, M. Benoussaad, J. Denys, R. Pissard-Gibollet, C. Geny, and C. Azevedo Coste, “Implementation and Validation of a Stride Length Estimation Algorithm , Using a Single Basic Inertial Sensor on Healthy Subjects and Patients Suffering from Parkinson ’ s Disease,” *Health (Irvine. Calif.)*, vol. 7, no. June, pp. 704–714, 2015.
- [58] M. Benoussaad, B. Sijobert, K. Mombaur, and C. Azevedo-Coste, “Robust Foot Clearance Estimation based on Acceleration Integration of Mounted Inertial Measurement Unit,” *Sensors*, no. October 2015, pp. 1–13, 2015.
- [59] C. A. Coste, B. Sijobert, C. Geny, J. Froger, and C. Fattal, “The Potential of Inertial Sensors in Posture, Gait and Cycling FES-Assistance,” in *Biosystems and Biorobotics*, vol. 15, 2017, pp. 699–704.
- [60] F. Feuvrier, B. Sijobert, C. Azevedo, A. Dupeyron, I. Laffont, and J. Froger, “Assessment of the metrological qualities of inertial sensors compared to the reference system for adaptive trigger functional electrical stimulation to correct dropfoot in poststroke hemiplegic patients,” *Ann. Phys. Rehabil. Med.*, vol. 60, p. e42, Sep. 2017.
- [61] C. Azevedo Coste, B. Sijobert, and J. Froger, “FES-Drop-Foot Correction: From Pre-programmed Patterns to Online Modulation,” Springer, Cham, 2017, pp. 971–974.
- [62] B. Sijobert, F. Feuvrier, J. Froger, and C. Azevedo, “A Sensor Fusion Approach for Inertial Sensors Based 3D Kinematics and Pathological Gait Assessments: Toward an Adaptive Control of Stimulation in Post-Stroke Subjects,” in *40th Annual International Conference of the IEEE Engineering in Medicine and Biology Society*, 2018.
- [63] E. R. Bachmann, “Inertial and magnetic tracking of limb segment orientation for

- inserting humans into synthetic environments,” *Electr. Eng.*, no. December, pp. 171–178, 2000.
- [64] A. M. Sabatini, “Estimating three-dimensional orientation of human body parts by inertial/magnetic sensing,” *Sensors (Basel)*, vol. 11, no. 2, pp. 1489–525, 2011.
- [65] D. Eberly, “Rotation representations and performance issues,” *Geom. Tools. Inc.*, pp. 1–13, 2002.
- [66] W. Hamilton, *Lectures on Quaternions: containing a systematic statement of a new mathematical method.* Dublin, 1853.
- [67] V. Cviklovič, D. Hrubý, M. Olejár, and O. Lukáč, “Comparison of numerical integration methods in strap-down inertial navigation algorithm,” *Res. Agr. Eng.*, vol. 57, pp. S30–S34, 2011.
- [68] M. Kirkko-Jaakkola, J. Collin, and J. Takala, “Bias Prediction for MEMS Gyroscopes.”
- [69] E. Munoz Diaz, F. de Ponte Müller, and J. J. García Domínguez, “Use of the Magnetic Field for Improving Gyroscopes’ Biases Estimation,” *Sensors (Basel)*, vol. 17, no. 4, Apr. 2017.
- [70] B. Fan, Q. Li, and T. Liu, “How Magnetic Disturbance Influences the Attitude and Heading in Magnetic and Inertial Sensor-Based Orientation Estimation,” *Sensors*, vol. 18, no. 2, p. 76, Dec. 2017.
- [71] S. Lambrecht, S. L. Nogueira, M. Bortole, A. A. G. Siqueira, M. H. Terra, E. Rocon, and J. L. Pons, “Inertial sensor error reduction through calibration and sensor fusion,” *Sensors (Switzerland)*, vol. 16, no. 2, p. 235, Feb. 2016.
- [72] Z. D. Z. Dong, G. Z. G. Zhang, Y. L. Y. Luo, C. C. T. C. C. Tsang, G. S. G. Shi, S. Y. K. S. Y. Kwok, W. J. Li, P. H. W. Leong, and M. Y. W. M. Y. Wong, “A Calibration Method for MEMS Inertial Sensors Based on Optical Tracking,” *2007 2nd IEEE Int. Conf. NanoMicro Eng. Mol. Syst.*, pp. 542–547, 2007.
- [73] K.-Y. Choi, S.-A. Jang, and Y.-H. Kim, “Calibration of Inertial Measurement Units Using Pendulum Motion,” *Int. J. Aeronaut. Sp. Sci.*, vol. 11, no. 3, pp. 234–239, 2010.
- [74] M. Peres, R. D. Sill, C. Negocio, S. a, and S. Clemente, “a New Solution for Shock and Vibration Calibration of Accelerometers,” *Shock Vib.*, no. in mV.
- [75] Z. F. Syed, P. Aggarwal, C. Goodall, X. Niu, and N. El-Sheimy, “A new multi-position calibration method for MEMS inertial navigation systems,” *Meas. Sci. Technol.*, vol. 18, no. 7, pp. 1897–1907, 2007.
- [76] I. Frosio, F. Pedersini, N. A. Borghese, and A. S. Model, “Autocalibration of MEMS Accelerometers,” *IEEE Trans. Instrum. Meas.*, vol. 58, no. 6, pp. 2034–2041, 2009.
- [77] J. C. Springmann, J. W. Cutler, and H. Bahcivan, “Magnetic Sensor Calibration and Residual Dipole Characterization for Application to Nanosatellites,” *AIAA/AAS Astrodyn. Spec. Conf.*, no. August, pp. 1–14, 2010.
- [78] N. Bowditch, “The American Practical Navigator,” *Deffense Mapp. Agency Hydrogr.*, no. 9, p. 882, 2002.
- [79] M. Kok, J. Hol, T. Schön, F. Gustafsson, and H. Luinge, “Calibration of a

- magnetometer in combination with inertial sensors,” *Proc. 15th Int. Conf. Inf. Fusion*, pp. 787–793, 2012.
- [80] V. Renaudin, M. H. Afzal, and G. Lachapelle, “New method for magnetometer based orientation estimation,” *Proc. IEEE/ION Position, Locat. Navig. Symp.*, no. D, pp. 348–356, 2010.
- [81] S. K. Hong and S. Park, “Minimal-drift heading measurement using a MEMS gyro for indoor mobile robots,” *Sensors*, vol. 8, no. 11, pp. 7287–7299, 2008.
- [82] A. Chatfield, *Fundamentals of high accuracy inertial navigation*, vol. 174. 1997.
- [83] M. J. B. Rogers, K. Hrovat, K. Mcpherson, M. E. Moskowitz, and T. Reckart, “Accelerometer data analysis and presentation techniques,” *Tech. Report, NASA*, 1997.
- [84] S. Colton, “The balance filter: a simple solution for integrating accelerometer and gyroscope measurements for a balancing platform,” *white Pap. Massachusetts Inst. Technol. Cambridge, MA*, 2007.
- [85] E. Charry, D. T. H. Lai, R. K. Begg, and M. Palaniswami, “A study on band-pass filtering for calculating foot displacements from accelerometer and gyroscope sensors,” in *2009 Annual International Conference of the IEEE Engineering in Medicine and Biology Society*, 2009, vol. 2009, pp. 4824–4827.
- [86] R. Mahony, T. Hamel, and J. M. Pflimlin, “Complementary filter design on the special orthogonal group  $SO(3)$ ,” in *Proceedings of the 44th IEEE Conference on Decision and Control, and the European Control Conference, CDC-ECC ’05*, 2005, vol. 2005, pp. 1477–1484.
- [87] M. Euston, P. Coote, R. Mahony, J. Kim, and T. Hamel, “A complementary filter for attitude estimation of a fixed-wing UAV,” in *2008 IEEE/RSJ International Conference on Intelligent Robots and Systems, IROS*, 2008, pp. 340–345.
- [88] W. Premerlani and P. Bizard, “Direction Cosine Matrix IMU: Theory,” 2009.
- [89] Starlino, “A Guide To using IMU ( Accelerometer and Gyroscope Devices ) in Embedded Applications .,” *IMU Theory Exp.*, pp. 1–72, 2009.
- [90] S. O. H. Madgwick, “An efficient orientation filter for inertial and inertial/magnetic sensor arrays,” *Tech. Rep. X-io*, p. 32, 2010.
- [91] R. Valenti, I. Dryanovski, and J. Xiao, “Keeping a Good Attitude: A Quaternion-Based Orientation Filter for IMUs and MARGs,” *Sensors*, vol. 15, no. 8, pp. 19302–19330, Aug. 2015.
- [92] R. Mahony, S. Member, T. Hamel, and J. Pflimlin, “Nonlinear Complementary Filters on the Special Orthogonal Group,” vol. 53, no. 5, pp. 1203–1218, 2008.
- [93] S. O. H. Madgwick, A. J. L. Harrison, and R. Vaidyanathan, “Estimation of IMU and MARG orientation using a gradient descent algorithm,” *2011 IEEE Int. Conf. Rehabil. Robot.*, pp. 1–7, 2011.
- [94] R. E. Kalman, “A New Approach to Linear Filtering and Prediction Problems,” *J. Basic Eng.*, vol. 82, no. 1, p. 35, 1960.
- [95] B. Barshan and H. F. Durrant-Whyte, “Inertial Navigation Systems for Mobile Robots,” *IEEE Trans. Robot. Autom.*, vol. 11, no. 3, pp. 328–342, 1995.
- [96] E. Foxlin, “Inertial head-tracker sensor fusion by a complementary separate-bias

- Kalman filter,” in *Proceedings of the IEEE 1996 Virtual Reality Annual International Symposium*, 1996, pp. 185–194.
- [97] H. J. Luinge, P. H. Veltink, and C. T. M. Baten, “Estimating orientation with gyroscopes and accelerometers,” *Technol. Heal. care*, vol. 7, no. 6, p. 455, 1999.
- [98] J. L. Marins, X. Y. X. Yun, E. R. Bachmann, R. B. McGhee, and M. J. Zyda, “An extended Kalman filter for quaternion-based orientation estimation using MARG sensors,” *Proc. 2001 IEEE/RSJ Int. Conf. Intell. Robot. Syst. Expand. Soc. Role Robot. Next Millenn. (Cat. No.01CH37180)*, vol. 4, pp. 2003–2011, 2001.
- [99] “XSens: 3D motion tracking technology: published papers,” *Eschede, Netherlands*, 2018. [Online]. Available: <https://www.xsens.com/research/published-papers/>.
- [100] “VectorNav: Embedded Navigation Solutions,” *Texas, USA*, 2018. [Online]. Available: <https://www.vectornav.com/support/library/ahrs>.
- [101] “InterSense Thales: motion tracking products,” *Massachusetts, USA*, 2018. [Online]. Available: <http://www.intersense.com/categories/44/>.
- [102] “PNI: sensor fusion coprocessor,” *California, USA*, 2018. [Online]. Available: <https://www.pnicorp.com/sentral/>.
- [103] “Yost: 3-space sensors,” *Ohio, USA*, 2018. [Online]. Available: <https://yostlabs.com/3-space-sensors/>.
- [104] A. M. Sabatini, “Quaternion-based extended Kalman filter for determining orientation by inertial and magnetic sensing,” *IEEE Trans. Biomed. Eng.*, vol. 53, no. 7, pp. 1346–1356, 2006.
- [105] M. Haid and J. Breitenbach, “Low cost inertial orientation tracking with Kalman filter,” *Appl. Math. Comput.*, vol. 153, no. 2, pp. 567–575, 2004.
- [106] D. Gebre-Egziabher, R. C. Hayward, and J. D. Powell, “Design of multi-sensor attitude determination systems,” *IEEE Trans. Aerosp. Electron. Syst.*, vol. 40, no. 2, pp. 627–649, 2004.
- [107] J. Friedman, “Introduction to human movement analysis,” no. October, 2010.
- [108] XSens, “MTi-G-710 XSens Sensor fusion sensor,” *Eschede, Netherlands*, 2018.
- [109] MicroStrain, “3DM-GX3®-35 Miniature Attitude Heading Reference System,” *Vermont, USA*, 2018.
- [110] F. L. Markley, “Attitude Error Representations for Kalman Filtering,” *J. Guid. Control. Dyn.*, vol. 26, no. 2, pp. 311–317, Mar. 2003.
- [111] J. L. Crassidis, F. L. Markley, and Y. Cheng, “Survey of Nonlinear Attitude Estimation Methods,” *J. Guid. Control. Dyn.*, vol. 30, no. 1, pp. 12–28, Jan. 2007.
- [112] M. Zimmermann and W. Sulzer, “High Bandwidth Orientation Measurement and Control Based on Complementary Filtering,” *IFAC Proc. Vol.*, vol. 24, no. 9, pp. 525–530, Sep. 1991.
- [113] A.-J. Baerveldt and R. Klang, “A low-cost and low-weight attitude estimation system for an autonomous helicopter,” in *Proceedings of IEEE International Conference on Intelligent Engineering Systems*, pp. 391–395.
- [114] B. Vik and T. I. Fossen, “A Nonlinear Observer for Integration of GPS and INS Attitude.”
- [115] P. Martin and E. Sala, “Design and implementation of a low-cost observer-based

- Attitude and Heading Reference System,” 2009.
- [116] A. I. Cuesta-Vargas, A. Galán-Mercant, and J. M. Williams, “The use of inertial sensors system for human motion analysis.”
- [117] S. O. H. Madgwick, “An efficient orientation filter for inertial and inertial/magnetic sensor arrays,” *Rep. x-io Univ. ...*, p. 32, 2010.
- [118] P. Martin and E. Salaün, “Design and implementation of a low-cost observer-based attitude and heading reference system,” *Control Eng. Pract.*, vol. 18, no. 7, pp. 712–722, Jul. 2010.
- [119] A. Muro-de-la-Herran, B. García-Zapirain, and A. Méndez-Zorrilla, “Gait analysis methods: An overview of wearable and non-wearable systems, highlighting clinical applications,” *Sensors (Switzerland)*, vol. 14, no. 2. pp. 3362–3394, 2014.
- [120] S. Yang and Q. Li, “Inertial Sensor-Based Methods in Walking Speed Estimation: A Systematic Review,” *Sensors*, vol. 12, no. 5, pp. 6102–6116, Jan. 2012.
- [121] K. Aminian, B. Najafi, C. Bila, P. F. Leyvraz, and P. Robert, “Spatio-temporal parameters of gait measured by an ambulatory system using miniature gyroscopes,” *J. Biomech.*, vol. 35, no. 5, pp. 689–699, 2002.
- [122] D. Trojaniello, A. Cereatti, E. Pelosin, L. Avanzino, A. Mirelman, J. M. Hausdorff, and U. Della Croce, “Estimation of step-by-step spatio-temporal parameters of normal and impaired gait using shank-mounted magneto-inertial sensors: application to elderly, hemiparetic, parkinsonian and choreic gait,” pp. 1–12, 2014.
- [123] A. Rampp, J. Barth, S. Schüle, K. G. Gaßmann, J. Klucken, and B. M. Eskofier, “Inertial Sensor-Based Stride Parameter Calculation From Gait Sequences in Geriatric Patients,” *IEEE Trans. Biomed. Eng.*, vol. 62, no. 4, pp. 1089–1097, 2015.
- [124] A. Kose, A. Cereatti, and U. Della Croce, “Bilateral step length estimation using a single inertial measurement unit attached to the pelvis,” *J. Neuroeng. Rehabil.*, vol. 9, no. 1, p. 9, 2012.
- [125] B. Mariani, C. Hoskovec, S. Rochat, C. Büla, J. Penders, and K. Aminian, “3D gait assessment in young and elderly subjects using foot-worn inertial sensors,” *J. Biomech.*, vol. 43, pp. 2999–3006, 2010.
- [126] F. N. Fritsch and R. E. Carlson, “Monotonicity preserving bicubic interpolation: A progress report,” *Comput. Aided Geom. Des.*, vol. 2, no. 1–3, pp. 117–121, 1985.
- [127] J. Taborri, E. Palermo, S. Rossi, and P. Cappa, “Gait Partitioning Methods: A Systematic Review,” no. November 2015, pp. 40–42, 2016.
- [128] J. A. Flórez and A. Velásquez, “Calibration of force sensing resistors (fsr) for static and dynamic applications,” *2010 IEEE Andescon Conf. Proceedings, Andescon 2010*, pp. 2–7, 2010.
- [129] V. C. Moulianitis, V. N. Syrimpeis, N. A. Aspragathos, and E. C. Panagiotopoulos, “A closed-loop drop-foot correction system with gait event detection from the contralateral lower limb using fuzzy logic,” in *2011 10th International Workshop on Biomedical Engineering*, 2011, pp. 1–4.
- [130] A. Mannini and A. M. Sabatini, “Gait phase detection and discrimination between

- walking–jogging activities using hidden Markov models applied to foot motion data from a gyroscope,” *Gait Posture*, vol. 36, no. 4, pp. 657–661, Sep. 2012.
- [131] N. Abaid, P. Cappa, E. Palermo, M. Petrarca, and M. Porfiri, “Gait Detection in Children with and without Hemiplegia Using Single-Axis Wearable Gyroscopes,” *PLoS One*, vol. 8, no. 9, p. e73152, Sep. 2013.
- [132] R. W. Selles, M. A. G. Formanoy, J. B. J. Bussmann, P. J. Janssens, and H. J. Stam, “Automated Estimation of Initial and Terminal Contact Timing Using Accelerometers; Development and Validation in Transtibial Amputees and Controls,” *IEEE Trans. Neural Syst. Rehabil. Eng.*, vol. 13, no. 1, pp. 81–88, Mar. 2005.
- [133] J. Rueterbories, E. G. Spaich, and O. K. Andersen, “Gait event detection for use in FES rehabilitation by radial and tangential foot accelerations,” *Med. Eng. Phys.*, vol. 36, no. 4, pp. 502–508, Apr. 2014.
- [134] J. Taborri, E. Palermo, S. Rossi, and P. Cappa, “Gait Partitioning Methods: A Systematic Review,” *Sensors*, vol. 16, no. 1, p. 66, Jan. 2016.
- [135] R. E. Mayagoitia, A. V Nene, and P. H. Veltink, “Accelerometer and rate gyroscope measurement of kinematics: an inexpensive alternative to optical motion analysis systems.,” *J. Biomech.*, vol. 35, no. 4, pp. 537–42, Apr. 2002.
- [136] K. Tong and M. H. Granat, “A practical gait analysis system using gyroscopes,” *Med. Eng. Phys.*, vol. 21, no. 2, pp. 87–94, Mar. 1999.
- [137] P. Catalfamo, S. Ghousayni, and D. Ewins, “Gait event detection on level ground and incline walking using a rate gyroscope.,” *Sensors (Basel)*, vol. 10, no. 6, pp. 5683–702, 2010.
- [138] A. Laudanski, S. Yang, and Q. Li, “A concurrent comparison of inertia sensor-based walking speed estimation methods,” *2011 Annu. Int. Conf. IEEE Eng. Med. Biol. Soc.*, pp. 3484–3487, 2011.
- [139] K. Abdulrahim, T. Moore, C. Hide, and C. Hill, “Understanding the Performance of Zero Velocity Updates in MEMS-based Pedestrian Navigation,” *Int. J. Adv. Technol.*, vol. 5, no. 2, 2014.
- [140] I. P. I. Pappas, T. Keller, S. Mangold, M. R. Popovic, V. Dietz, and M. Morari, “A Reliable Gyroscope-Based Gait-Phase Detection Sensor Embedded in a Shoe Insole,” *IEEE Sens. J.*, vol. 4, no. 2, pp. 268–274, 2004.
- [141] Q. Li, M. Young, V. Naing, and J. M. Donelan, “Walking speed estimation using a shank-mounted inertial measurement unit,” *J. Biomech.*, vol. 43, no. 8, pp. 1640–1643, 2010.
- [142] M. A. Hely, W. G. J. Reid, M. A. Adena, G. M. Halliday, and J. G. L. Morris, “The Sydney Multicenter Study of Parkinson’s disease: The inevitability of dementia at 20 years,” *Mov. Disord.*, vol. 23, no. 6, pp. 837–844, 2008.
- [143] S. T. Moore, H. G. MacDougall, J. M. Gracies, H. S. Cohen, and W. G. Ondo, “Long-term monitoring of gait in Parkinson’s disease,” *Gait Posture*, vol. 26, no. 2, pp. 200–207, 2007.
- [144] N. Giladi and A. Nieuwboer, “Understanding and treating freezing of gait in Parkinsonism, proposed working definition, and setting the stage,” *Movement*

- Disorders*, vol. 23, no. SUPPL. 2, 2008.
- [145] A. Nieuwboer, K. Baker, A.-M. Willems, D. Jones, J. Spildooren, I. Lim, G. Kwakkel, E. Van Wegen, and L. Rochester, “The short-term effects of different cueing modalities on turn speed in people with Parkinson’s disease.,” *Neurorehabil. Neural Repair*, vol. 23, no. 8, pp. 831–836, 2009.
- [146] J. G. Nutt, B. R. Bloem, N. Giladi, M. Hallett, F. B. Horak, and A. Nieuwboer, “Freezing of gait: Moving forward on a mysterious clinical phenomenon,” *The Lancet Neurology*, vol. 10, no. 8, pp. 734–744, 2011.
- [147] B. R. Bloem, J. M. Hausdorff, J. E. Visser, and N. Giladi, “Falls and freezing of Gait in Parkinson’s disease: A review of two interconnected, episodic phenomena,” *Mov. Disord.*, vol. 19, no. 8, pp. 871–884, 2004.
- [148] S. T. Moore, D. a Yungher, T. R. Morris, V. Dilda, H. G. MacDougall, J. M. Shine, S. L. Naismith, and S. J. G. Lewis, “Autonomous identification of freezing of gait in Parkinson’s disease from lower-body segmental accelerometry.,” *J. Neuroeng. Rehabil.*, vol. 10, no. 1, p. 19, Jan. 2013.
- [149] D. W. Fell, K. Y. Lunnen, and R. P. Rauk, *Lifespan neurorehabilitation: a patient-centered approach from examination to interventions and outcomes*. .
- [150] C. Azevedo Coste, B. Sijobert, J. Froger, and C. Fattal, “Preliminary developments towards closed-loop FES-assistance of posture and gait,” in *IFAC-PapersOnLine*, 2015, vol. 28, no. 20, pp. 333–337.
- [151] B. Sijobert, C. Azevedo-Coste, D. Andreu, C. Verna, and C. Geny, “Effects of sensitive electrical stimulation based cueing in Parkinson’s disease: a preliminary study,” *Eur. J. Transl. Myol.*, vol. 26, no. 2, p. [1] P. Lorenzi, R. Rao, A. Suppa, A. Kita, R. Pari, 2016.
- [152] B. Sijobert, C. Azevedo, D. Andreu, C. Verna, and C. Geny, “Effects of sensitive electrical stimulation-based somatosensory cueing in Parkinson’s disease gait and Freezing of Gait assessment,” *Artif. Organs*, 2017.
- [153] B. Sijobert, C. Fattal, A. Daubigney, and C. Azevedo-Coste, “Participation to the first Cybathlon: an overview of the FREEWHEELS team FES-cycling solution.,” *Eur. J. Transl. Myol.*, vol. 27, no. 4, p. 7120, 2017.
- [154] B. Sijobert, A. Daubigney, E. F. Martins, C. Azevedo, C. Fattal, and I. Lirimm, “Longitudinal feasibility study of a SCI subject one-year training based on sublesional muscles FES assisted cycling,” in *International FES Society*, 2017, p. 2017.
- [155] C. Fattal, B. Sijobert, A. Daubigney, B. Lucas, and C. Azevedo-Coste, “The feasibility of training with FES-assisted cycling: Psychological, physical and physiological consideration,” *Ann. Phys. Rehabil. Med.*, vol. 60, p. e15, Sep. 2017.
- [156] A. Daubigney, C. A. Coste, B. Sijobert, J. Parent, and C. Fattal, “Stimulation électrique fonctionnelle et vélo couché : un apport rééducatif et récréatif dans la prise en charge du blessé médullaire,” *Kinésithérapie, la Rev.*, vol. 17, no. 184, p. 88, Apr. 2017.
- [157] C. Fattal, B. Sijobert, A. Daubigney, E. Fachin-Martins, and C. Azevedo, “Training with FES-assisted cycling in a subject with spinal cord injury:

- psychological, physical and physiological considerations,” *J. Spinal Cord Med.*, 2018.
- [158] B. Sijobert, F. Charles, J. Pontier, and C. Azevedo, “FES-based control of knee joint to reduce stance phase asymmetry in post-stroke gait: feasibility study,” in *International Conference On Neurorehabilitation (ICNR)*, 2018.
- [159] R. Baptista, B. B. Sijobert, C. A. Coste, and C. Azevedo, “New approach of cycling phases detection to improve FES-pedaling in SCI individuals,” in *International Conference on Intelligent Robots and Systems (IROS)*, 2018.
- [160] T. C. Rubinstein, N. Giladi, and J. M. Hausdorff, “The power of cueing to circumvent dopamine deficits: A review of physical therapy treatment of gait disturbances in Parkinson’s disease,” *Mov. Disord.*, vol. 17, no. 6, pp. 1148–1160, 2002.
- [161] E. Jovanov, E. Wang, L. Verhagen, M. Fredrickson, and R. Fratangelo, “deFOG - A real time system for detection and unfreezing of gait of Parkinson’s patients,” *Proc. 31st Annu. Int. Conf. IEEE Eng. Med. Biol. Soc. Eng. Futur. Biomed. EMBC 2009*, pp. 5151–5154, 2009.
- [162] Y. Baram, “Virtual Sensory Feedback for Gait Improvement in Neurological Patients,” *Front. Neurol.*, vol. 4, no. October, p. 138, 2013.
- [163] M. Suteerawattananon, G. S. Morris, B. R. Etnyre, J. Jankovic, and E. J. Protas, “Effects of visual and auditory cues on gait in individuals with Parkinson’s disease,” *J. Neurol. Sci.*, vol. 219, no. 1–2, pp. 63–69, 2004.
- [164] S. J. Spaulding, B. Barber, M. Colby, B. Cormack, T. Mick, and M. E. Jenkins, “Cueing and gait improvement among people with Parkinson’s disease: A meta-analysis,” *Arch. Phys. Med. Rehabil.*, vol. 94, no. 3, pp. 562–570, 2013.
- [165] E. van Wegen, C. de Goede, I. Lim, M. Rietberg, A. Nieuwboer, A. Willems, D. Jones, L. Rochester, V. Hetherington, H. Berendse, J. Zijlmans, E. Wolters, and G. Kwakkel, “The effect of rhythmic somatosensory cueing on gait in patients with Parkinson’s disease,” *J. Neurol. Sci.*, vol. 248, no. 1–2, pp. 210–214, 2006.
- [166] L.-A. Leow, T. Parrott, and J. A. Grahn, “Individual differences in beat perception affect gait responses to low- and high-groove music,” *Front. Hum. Neurosci.*, vol. 8, no. October, p. 811, 2014.
- [167] M. Vaugoyeau, S. Viel, C. Assaiante, B. Amblard, and J. P. Azulay, “Impaired vertical postural control and proprioceptive integration deficits in Parkinson’s disease,” *Neuroscience*, vol. 146, no. 2, pp. 852–863, 2007.
- [168] S. Mesure, J. P. Azulay, J. Pouget, and B. Amblard, “Strategies of segmental stabilization during gait in Parkinson’s disease,” *Exp. Brain Res.*, vol. 129, no. 4, pp. 573–581, 1999.
- [169] F. Qiu, M. H. Cole, K. W. Davids, E. M. Hennig, P. A. Silburn, H. Netscher, and G. K. Kerr, “Effects of textured insoles on balance in people with Parkinson’s disease,” *PLoS One*, vol. 8, no. 12, 2013.
- [170] E. Khudados, F. W. J. Cody, and D. J. O’Boyle, “Proprioceptive regulation of voluntary ankle movements, demonstrated using muscle vibration, is impaired by Parkinson’s disease,” *J. Neurol. Neurosurg. Psychiatry*, vol. 67, no. 4, pp. 504–510,

- 1999.
- [171] M. S. El-Tamawy, M. H. Darwish, and M. E. Khallaf, “Effects of augmented proprioceptive cues on the parameters of gait of individuals with Parkinson’s disease,” *Ann. Indian Acad. Neurol.*, vol. 15, no. 4, pp. 267–72, 2012.
- [172] A. Kleiner, M. Galli, M. Gaglione, D. Hildebrand, P. Sale, G. Albertini, F. Stocchi, and M. F. De Pandis, “The Parkinsonian Gait Spatiotemporal Parameters Quantified by a Single Inertial Sensor before and after Automated Mechanical Peripheral Stimulation Treatment,” *Parkinsons. Dis.*, vol. 2015, 2015.
- [173] G. E. Mann, S. M. Finn, and P. N. Taylor, “A pilot study to investigate the feasibility of electrical stimulation to assist gait in Parkinson’s disease,” *Neuromodulation*, vol. 11, no. 2, pp. 143–9, 2008.
- [174] L. Popa and P. Taylor, “Functional electrical stimulation may reduce bradykinesia in Parkinson’s disease: A feasibility study,” *J. Rehabil. Assist. Technol. Eng.*, vol. 2, no. 0, pp. 1–8, 2015.
- [175] M. Djurić-Jovičić, S. Radovanović, I. Petrović, C. Azevedo, G. Mann, and M. B. Popović, “The impact of functional electrical stimulation (FES) on freezing of gait (FOG) in patients with Parkinson’s disease,” *Clin. Neurophysiol.*, vol. 124, no. 7, p. e11, Jul. 2013.
- [176] S. R. Hundza, W. R. Hook, C. R. Harris, S. V. Mahajan, P. A. Leslie, C. A. Spani, L. G. Spalteholz, B. J. Birch, D. T. Commandeur, and N. J. Livingston, “Accurate and reliable gait cycle detection in parkinson’s disease,” *IEEE Trans. Neural Syst. Rehabil. Eng.*, vol. 22, no. 1, pp. 127–137, 2014.
- [177] J. D. Schaafsma, Y. Balash, T. Gurevich, A. L. Bartels, J. M. Hausdorff, and N. Giladi, “Characterization of freezing of gait subtypes and the response of each to levodopa in Parkinson’s disease,” *Eur. J. Neurol.*, vol. 10, no. 4, pp. 391–398, 2003.
- [178] M. Plotnik, N. Giladi, Y. Balash, C. Peretz, and J. M. Hausdorff, “Is freezing of gait in Parkinson’s disease related to asymmetric motor function?,” *Ann. Neurol.*, vol. 57, no. 5, pp. 656–663, 2005.
- [179] P. Crenna, I. Carpinella, M. Rabuffetti, E. Calabrese, P. Mazzoleni, R. Nemni, and M. Ferrarin, “The association between impaired turning and normal straight walking in Parkinson’s disease,” *Gait Posture*, vol. 26, no. 2, pp. 172–178, 2007.
- [180] D. Podsiadlo and S. Richardson, “The timed ‘Up & Go’: a test of basic functional mobility for frail elderly persons,” *J. Am. Geriatr. Soc.*, vol. 39, no. 2, pp. 142–148, 1991.
- [181] D. G. Dotov, S. Bayard, V. Cochen de Cock, C. Geny, V. Driss, G. Garrigue, B. Bardy, and S. Dalla Bella, “Biologically-variable rhythmic auditory cues are superior to isochronous cues in fostering natural gait variability in Parkinson’s disease,” *Gait Posture*, vol. 51, pp. 64–69, 2017.
- [182] A. Anzak, H. Tan, A. Pogosyan, A. Djamshidian, H. Ling, A. Lees, and P. Brown, “Improvements in rate of development and magnitude of force with intense auditory stimuli in patients with Parkinson’s disease,” *Eur. J. Neurosci.*, vol. 34, no. 1, pp. 124–132, 2011.
- [183] C.-E. Benoit, S. Dalla Bella, N. Farrugia, H. Obrig, S. Mainka, and S. Kotz,

- “Musically Cued Gait-Training Improves Both Perceptual and Motor Timing in Parkinson’s Disease,” *Front. Hum. Neurosci.*, vol. 8, no. July, p. 494, 2014.
- [184] A. Ashoori, D. M. Eagleman, and J. Jankovic, “Effects of auditory rhythm and music on gait disturbances in Parkinson’s disease,” *Frontiers in Neurology*, vol. 6, no. NOV. 2015.
- [185] B. Sijobert, M. Benoussaad, J. Denys, R. Pissard-gibollet, and C. A. Coste, “Implementation and validation of a stride length estimation algorithm , using a single inertial sensor on healthy and Parkinson ’ s disease subjects,” *Health (Irvine. Calif.)*, vol. 13, no. 9, pp. 1–7, 2015.
- [186] B. Sijobert, J. Denys, C. A. Coste, and C. Geny, “IMU based detection of freezing of gait and festination in Parkinson’s disease,” in *2014 IEEE 19th International Functional Electrical Stimulation Society Annual Conference, IFESS 2014 - Conference Proceedings*, 2014.
- [187] E. G. Spaich, L. Arendt-Nielsen, and O. K. Andersen, “Modulation of lower limb withdrawal reflexes during gait: a topographical study.,” *J. Neurophysiol.*, vol. 91, no. 1, pp. 258–66, 2004.
- [188] R. M. Glaser, “Physiologic aspects of spinal cord injury and functional neuromuscular stimulation.,” *Cent. Nerv. Syst. Trauma*, vol. 3, no. 1, pp. 49–62, 1986.
- [189] C. Fornusek and G. M. Davis, “Cardiovascular and Metabolic Responses During Functional Electric Stimulation Cycling at Different Cadences,” *Arch. Phys. Med. Rehabil.*, vol. 89, no. 4, pp. 719–725, 2008.
- [190] R. Berkelmans, J. Duysens, and D. van Kuppevelt, “Development of a tricycle for spinal cord injured,” *Rehabil. Mobility, Exerc. Sport. 4th Int. State-of-the-Art Congr.*, vol. 31, no. 0, pp. 329–331, 2010.
- [191] D. J. Newham and N. D. N. Donaldson, “FES cycling,” *Acta Neurochirurgica, Supplementum*, no. 97 PART 1. pp. 395–402, 2007.
- [192] J. A. Guimarães, L. O. da Fonseca, C. C. Dos Santos-Couto-Paz, A. P. L. Bó, C. Fattal, C. Azevedo-Coste, and E. Fachin-Martins, “Towards Parameters and Protocols to Recommend FES-Cycling in Cases of Paraplegia: A Preliminary Report.,” *Eur. J. Transl. Myol.*, vol. 26, no. 3, p. 6085, Jun. 2016.
- [193] S. F. Figoni and R. M. Glaser, “Acute hemodynamic responses of spinal cord injured individuals to functional neuromuscular...,” *J. Rehabil. Res. Dev.*, vol. 28, no. 4, p. 9, 1991.
- [194] E. Peri, E. Ambrosini, A. Pedrocchi, G. Ferrigno, C. Nava, V. Longoni, M. Monticone, and S. Ferrante, “Can FES-Augmented Active Cycling Training Improve Locomotion in Post-Acute Elderly Stroke Patients?,” *Eur. J. Transl. Myol.*, vol. 26, no. 3, p. 6063, Jun. 2016.
- [195] S. F. Pollack, K. Axen, N. Spielholz, N. Levin, F. Haas, and K. T. Ragnarsson, “Aerobic training effects of electrically induced lower extremity exercises in spinal cord injured people.,” *Arch. Phys. Med. Rehabil.*, vol. 70, no. 3, pp. 214–9, 1989.
- [196] J. Szecsi, P. Krause, S. Krafczyk, T. Brandt, and A. Straube, “Functional output improvement in FES cycling by means of forced smooth pedaling,” *Med. Sci.*

- Sports Exerc.*, vol. 39, no. 5, pp. 764–780, 2007.
- [197] R. Riener, “The Cybathlon promotes the development of assistive technology for people with physical disabilities,” *J. Neuroeng. Rehabil.*, vol. 13, no. 1, p. 49, Dec. 2016.
- [198] C. Wiesener, S. Ruppin, and T. Schauer, “Robust Discrimination of Flexion and Extension Phases for Mobile Functional Electrical Stimulation (FES) Induced Cycling in Paraplegics,” *IFAC-PapersOnLine*, vol. 49, no. 32, pp. 210–215, Jan. 2016.
- [199] C. Stein, C. G. Fritsch, C. Robinson, G. Sbruzzi, and R. D. M. Plentz, “Effects of Electrical Stimulation in Spastic Muscles After Stroke: Systematic Review and Meta-Analysis of Randomized Controlled Trials,” *Stroke*, vol. 46, no. 8, pp. 2197–205, Aug. 2015.
- [200] Z. Tan, H. Liu, T. Yan, D. Jin, X. He, X. Zheng, S. Xu, and C. Tan, “The Effectiveness of Functional Electrical Stimulation Based on a Normal Gait Pattern on Subjects with Early Stroke: A Randomized Controlled Trial,” *Biomed Res. Int.*, vol. 2014, pp. 1–9, 2014.
- [201] J. P. Holden, G. Chou, and S. J. Stanhope, “Changes in knee joint function over a wide range of walking speeds,” *Clin. Biomech.*, vol. 12, no. 6, pp. 375–382, 1997.
- [202] J. Perry, D. Antonelli, and W. Ford, “Analysis of knee-joint forces during flexed-knee stance,” *J. Bone Joint Surg. Am.*, vol. 57, no. 7, pp. 961–7, Oct. 1975.
- [203] F. Chantraine, C. Schreiber, E. Kolanowski, and F. Moissenet, “Control of Stroke-Related Genu Recurvatum With Prolonged Timing of Dorsiflexor Functional Electrical Stimulation,” *J. Neurol. Phys. Ther.*, vol. 40, no. 3, pp. 209–215, Jul. 2016.
- [204] J. Rose and J. G. Gamble, *Human walking*, 2nd ed. Baltimore: Williams & Wilkins, 1994.
- [205] J. A. Reinbolt, M. D. Fox, A. S. Arnold, S. Öunpuu, and S. L. Delp, “Importance of preswing rectus femoris activity in stiff-knee gait,” *J. Biomech.*, vol. 41, no. 11, pp. 2362–2369, 2008.
- [206] M. van Bloemendaal, S. A. Bus, C. E. de Boer, F. Nollet, A. C. H. Geurts, and A. Beelen, “Gait training assisted by multi-channel functional electrical stimulation early after stroke: study protocol for a randomized controlled trial,” *Trials*, vol. 17, no. 1, p. 477, 2016.
- [207] K. K. Patterson, W. H. Gage, D. Brooks, S. E. Black, and W. E. McIlroy, “Evaluation of gait symmetry after stroke: A comparison of current methods and recommendations for standardization,” *Gait Posture*, vol. 31, no. 2, pp. 241–246, Feb. 2010.
- [208] J. Mizrahi, P. Solzi, H. Ring, and R. Nisell, “Postural stability in stroke patients: vectorial expression of asymmetry, sway activity and relative sequence of reactive forces,” *Med. Biol. Eng. Comput.*, vol. 27, no. 2, pp. 181–90, Mar. 1989.
- [209] G. Borg, “Perceived exertion as an indicator of somatic stress,” *Scand. J. Rehabil. Med.*, vol. 2, no. 2, pp. 92–8, 1970.
- [210] M. A. Thirunarayan, D. C. Kerrigan, M. Rabuffetti, U. Della Croce, and M. Saini,

- “Comparison of three methods for estimating vertical displacement of center of mass during level walking in patients,” *Gait Posture*, vol. 4, no. 4, pp. 306–314, 1996.
- [211] Y. Enomoto, T. Aibara, K. Sugimoto, and K. Seki, “Estimation of the center of mass and pelvis movement in running using an inertia sensor mounted on sacrum,” *ISBS Proc. Arch.*, vol. 35, no. 1, pp. 3–6, Oct. 2016.
- [212] D. Popovic, “Control of functional electrical stimulation for restoration of motor function,” *Facta Univ. - Ser. Electron. Energ.*, vol. 30, no. 3, pp. 295–312, 2017.
- [213] B. J. Andrews, R. H. Baxendale, R. Barnett, G. F. Phillips, T. Yamazaki, J. P. Paul, and P. A. Freeman, “Hybrid FES orthosis incorporating closed loop control and sensory feedback,” *J. Biomed. Eng.*, vol. 10, no. 2, pp. 189–195, 1988.
- [214] H. Herr and A. Wilkenfeld, “User-adaptive control of a magnetorheological prosthetic knee,” *Ind. Robot An Int. J.*, vol. 30, no. 1, pp. 42–55, Feb. 2003.
- [215] S. R. Hundza, W. R. Hook, C. R. Harris, S. V. Mahajan, P. A. Leslie, C. A. Spani, L. G. Spalteholz, B. J. Birch, D. T. Commandeur, and N. J. Livingston, “Accurate and reliable gait cycle detection in parkinson’s disease,” *IEEE Trans. Neural Syst. Rehabil. Eng.*, vol. 22, no. 1, pp. 127–137, 2014.
- [216] A. Nandy, S. Mondal, L. Rai, P. Chakraborty, and G. C. Nandi, “A study on damping profile for prosthetic knee,” in *Proceedings of the International Conference on Advances in Computing, Communications and Informatics - ICACCI '12*, 2012, p. 511.
- [217] E. Munoz Diaz, O. Heirich, M. Khider, and P. Robertson, “Optimal sampling frequency and bias error modeling for foot-mounted IMUs,” in *International Conference on Indoor Positioning and Indoor Navigation*, 2013, pp. 1–9.
- [218] M. Toussaint, D. Andreu, P. Fraisse, and D. Guiraud, “Wireless Distributed Architecture for Therapeutic Functional Electrical Stimulation: a technology to design network-based muscle control,” in *2010 Annual International Conference of the IEEE Engineering in Medicine and Biology*, 2010, pp. 6218–6221.